Long Term Pavement Performance Computed Parameter: Moisture Content

PUBLICATION NO. FHWA-HRT-08-035

MARCH 2008

U.S. Department of Transportation
Federal Highway Administration

Research, Development, and Technology
Turner-Fairbank Highway Research Center
6300 Georgetown Pike
McLean, VA 22101-2296

LTPP

FOREWORD

The ability to accurately monitor subsurface soil parameters on a continuous basis is extremely beneficial in pavement design, evaluation, and performance prediction. The time domain reflectometry (TDR) data collected as part of the Long Term Pavement Performance seasonal monitoring program (SMP) can be used to estimate moisture content, conductivity, reflectivity, and density. This report provides valuable information on calculating these parameters utilizing TDR traces and documents the process of interpreting over 270,000 TDR traces taken at SMP sites across North America.

In situ data availability is critical to pavement engineering, particularly as the process moves toward mechanistic-empirical techniques. This study not only provides useful information from in-service pavements, but also provides a method that can be utilized by State highway agencies interested in monitoring subsurface conditions and analyzing their effect on pavement response.

Gary Henderson
Director, Office of Infrastructure
Research and Development

Notice

Quality Assurance Statement

The Federal Highway Administration (FHWA) provides high-quality information to serve Government, industry, and the public in a manner that promotes public understanding. Standards and policies are used to ensure and maximize the quality, objectivity, utility, and integrity of its information. FHWA periodically reviews quality issues and adjusts its programs and processes to ensure continuous quality improvement.

TECHNICAL REPORT DOCUMENTATION PAGE

1. Report No. FHWA-HRT-08-035	2. Government Accession No.	3. Recipient's Catalog No.
4. Title and Subtitle LTPP Computed Parameter: Moisture Content		5. Report Date January 2008
		6. Performing Organization Code
7. Author(s) D. Zollinger, S. Lee, J. Puccinelli, and N. Jackson		8. Performing Organization Report No. 1236.10
9. Performing Organization Name and Address Nichols Consulting Engineers 1885 South Arlington Avenue Suite 111 Reno, NV 89509-3370	Texas A & M Zachry Department of Civil Engineering 503E CE/TTI Building College Station, TX 77843	10. Work Unit No. (TRAIS)
		11. Contract or Grant No. DTFH61-02-D-00139
12. Sponsoring Agency Name and Address Office of Infrastructure R&D Federal Highway Administration 6300 Georgetown Pike McLean, VA 22101-2296		13. Type of Report and Period Covered Final Report July 2005 to September 2007
		14. Sponsoring Agency Code
15. Supplementary Notes Contracting Officer's Technical Representative (COTR): Larry Wiser, Long Term Pavement Performance Team		

16. Abstract

A study was conducted to compute in situ soil parameters based on time domain reflectometry (TDR) traces obtained from Long Term Pavement Performance (LTPP) test sections instrumented for the seasonal monitoring program (SMP). Ten TDR sensors were installed in the base and subgrade layers at each of the 70 SMP test sites monitored as part of the LTPP program. A comprehensive description of a new method developed as part of the study to estimate moisture content, dry density, reflectivity, and conductivity of the soil from TDR traces is provided in the report. This new method utilizes transmission line equations and micromechanics models calibrated to site-specific conditions for each site/layer combination. Background information on existing empirical methodologies used to estimate subsurface moisture content from TDR traces is also documented. The results were compared to previous methods as well as ground truth data to evaluate the ability of the new model to predict soil parameters. The transmission line equation and micromechanics method was found to provide accurate results and was used to interpret over 270,000 TDR records stored in the LTPP database. A computer program (MicroMoist) was developed to aid in the computation of soil parameters based on TDR trace data and calibration information. Details on the program are provided along with descriptions of the tables developed to store the computed values in the LTPP Information Management System database.

17. Key Words LTPP, SMP, TDR, moisture content, soil parameters, dry density, reflectivity, conductivity, transmission line equation, micromechanics, pavements	18. Distribution Statement No restrictions. This document is available to the public through the National Technical Information Service, Springfield, VA 22161.

19. Security Classification (of this report) Unclassified	20. Security Classification (of this page) Unclassified	21. No. of Pages 104	22. Price

SI* (MODERN METRIC) CONVERSION FACTORS

APPROXIMATE CONVERSIONS TO SI UNITS

Symbol	When You Know	Multiply By	To Find	Symbol
		LENGTH		
in	inches	25.4	millimeters	mm
ft	feet	0.305	meters	m
yd	yards	0.914	meters	m
mi	miles	1.61	kilometers	km
		AREA		
in^2	square inches	645.2	square millimeters	mm^2
ft^2	square feet	0.093	square meters	m^2
yd^2	square yard	0.836	square meters	m^2
ac	acres	0.405	hectares	ha
mi^2	square miles	2.59	square kilometers	km^2
		VOLUME		
fl oz	fluid ounces	29.57	milliliters	mL
gal	gallons	3.785	liters	L
ft^3	cubic feet	0.028	cubic meters	m^3
yd^3	cubic yards	0.765	cubic meters	m^3
	NOTE: volumes greater than 1000 L shall be shown in m^3			
		MASS		
oz	ounces	28.35	grams	g
lb	pounds	0.454	kilograms	kg
T	short tons (2000 lb)	0.907	megagrams (or "metric ton")	Mg (or "t")
		TEMPERATURE (exact degrees)		
°F	Fahrenheit	5 (F-32)/9 or (F-32)/1.8	Celsius	°C
		ILLUMINATION		
fc	foot-candles	10.76	lux	lx
fl	foot-Lamberts	3.426	candela/m^2	cd/m^2
		FORCE and PRESSURE or STRESS		
lbf	poundforce	4.45	newtons	N
lbf/in^2	poundforce per square inch	6.89	kilopascals	kPa

APPROXIMATE CONVERSIONS FROM SI UNITS

Symbol	When You Know	Multiply By	To Find	Symbol
		LENGTH		
mm	millimeters	0.039	inches	in
m	meters	3.28	feet	ft
m	meters	1.09	yards	yd
km	kilometers	0.621	miles	mi
		AREA		
mm^2	square millimeters	0.0016	square inches	in^2
m^2	square meters	10.764	square feet	ft^2
m^2	square meters	1.195	square yards	yd^2
ha	hectares	2.47	acres	ac
km^2	square kilometers	0.386	square miles	mi^2
		VOLUME		
mL	milliliters	0.034	fluid ounces	fl oz
L	liters	0.264	gallons	gal
m^3	cubic meters	35.314	cubic feet	ft^3
m^3	cubic meters	1.307	cubic yards	yd^3
		MASS		
g	grams	0.035	ounces	oz
kg	kilograms	2.202	pounds	lb
Mg (or "t")	megagrams (or "metric ton")	1.103	short tons (2000 lb)	T
		TEMPERATURE (exact degrees)		
°C	Celsius	1.8C+32	Fahrenheit	°F
		ILLUMINATION		
lx	lux	0.0929	foot-candles	fc
cd/m^2	candela/m^2	0.2919	foot-Lamberts	fl
		FORCE and PRESSURE or STRESS		
N	newtons	0.225	poundforce	lbf
kPa	kilopascals	0.145	poundforce per square inch	lbf/in^2

*SI is the symbol for the International System of Units. Appropriate rounding should be made to comply with Section 4 of ASTM E380.
(Revised March 2003)

TABLE OF CONTENTS

CHAPTER 1. INTRODUCTION 1

CHAPTER 2. BACKGROUND AND LITERATURE REVIEW 3

OVERVIEW OF TIME DOMAIN REFLECTOMETRY (TDR) 3
INTERPRETATION OF TDR TRACE 6
PREVIOUS COMPUTATION METHODOLOGY OF DIELECTRIC CONSTANT 7
PREVIOUS METHODOLOGY FOR DETERMINATION OF IN SITU VOLUMETRIC MOISTURE CONTENT 9
CALCULATION OF GRAVIMETRIC MOISTURE CONTENT 14

CHAPTER 3. RESEARCH APPROACH 17

SOLUTION METHODOLOGY (STEP 1) 20
DETERMINATION AND CALIBRATION OF SOIL COMPONENT DIELECTRIC CONSTANTS (STEP 2) 22
FORWARD COMPUTATION OF WATER CONTENT AND DRY DENSITY (STEP 3) 25
VALIDATION 25

CHAPTER 4. COMPUTER PROGRAM DEVELOPMENT 33

OVERVIEW OF THE LTPP MICROMOIST PROGRAM 33
PROGRAM ALGORITHM 34
Inflection Point Determination 34
Calculation of Dielectric Constant, Reflectivity, and Conductivity 37
Calculation of Moisture Content and Dry Density 39
DEVELOPMENT OF THE CALIBRATION TABLE 40
Calculation of Dielectric Data from Manual TDR Traces 41
Sources of Ground Truth Dry Density and Moisture Content 42
Adjustment of Dry Density 42
Calculation of Calibrated Values 48
MICROMOIST INPUT AND OUTPUT DATA TABLE 50
Input Tables 50
Output Tables 52

CHAPTER 5. PARAMETER COMPUTATION AND QUALITY REVIEW 55

INTERNAL PROGRAM QUALITY CONTROL FEATURES 55
SHIFT ZONE IN TREND LINE BETWEEN DIELECTRIC CONSTANT AND MOISTURE CONTENT 57
Soil-Water Characteristic Curve 58
Recalibration for Shift Zone 59
POST-PROCESSING QUALITY CONTROL REVIEW 60
ESTIMATE OF ERROR 61

CHAPTER 6. LTPP DATABASE DELIVERY 63

CHAPTER 7. DATA OBSERVATIONS 65

COMPARISON BETWEEN NEW AND EXISTING DATA 65
FROST EFFECTS 68
SOURCES OF ERROR IN CALIBRATION DATA 69

CHAPTER 8. RECOMMENDATIONS FOR FUTURE RESEARCH 71

INVESTIGATE THE EFFECTS OF SOIL SUCTION ON THE COMPOSITE DIELECTRIC CONSTANT 71
INVESTIGATE THE USE OF CONDUCTIVITY AND REFLECTIVITY 71
INVESTIGATE REPEATABILITY OF TDR TRACES 71
SENSITIVITY OF MICROMOIST PROGRAM OUTPUT TO VARIATION IN INPUT VALUES 72

CHAPTER 9. SUMMARY AND CONCLUSIONS 73

APPENDIX A. TRANSMISSION LINE EQUATION 77
MAXWELL'S EQUATIONS 77
CONSERVATION LAW OF ELECTRIC CHARGE 78
CONSTITUTIVE RELATIONS 78
MAXWELL'S EQUATIONS FOR TIME-HARMONIC FIELDS 79
UNIFORM PLANE WAVES IN FREE SPACE 80
TRANSMISSION LINE EQUATION OF COAXIAL TRANSMISSION LINE 82
COAXIAL LINES 82
TRANSVERSE ELECTRIC AND MAGNETIC (TEM) MODE IN A COAXIAL LINE 83
TRANSFORMATION RULES FOR TRANSMISSION LINES 84
TRANSMISSION LINE EQUATION 84
APPENDIX B. CHARACTERIZATION OF ERROR IN THE SID 87
APPENDIX C. MICROMOIST USER'S MANUAL 91
INTRODUCTION TO THE PROGRAM 91
GETTING STARTED IN THE PROGRAM 92
System Requirements 92
Installing and Running the Program 92
PROGRAM FEATURES 92
Raw TDR Trace Data 93
TDR Depth Records 93
TDR Calibration Records 93
Starting the Program 93
Output Table after Running Program 94
REFERENCES 95

LIST OF FIGURES

Figure 1. Diagram. TDR probe for SMP 4
Figure 2. Graph. Typical TDR signal 5
Figure 3. Diagram. Illustration of instrumentation installation 6
Figure 4. Graph. Illustration of trace interpretation methods 7
Figure 5. Flowchart. Volumetric moisture model selection process 13
Figure 6. Diagram. Soil mixture with volume of soil solids equal to 1 15
Figure 7. Diagram. Coaxial line dimensions 19
Figure 8. Graph. Bounding of dielectric constant as a function of the computed volumetric moisture content (θ) using equation 28 23
Figure 9. Bar Chart. Errors in volumetric moisture content estimates (calibration validation) 27
Figure 10. Bar Chart. Errors of volumetric moisture contents on ground truth data 28
Figure 11. Bar Chart. Errors of laboratory estimated dry density on ground truth data 29
Figure 12. Bar Chart. Errors of volumetric moisture contents on ground truth data 30
Figure 13. Bar Chart. Errors of estimated dry density on ground truth data (field validation) 31
Figure 14. Photo. Interface of new program 33
Figure 15. Graph. Inflection points in TDR trace 35
Figure 16. Flowchart. Determination of inflection points 36
Figure 17. Flowchart. Calculation of dielectric constant, conductivity, and reflectivity 38
Figure 18. Flowchart. Calculation of moisture content and dry density 40
Figure 19. Graph. TDR traces of Section 308129, TDR No. 8 41
Figure 20. Diagram. Three separate phases of a soil element 43
Figure 21. Diagram. Profile of TDR and depth at each layer 44
Figure 22. Graph. Uninterpretable TDR trace 56
Figure 23. Graph. Incomplete TDR trace 56
Figure 24. Graph. Shift zone in LTPP section 091803, TDR sensor No. 7 57
Figure 25. Graph. Soil-water characteristic curve for sandy soil 58
Figure 26. Diagram. Diagrams of soil having different volume 59
Figure 27. Graph. Comparison of SWCC and VMC-DC trend 59
Figure 28. Graph. Sample plot of moisture content seasonal trend 60
Figure 29. Graph. Results from the apparent length approach for LTPP section 063042 66
Figure 30. Graph. Results from the TLE micromechanics method for LTPP section 063042 66
Figure 31. Graph. Results from the apparent length approach for LTPP section 313018 67
Figure 32. Graph. Results from the TLE micromechanics method for LTPP section 313018 68
Figure 33. Graph. Time-harmonic function $V(t)$ 79
Figure 34. Graph. Electric field as a function of z direction at different times 81
Figure 35. Diagram. Coaxial line 82
Figure 36. Graph. Cylindrical coordinate system 83
Figure 37. Diagram. Coaxial line developed into a parallel-plate waveguide 83

LIST OF TABLES

Table 1. Instrumentation for SMP 3
Table 2. SMP core experiment sectioning category 3
Table 3. Coefficient for mixing model 10
Table 4. Third order polynomial K_a-soil model parameters 11
Table 5. Refined third order polynomial K_a-soil model parameters 12
Table 6. Comparison of volumetric moisture contents during TDR installation 24
Table 7. Calibrated and calculated values determined by micromechanics method 24
Table 8. Calibration of dielectric constants by transmission line equation 27
Table 9. Comparison of moisture contents 27
Table 10. Calibration of dielectric constants for Section 091803 29
Table 11. Comparison of moisture contents for Section 091803 30
Table 12. Overview of LTPP MicroMoist program 34
Table 13. Dry density adjustment of Section 331001 and 533813 47
Table 14. Calibrated values of Section 331001 and 533813 49
Table 15. Field names and description of MICROMOIST_SMP_TDR_AUTO table 50
Table 16. Field names and description of MICROMOIST_SMP_TDR_DEPTHS_LENGTH table 51
Table 17. Field names and description of MICROMOIST_SMP_TDR_CALIBRATE table 51
Table 18. Field names and description of MICROMOIST_SMP_TDR_AUTO_DIELECTRIC table 52
Table 19. Field names and description of MICROMOIST_SMP_TDR_AUTO_MOISTURE table 53
Table 20. Error codes used in the program 57
Table 21. Description of SMP_TDR_CALIBRATE table for the LTPP IMS Database 63
Table 22. Description of SMP_TDR_MOISTURE table for the LTPP IMS Database 64

LIST OF ACRONYMS AND ABBREVIATIONS

AASHTO	American Association of State Highway and Transportation Officials
AC	asphalt concrete
FHWA	Federal Highway Administration
IMS	Information Management System
LTPP	Long Term Pavement Performance
QC	quality control
SID	system identification method
SMP	seasonal monitoring program
SPS	Specific Pavement Study
SWCC	soil-water characteristic curve
TDR	time domain reflectometry
TEM	transverse electromagnetic mode
TLE	transmission line equation
VMC	volumetric moisture content

CHAPTER 1. INTRODUCTION

Time domain reflectometry (TDR) information has been collected as a key component of the Long Term Pavement Performance (LTPP) program's seasonal monitoring program (SMP) to monitor subsurface moisture conditions in pavement structures. The TDR waveform data do not provide in situ moisture contents directly. Rather, the data must be analyzed to determine parameters—such as volumetric moisture content (VMC)—that are of use in pavement design and performance prediction.

Interpretation that included the development of empirical-based methodologies to convert waveform characteristics and in situ soil properties to moisture parameters was performed on a portion of these TDR data under previous analysis.[1] The computed parameter data from this effort are currently available in the LTPP Pavement Performance database. Since then, approximately 175,000 more automated TDR measurements have been added to the database but have not been interpreted. The current study was performed to not only compute the moisture parameters for these additional TDR measurements but also to assess other feasible computational procedures.

The objectives of the current study were to:

- Investigate the differences between the automated and manual TDR trace interpretation methods.
- Investigate the adequacy of the models used to estimate VMC from the TDR interpreted dielectric constant.
- Investigate the adequacy of data used to compute gravimetric moisture content from VMC.
- Determine adequacy of data to support computation of other moisture-related indices such as degree of saturation.

A significant portion of the analysis was focused on alternative computational processes, wherein previously uninterpretable traces could be utilized. Based on this investigation, a new approach was recommended that computed the soil dielectric constant using a solution of the transmission line equation (TLE) for each TDR trace and the computation of the dry density and the moisture content using a micromechanics model. The new approach eliminated many of the issues related to the trace interpretations and provided a relatively accurate assessment of the in situ moisture content.

In phase 1 of this project, the basic procedures of the new approach were developed and evaluated using measured moisture contents from the SMP Installation Reports and other sources.[2] The new approach was shown to work and to produce reasonable estimates of the in situ moisture contents compared with ground truth measurements in both field and laboratory settings. Phase 2 of the project entailed the development of a new computer program to automate the computation process, the computation of the moisture content for 274,000 TDR traces, and the uploading of this data into the LTPP database. Quality control (QC) checks were developed and performed on all of the computed data.

This report presents the development of the new computational procedures, evaluation of results from the new approach, development of the computer program automating the process, and the QC initiatives implemented to ensure data reported in the LTPP database are of research quality.

CHAPTER 2. BACKGROUND AND LITERATURE REVIEW

Environmental factors such as moisture content, temperature gradient, and depth of frost penetration have a significant effect on pavement performance. Understanding the effect of these factors on performance is crucial to the optimal design of pavement structures and involves consideration of not only seasonal variations but also changes throughout the day.

To provide a means for studying the contribution of environmental factors on pavement structures, SMP was initiated within LTPP. This program was designed to provide (1) the means to link pavement response data obtained at random points in time relative to critical design conditions, (2) the means to validate models for relationships between environmental conditions and in situ structural properties of pavement materials, and (3) expanded knowledge of the magnitude and impact of the changes involved. To accomplish this, SMP sites were instrumented with the equipment in table 1.

Table 1. Instrumentation for SMP. [3]

Instruments	Measurement
TDR (time domain reflectometry)	Moisture content of subsurface
Thermistor sensors	Pavement temperature gradients and air temperature
Electrical resistivity probes	Depth of frost/thaw
Piezometer	Depth of ground water table
Tipping-bucket rain gauge	Precipitation

The design of SMP was a two-tiered approach including the core experiment and supplemental studies. The core experiment included 64 LTPP test sections selected by the categories listed in table 2. An additional six test sections were included as supplemental studies to the original SMP experimental design. To capture seasonal and diurnal changes, pavement response data were collected more frequently than routine LTPP monitoring. The supplemental studies were carried out in response to highway agencies' desire to collect data on LTPP test sections not included in the core sites.

Table 2. SMP core experiment sectioning category. [3]

Pavement type	- Flexible-thin asphalt concrete (AC) surface (<127 mm (5 inches)) - Flexible-thick AC surface (>127 mm (5 inches)) - Rigid-jointed plain concrete - Rigid-jointed reinforced concrete	
Subgrade soil	- Fine grained	- Coarse grained
Environment	- Wet-freeze - Dry-freeze	- Wet-no freeze - Dry-no freeze

OVERVIEW OF TIME DOMAIN REFLECTOMETRY (TDR)

The collection of TDR waveforms from subsurface materials is of particular interest in this study. Although the importance of in situ moisture content of subsurface layers in

pavement structures has been well recognized, moisture measurement has sometimes been difficult because of the limitations of existing measurement and computational methods.

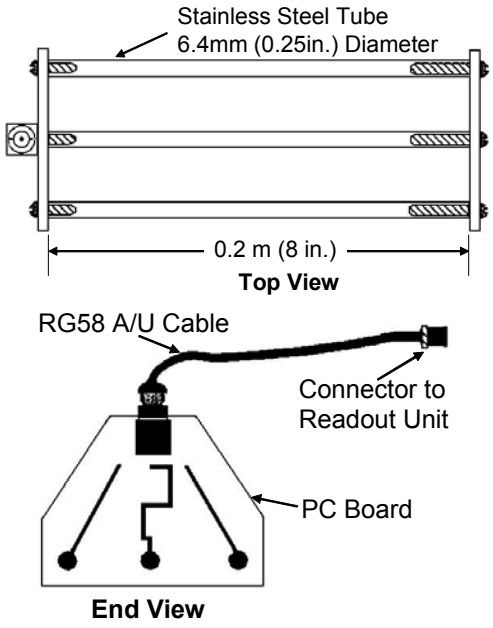

Figure 1. Diagram. TDR probe for SMP. [3]

The TDR method was selected for use in the SMP core experiment. TDR equipment was originally developed for measuring electromagnetic wave travel times to detect breaks or shorts in electrical conductors and subsequently was adapted to collect sufficient data to allow for soil moisture to be estimated. The TDR system records an electromagnetic waveform that can be analyzed as it is transmitted and reflected to characterize the nature of objects that reflect the waves. The waveform pulse is transmitted along a coaxial metallic cable shielded by a waveguide at a velocity that is influenced by the dielectric constant (ε) of material surrounding the conductors. This dielectric constant is a dimensionless ratio of a material's dielectric permittivity to the permittivity of free space. Changes in the dielectric constant of the surrounding material occur as its moisture content or conductivity (the reciprocal of resistance) changes. Signal reflectivity also varies (from 1 to -1) as a function of the degree of open to short circuitry, respectively, and exists in the wave reflections as evidenced by slope changes in the return wave pulse recorded by the TDR readout unit. A full short circuit eliminates any additional return signals, while varying degrees of an open circuit results in a variety of return signals.[3]

The Federal Highway Administration (FHWA) TDR moisture probe is shown in figure 1. The coaxial lead cable (signal lead) is connected to the center of the three stainless steel rods, which are inserted horizontally into the soil at the point of monitoring. The cable's outer shield is connected to the outer rods, which serve as the waveguide. The recorded TDR signal rises to a peak (initial inflection point), as the electromagnetic wave enters

the probe rods, followed by a fall in the return signal to a second inflection point as the wave hits the end of the probes as illustrated in figure 2. The distance between the first inflection point (point D_1) and final inflection point (point D_2) is known as the "apparent" length of the probe, L_a. [3]

Ten TDR probes were used to measure in situ moisture content of pavement sublayers at SMP test sections that were placed in one hole located in the outer wheel path. [4] At most sites, the TDR installation hole was located at approximately 0.76 m (2.5 ft) from the outside edge of the white stripe and at least 1.2 m (4 ft) away from joints and/or cracks to avoid unrepresentative surface moisture infiltration. Figure 3 provides a schematic of the instrumentation.

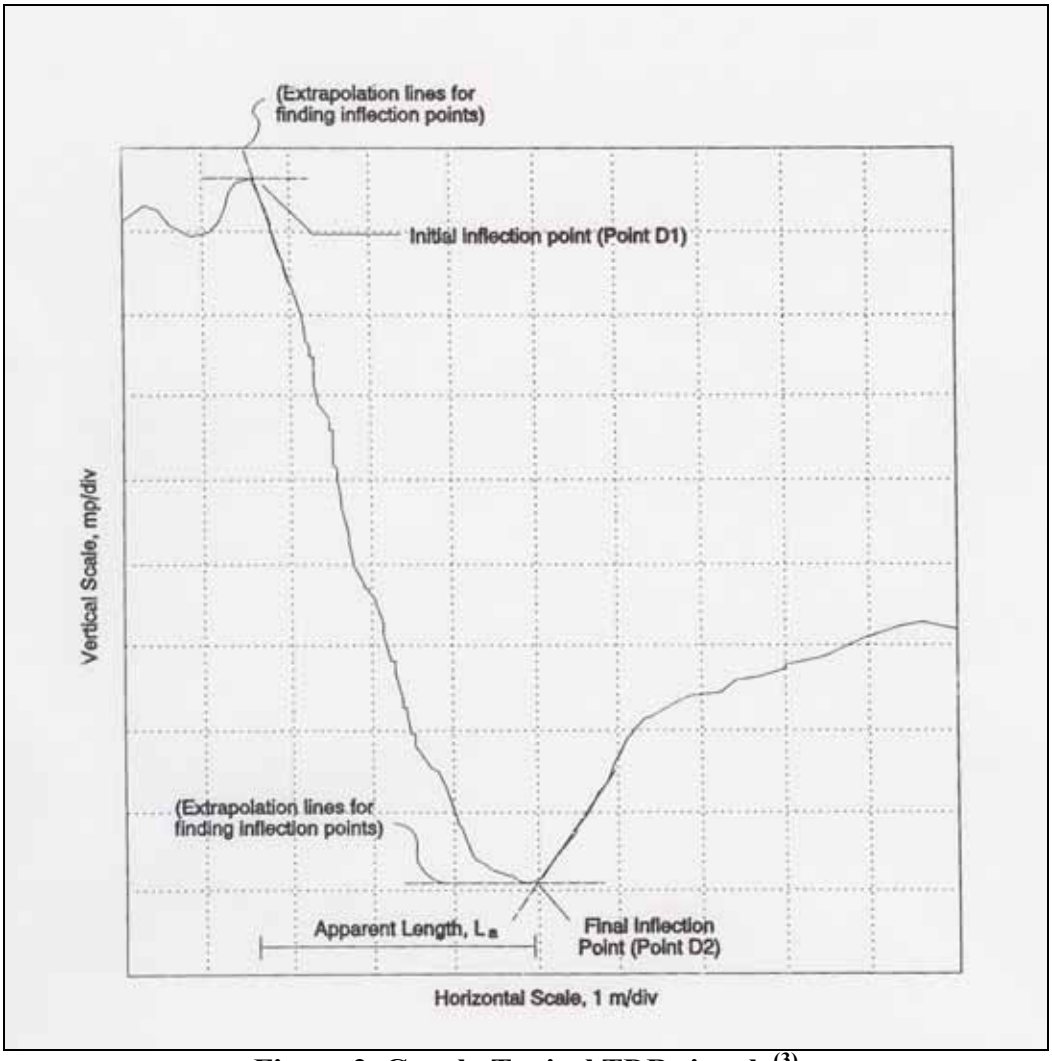

Figure 2. Graph. Typical TDR signal. [3]

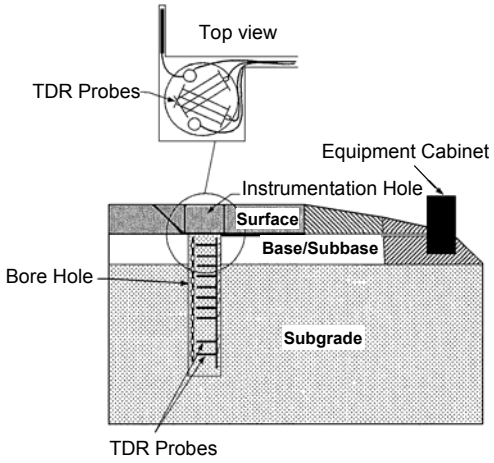

Figure 3. Diagram. Illustration of instrumentation installation. [3]

The TDR probes were placed at specified depths as the type of sublayer and its thickness varied. If the top granular base (or subbase) layer was greater than 305 mm (12 in), the first TDR probe was placed 152 mm (6 in) below the surface layer and/or bottom of the lowest stabilized layer; otherwise, the probe was placed at mid depth of the top granular base (or subbase) layer. The next seven TDR probes were placed at 152 mm (6 in) intervals and the last two probes were placed at 305 mm (12 in) intervals. [3]

INTERPRETATION OF TDR TRACE

The waveform obtained from the TDR sensor must be analyzed to determine in situ soil parameters. Existing procedures for the interpretation of TDR data have included determining the apparent length (L_a) so as to compute the dielectric constant and the VMC for the material surrounding the TDR probe.

The initial inflection point (D_1) is located where the signal enters the probe rods while the final inflection point (D_2) occurs at the end of the probes. Both are displayed in the TDR readout device. The distance between Point D_1 and D_2 is the L_a value used to determine the dielectric constant of surrounding material. The L_a value can be determined using a variety of methods. Klemunes studied ways to find the most accurate methodology to determine the L_a value of the TDR signal response. [5] The study investigated and compared five methods: (1) Method of Tangents, (2) Method of Peaks, (3) Method of Diverging Lines, (4) Alternate Method of Tangents, and (5) the Campbell Scientific Method.

Differences among the methods are centered on the procedure of locating the initial and final inflection points of the TDR trace. From the study, the method of tangents was found to be the most accurate while the least accurate methods are the alternate method of tangents and the method of diverging lines.

The method of tangents employs the tangent lines at the local values of the TDR traces to isolate the inflection points. D_1 is located at the intersection of the horizontal and negatively sloped tangents (i.e., local maximum) of the TDR trace, and D_2 is located at the intersection of the horizontal and positively sloped tangents (i.e., local minimum) as

shown in figure 4(a). However, the method cannot be applied to very dry or partially frozen soils, so the method of peaks is used for those soil type situations. [6] In the Method of Peaks, D_1 is determined by locating the intersection of the tangents drawn on both sides of the initial inflection point, and D_2 is at the intersection of the tangents drawn of both sides of the final inflection point, as shown in figure 4(b).

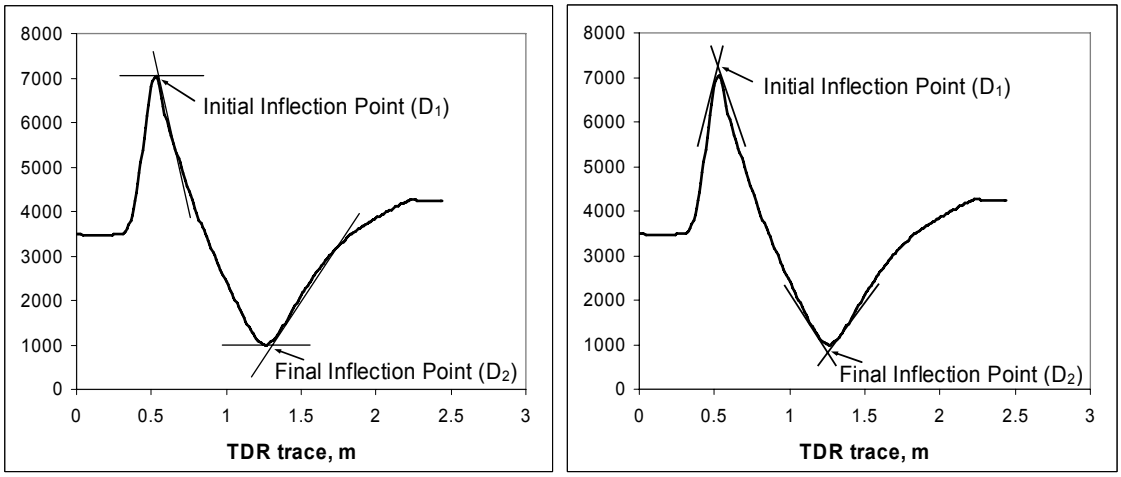

(a) Method of Tangents (b) Method of Peaks

Figure 4. Graph. Illustration of trace interpretation methods. [5, 6]

PREVIOUS COMPUTATION METHODOLOGY OF DIELECTRIC CONSTANT

An electromagnetic signal is transmitted along the TDR probe. When the signal reaches the end of the probe, it is reflected back to the data acquisition unit and the reflected signal is recorded. The velocity of this reflected electromagnetic wave in the probe depends on the dielectric constant and magnetic permeability of the surrounding material (relative to the speed of light in a vacuum) and is given in equation 1 as: [7]

$$c = \frac{1}{\sqrt{\varepsilon\mu}} c_0 \qquad (1)$$

Where:

c = velocity of electromagnetic wave,
ε = dielectric constant, (approximately 1.0 for air, 80 for water, and 3–5 for dry soil)
μ = relative magnetic permeability of the soil
c_0 = speed of light in vacuum

Assuming the effects of ferromagnetic components in soils are not significant, the magnetic permeability of soil can be set to unity ($\mu = 1$). [8] By substituting the velocity

of electromagnetic wave with the travel time and the length of probe ($c = 2L/\Delta t$), the dielectric constant is:

$$\varepsilon = \left(\frac{\Delta t \cdot c_0}{2L} \right)^2 \quad (2)$$

Where:

Δt = the travel time of the TDR signal
L = actual length of TDR probe

The travel time of the signal is also dependent on the dielectric constant, which includes signal propagation in the soil-moisture mixture; hence, the apparent probe length can be determined by the travel time of the signal if it were propagating at the speed of light:

$$L_a = \frac{\Delta t \cdot c_0}{2} \quad (3)$$

Therefore, the dielectric constant of soil can be expressed as the ratio of apparent length to actual length of TDR probe from equations 2 and 3:

$$\varepsilon = \left(\frac{L_a}{L} \right)^2 \quad (4)$$

Where:

L_a = apparent length of probe, m

The dielectric constant can be determined with the phase velocity considering the propagation as follows: [5]

$$\varepsilon = \left(\frac{L_a}{L \cdot V_p} \right)^2 = \left(\frac{D_2 - D_1}{L \cdot V_p} \right)^2 \quad (5)$$

Where:

L = actual length of TDR probe, 0.203 m (8 inches) for FHWA probes
V_p = phase velocity setting on TDR cable tester (usually 0.99); this is the ratio of the actual propagation velocity to the speed of light.

In short, the dielectric constant is derived from the relationship between the speed of light and the wave velocity (delayed due to wave propagation caused by the dielectric properties of the soil surrounding the TDR probe).

PREVIOUS METHODOLOGY FOR DETERMINATION OF IN SITU VOLUMETRIC MOISTURE CONTENT

The methods currently used to determine soil VMC from dielectric constants are mainly based on empirical approaches:

(1) Topp's equation
(2) Klemunes' model
(3) Third-order polynomial K_a – soil gradation model

Topp's equation employs empirical regression functions to relate the dielectric constant to the VMC. [8] The third-order polynomial function developed by Topp is widely used for calculating moisture content of soil materials. Topp's equation can be applied to all types of soils but is inaccurate for certain scenarios: [1,8]

$$\theta = -5.3 + 2.923\varepsilon - 0.055\varepsilon^2 + 0.00043\varepsilon^3 \quad (6)$$

Where:

θ = volumetric moisture content (%)

Klemunes developed calibrated mixing models for soil samples obtained from 28 LTPP sites. [5, 6] TDR traces were obtained from the soil samples prepared at various combinations of moisture content and compaction levels. The moisture content and dry density of each combination was determined by laboratory testing after the TDR trace was obtained. A total of 415 data points were obtained; however, outliers and TDR traces that were impossible to interpret were removed from the dataset. Consequently, 397 data points were available and used to develop Klemunes' moisture models, which employ a hierarchal methodology (i.e., level 1 to level 4) relative to the level of information available and the desired accuracy.

At level 1, the moisture content would be determined without any information about the properties of the soil, such as coarse-/fine-grained or American Association of State Highway and Transportation Officials (AASHTO) classification. Therefore, level 1 has the lowest explained variance and the highest standard error. At level 2, moisture content is determined on the basis of the soil being identified as either coarse- or fine-grained. The accuracy of this level is better than that of level 1. At level 3, the VMC is based on the AASHTO soil classification, accounting for the soil's gradation and the characteristics of fraction passing No. 40.

The most accurate level of Klemunes' model is level 4 since this involves testing the soil at various moisture and density levels in the laboratory and correlating the results with the TDR recordings. Accordingly, a calibration curve is developed for a range of VMC expected in the field. The following equation is used to predict the VMC for each of the four levels. Table 3 provides the specific regression coefficients for each level.

$$\theta(\%) = \frac{(5L_a - 1) - B_0 \dfrac{\gamma_d}{G_s \gamma_w}}{B_1} \qquad (7)$$

Where:

γ_d , γ_w = unit weight of the soil and water
G_s = specific gravity of the soil
B_0, B_1 = regression coefficients

Table 3. Coefficient for mixing model. [5, 6]

Level	Soil Type	B_0	B_1
Level 1	All-type	1.41	7.98
Level 2	Coarse	1.06	9.30
	Fine	1.50	7.56
Level 3	A-1-b	1.43	7.69
	A-2-4	1.00	9.57
	A-3	1.11	9.02
	A-4	1.77	6.25
	A-6	-1.56	12.26
	A-7-5	1.04	8.49
	A-7-6	1.02	10.31
Level 4	Determined based on a site-specific calibration		

As part of the third-order polynomial K_a-soil gradation approach, four models were developed for the VMC computation. The first three models take the third-order polynomial K_a model based on soil type while the fourth model applies to only fine-gradation soils and incorporates the contribution of the gradation into the model. [1] A computer program entitled MOISTER incorporates all four of the third-order polynomial K_a models to determine the VMC of soil, the method of tangents, and the method of peaks to determine the apparent length (and dielectric constant) of the TDR trace.

The third-order polynomial K_a models were developed based on the regression of dielectric constants and VMC from the dataset obtained in Klemunes' study. The coarse-grained soil has a different trend compared with fine- grained soil, but both of them show a third-order polynomial functional form. Hence, in order to provide a more accurate model, data for coarse-grained soil and fine-grained soil were modeled separately. The models are valid only within the dielectric constant range or the inference space that was used to develop the model. [1] The three empirical regression equations developed using the dielectric constant as the sole independent variable are given below with the regression coefficients shown in table 4.

$$\theta\ (\%) = a_0 + a_1\varepsilon + a_2\varepsilon^2 + a_3\varepsilon^3 \quad (8)$$

Where:

ε = dielectric constant
a_0, a_1, a_2, a_3 = regression coefficients

Table 4. Third order polynomial K_a-soil model parameters. [1]

Model type	a_0	a_1	a_2	a_3
Coarse-K_a model	-5.7875	3.41763	-0.13117	0.00231
Fine-K_a model	0.4756	2.75634	-0.061667	0.000476
All soil-K_a model	-0.8120	2.38682	-0.04427	0.000292

To refine the regression model and to increase the R^2 for fine-grained soil, another model was developed using gradation, plastic limit, and liquid limit as independent variables. Equation 9 provides the VMC model for fine-grained soil with variables: [1]

$$\theta(\%) = a_0 + a_1\varepsilon + a_2\varepsilon^2 + a_3\varepsilon^3 + a_4 G11\_2 + a_5 G1\_2 + a_6 No4 + a_7 No10 + a_8 No200 + a_9 PL + a_{10} LL \quad (9)$$

Where:

θ = volumetric moisture content
ε = dielectric constant
$a_0, a_1, \ldots, a_{10}$ = regression coefficients (see table 5)

This model was used for computing the VMC for the fine-grained soils where gradation and other parameters were available and within the inference region of the model. Table 5 shows the descriptions, values, and inference ranges of these variables.

Table 5. Refined third order polynomial K_a-soil model parameters. [1]

Variable	Description	Coef.	Value	Inference Range
Intercept		a_0	1761.78	
K_a	Dielectric constant	a_1	2.9145	3 - 58.4
K_a^2		a_2	-0.07674	
K_a^3		a_3	0.000722	
G11_2	%passing 1½-sieve	a_4	-19.6649	99 - 100
G1_2	%passing ½-sieve	a_5	4.3667	97 - 100
No4	%passing No.4 sieve	a_6	-5.1516	90 - 100
No10	%passing No.10 sieve	a_7	2.7737	84 - 100
No200	%passing No.200 sieve	a_8	0.06057	12.6 - 94.6
PL	Plastic limit	a_9	-0.2057	0 - 45
LL	Liquid limit	a_{10}	0.10231	0 - 69

The four models are selected based on the dielectric constant and properties of soil to calculate moisture content. The flow chart of the model selection scheme is shown in figure 5.

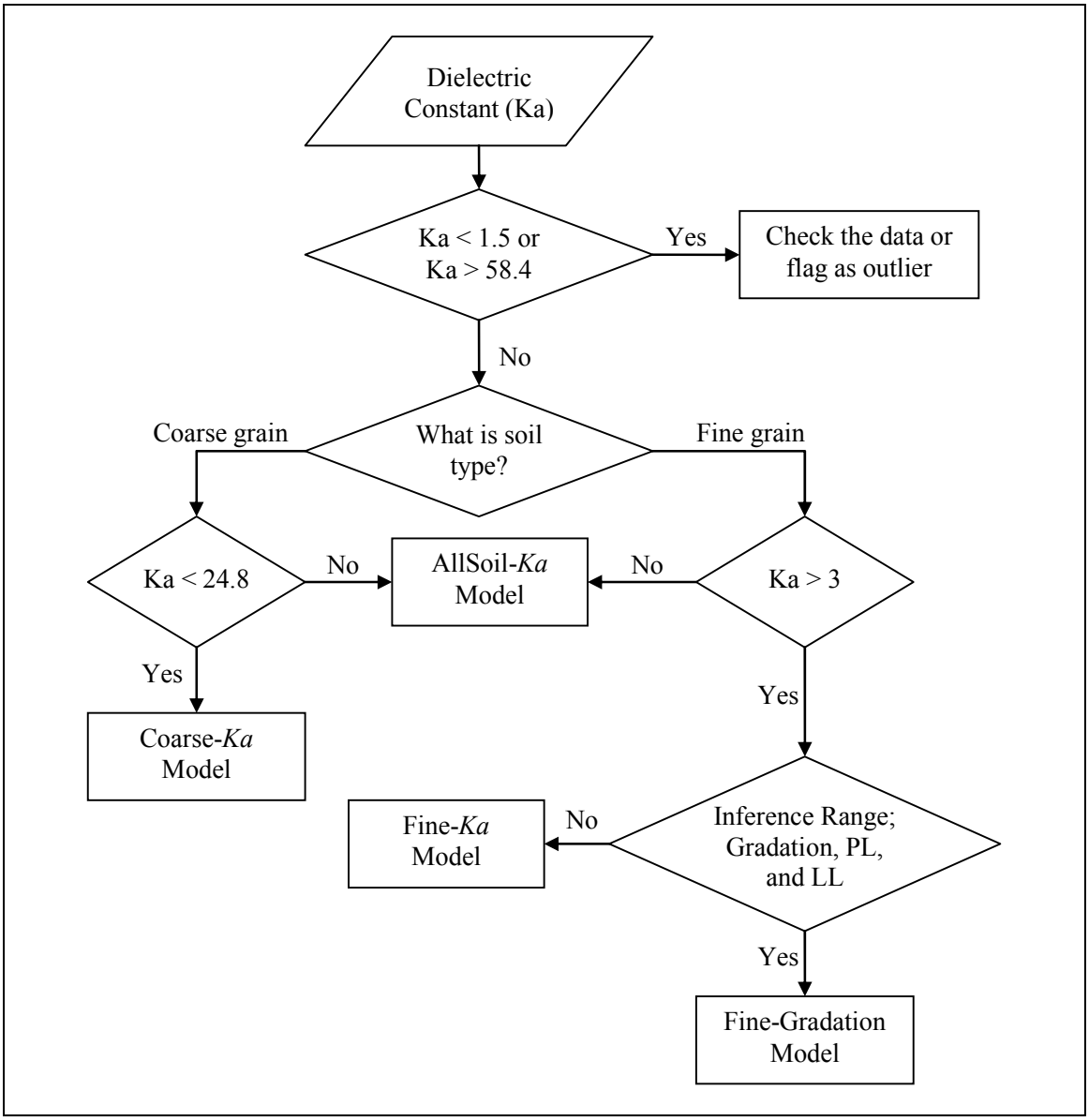

Figure 5. Flowchart. Volumetric moisture model selection process. [9]

CALCULATION OF GRAVIMETRIC MOISTURE CONTENT

VMC can be converted to a gravimetric basis using volume and weight relationships. The volume relationships used for soil solid-moisture-air mixture are degree of saturation, void ratio, and porosity as shown below: [10]

$$S = \frac{V_w}{V_v} \tag{10}$$

$$e = \frac{V_v}{V_s} = \frac{n}{1-n} \tag{11}$$

$$n = \frac{V_v}{V} = \frac{e}{1+e} \tag{12}$$

Where:

S = degree of saturation
e = void ratio
n = porosity
V_s = volume of soil solids (cm^3)
V_w = volume of water (cm^3)
V_v = volume of void (cm^3)
V = total volume of mixture (cm^3)

The weight relationship can be represented by moisture content and unit weight:

$$w = \frac{W_w}{W_s} \tag{13}$$

$$\gamma = \frac{W}{V} \tag{14}$$

Where:

w = gravimetric moisture content (%)
γ = unit weight (g/cm^3)
W_w = weight of water (g)
W_s = weight of solids (g)
W = total weight of mixture (g)

To calculate gravimetric moisture content, a relationship among moisture content and unit weight can be derived from a volume of soil mixture in which the volume of the soil solids is set to 1 as shown in figure 6. The volume of water can be defined as:

$$V_w = \frac{W_w}{\gamma_w} = wG_s \tag{15}$$

Where:

γ_w = unit weight of water (g/cm^3)
G_s = specific gravity of solids

The dry density of soil can be written as:

$$\gamma_d = \frac{W_s}{V} = \frac{G_s \gamma_w}{1+e} \tag{16}$$

Where:

γ_d = dry unit weight of soil (or soil dry density, g/cm^3)

Also, the degree of saturation is changed as follows:

$$S = \frac{V_w}{V_v} = \frac{wG_s}{e} \tag{17}$$

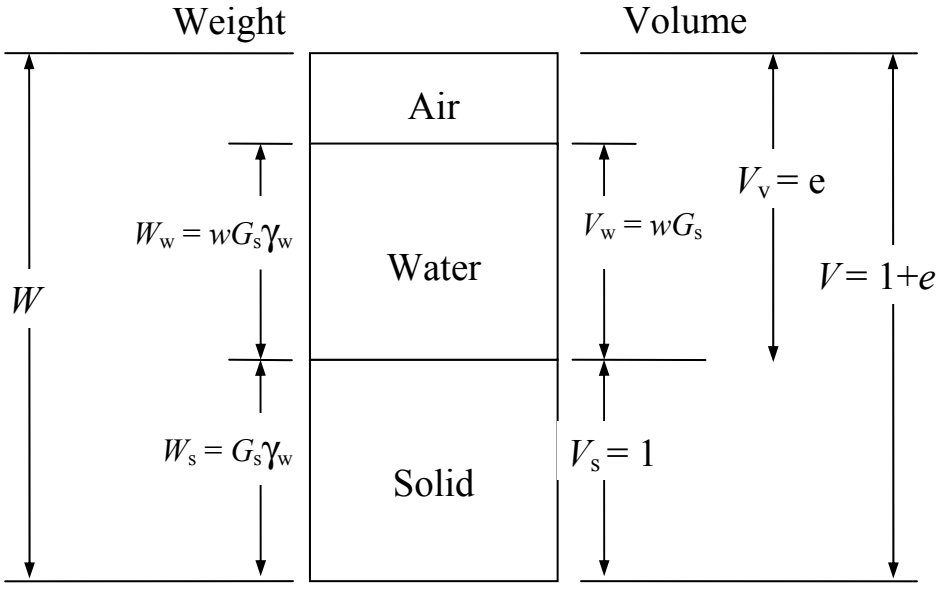

Figure 6. Diagram. Soil mixture with volume of soil solids equal to 1.

Thus, the gravimetric moisture content can be expressed in terms of the unit weight of water, unit weight of solids, and VMC by combining equations 16 and 17:

$$w = \frac{S \cdot e}{G_s} = \frac{V_w}{V}\frac{\gamma_w}{\gamma_d} = \theta\frac{\gamma_w}{\gamma_d} \tag{18}$$

Where:

θ = volumetric moisture content (%)

Equation 18 is used to convert soil moisture from a volume to a weight basis as needed in pavement engineering applications. Reasonably accurate in situ dry density estimates of material surrounding the TDR sensors must be made for moisture conversion. During installation, field moisture measurements were performed on the material placed around TDR probes with additional material samples retained for laboratory analyses. [3]

CHAPTER 3. RESEARCH APPROACH

The existing empirical methodology used to determine dielectric constant and VMC were evaluated along with new mechanistic-based techniques to determine to determine the best approach to use in computing TDR traces collected at LTPP SMP sites. This section provides details on the evaluation conducted and details on the methodology selected for use on SMP TDR data.

The existing methodology used in the analysis of SMP TDR traces to determine the dielectric constant is shown in equation 5. The dielectric constant for the soil-moisture-air mixture has been determined by comparing the "apparent" electrical length (L_a) of the probe from the TDR signal to its actual length. This method of determination of the dielectric constant is independent of the conducting medium's other electrical properties besides the dielectric constant, which influences the resultant computed parameters because the soil magnetic permeability is, for instance, assumed to be unity. Saline or alkaline soils can create an effective electrical short with the shielding rods due to the ions in the water, which can increase the effect of conductivity on the value of the dielectric constant. Consequently, trace interpretation difficulties and erroneous determinations result because of the soil's high electrical conductivity, suggesting that an improved method of determining the dielectric constant would involve the consideration of the effect of the soil conductivity. Furthermore, the difficult-to-interpret wave forms result from "dispersion" and "attenuation," which are directly related to the level of electrical conductivity in the medium.

The dielectric constant—or permittivity—of a soil is really a complex number, composed of a real and an imaginary part. It is assumed in the above method of analyzing TDR data that the imaginary part is negligible. The imaginary part is a measure of the ratio of the electrical conductivity of the soil to the dielectric property that is computed from TDR data. Conductivity is important in identifying corrosive soils and in indicating the presence of anions, such as sulfates, which are capable of expanding to produce large buckling movements in lime-stabilized pavement layers. Reduction in the wave form distortion over time indicates that the conductive elements in the soil are leaching out. In short, when the TDR signal is distorted and, consequently, difficult to interpret, it is providing additional information about the soil permittivity.

The wave form shown in figure 2 is typical of a soil with low conductivity. The horizontal axis in that graph is labeled as an apparent length, L_a. However, it is a plot of the voltage measured by the TDR device versus the time of arrival of that voltage. This is a signal of voltage as a function of time exactly as is analyzed when using ground-penetrating radar signals. A distorted wave form can be further analyzed to produce both the real and the imaginary parts of the permittivity of the soil—and what has been previously considered to be a limitation of the equipment is actually a benefit.

In terms of the sources of error in TDR measurements, there is a difference between the meaning of "regular" and "distorted" waveforms. Measurement error is inherent in the instrumentation itself. This type of error is normally random and can be reduced by

repeating the measurement. [11] The other kind of error is systematic error and arises from the assumptions that are made in the analysis of the data, precisely the type of error referred to in the above discussion. Further discussion in this regard will be presented later relative to the new approach to evaluate the soil dielectric property.

The new approach for the calculation of the VMC consists of three steps:

1. Calculate the dielectric constant, conductivity, and reflectivity from the TLE.

2. Given the ground truth moisture content data recorded at the installation of each device and the above parameters, backcalculate the permittivity of the solids for the particular TDR location and calibrate the micromechanics volumetric water model to site specific conditions. [12]

3. Using the calibrated micromechanics volumetric water model (specific to each TDR and location), forward calculate the volumetric water content and the dry density of the soil for other times and seasons based on the TDR traces and the associated dielectric constant.

Step (1) involves the use of the TLE for voltage (V):[12]

$$V(z) = V_{+}e^{-jkz} + V_{-}e^{+jkz} \tag{19}$$

Where:

V = applied voltage

z = distance along the transmission line (TDR probe), m

$= \frac{c}{\sqrt{\varepsilon_0}}t$

c $= \frac{1}{\sqrt{\mu_0 \varepsilon_0}}$

μ_0 = magnetic permeability of free space

$= 4\pi \times 10^{-7}$ H/m

ε_0 = electric permittivity of free space

$= \frac{1}{36\pi} x10^{-9}$ F/m

t = time of travel relative to the peak relative voltage

V_+ = voltage amplitude in the positive z direction

V_- = voltage amplitude in the negative z direction

k = dispersion coefficient = $k_R - jk_I$ (real and imaginary components)

$= \omega\sqrt{LC} = \omega\sqrt{\mu_0 \varepsilon}$

$= \omega\sqrt{\mu_0 \varepsilon}\left[1 - j\left(\frac{\sigma}{2\omega\varepsilon}\right)\right]$ for a slightly conducting medium

(i.e., $k_r = \omega\sqrt{\mu_0\varepsilon}$; $k_I = \frac{\sigma}{2}\sqrt{\frac{\mu_0}{\varepsilon}}$); $= \sqrt{\omega\mu}\left[1-j\right]$ for a highly conducting medium)

ε = dielectric constant of the soil

ω = waveform frequency (Hz)

σ = soil conductivity (S/m)

L = inductance (H/m)

$= \frac{\mu}{2\pi}\ln\left(\frac{b}{a}\right)$

a, b = inside and outside coaxial transmission line diameters, respectively (see figure 7)

μ = soil magnetic permeability (H/m)

C = capacitance (F/m)

$= \frac{2\pi\varepsilon}{\ln\frac{b}{a}}$

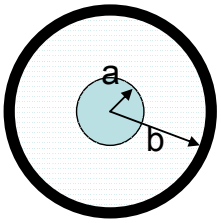

Figure 7. Diagram. Coaxial line dimensions. [12]

Developing further:

$$V(z) = V_+(e^{-jkz} + \Gamma_L e^{+jkz})$$
$$v(z) = e^{-jkz} + \Gamma_L e^{+jkz} = e^{-j(k_R - jk_I)z} + \Gamma_L e^{+j(k_R - jk_I)z}$$
$$= e^{-jk_R z - k_I z} + \Gamma_L e^{+jk_R + k_I z} \quad (20)$$

Where:

Γ_L = reflection coefficient

$= \frac{V_-}{V_+}$

$v(z)$ = relative voltage as a function of the dimension z

$= \frac{V(z)}{V_+}$

Writing the relative voltage ($v(z)$) in terms of time of travel (t) of the microwave:

$$v(t) = e^{-j\omega c\sqrt{\mu_0}t - \frac{\sigma c\sqrt{\mu_0}}{2\varepsilon}t} + \Gamma_L e^{+j\omega c\sqrt{\mu_0}t + \frac{\sigma c\sqrt{\mu_0}}{2\varepsilon}t}$$

$$= Re\left[e^{-j\omega\frac{t}{\sqrt{\varepsilon_0}} - \frac{\sigma t}{2\varepsilon\sqrt{\varepsilon_0}}} + \Gamma_L e^{+j\omega\frac{t}{\sqrt{\varepsilon_0}} + \frac{\sigma t}{2\varepsilon\sqrt{\varepsilon_0}}} \right] = e^{-\frac{\sigma t}{2\varepsilon\sqrt{\varepsilon_0}}} \cos\left(\omega\frac{t}{\sqrt{\varepsilon_0}} \right) + \Gamma_L e^{+\frac{\sigma t}{2\varepsilon\sqrt{\varepsilon_0}}} \cos\left(\omega\frac{t}{\sqrt{\varepsilon_0}} \right) \quad (21)$$

$$= \left(e^{-\frac{\sigma t}{2\varepsilon\sqrt{\varepsilon_0}}} + \Gamma_L e^{+\frac{\sigma t}{2\varepsilon\sqrt{\varepsilon_0}}} \right) \cos\left(\omega\frac{t}{\sqrt{\varepsilon_0}} \right)$$

The above expression can be used to analyze the voltage trace that is obtained from the TDR device. Notice that the voltage is a function of not only the dielectric constant but also of the conductivity and the reflectivity. Both of these parameters affect the inferred dielectric constant, or, in other words, they influence the value as it would be deducted from the characteristics of the trace. Systematic errors that would result from not accounting for conductivity and reflectivity are corrected by accurately accounting for the actual physics of wave transmission through a dielectric medium in the model. The use of the TLE to analyze the data reduces the systematic error introduced by assuming that conductivity and reflectivity have no influence on the shape of the transmitted voltage with distance down the length of the TDR probe. The dielectric constants produced after correcting for the effects of conductivity and reflectivity more accurately and precisely reflect the actual moisture state of the soil. The concept of the TLE and electromagnetics involved in the new approach is addressed in more detail in appendix A.

The constants used to compute the dielectric constant are the voltage and relative distance, the magnetic permeability of free space, and the electric permittivity of free space. While the voltage and relative distance are obtained from the TDR trace, the magnetic permeability and electric permittivity are fixed values, which are $4\pi \times 10^{-7}$ H/m and $1/36\pi \times 10^{-9}$ F/m, respectively. The inside and outside diameters of the coaxial cable are not required to compute dielectric constant values using the TLE.

SOLUTION METHODOLOGY (STEP 1)

The method of solving for the dielectric, conductivity, and reflectivity parameters (step 1) is by use of the system identification method (SID).[11] This method is used to fit the equation for relative voltage (v(z)) to the form of the TDR trace (an example of which is shown in figure 2) by iterating ΔX_i until it equals zero by satisfying the following expression for each point selected from the trace:

$$\sum_{1}^{i=m} \left(\frac{\partial v(z)_i}{\partial X_i} \frac{X_i^n}{v(z)_i^n} \right) \left(\frac{\Delta X_i^n}{X_i^n} \right) = \frac{\Delta v(z)_i^n}{v(z)_i^n} \quad (22)$$

Where:

X_i^n = conductivity (σ), dielectric constant (ε), or reflection coefficient (Γ)

m = number of X_i (in this case = 3) that are determined for each voltage recorded from the TDR trace

$\Delta X_i^n = X_i^{n+1} - X_i^n$

n = iteration count

$\Delta v(z)_i^n = v(z)_i^n - v(z)_m$

$v(z)_m$ = the measured voltage

$v(z)_i^n$ = the current calculated voltage based on the current values of X_i^n

In matrix form, the iteration process is capable of solving a set of simultaneous equations developed for each set of data points taken from the TDR trace:

$$[F]\{\beta\} = [\underline{r}] \tag{23}$$

Where:

$[F]$ = matrix of $\frac{\partial v(z)_i}{\partial X_i}\frac{X_i^n}{v(z)_i^n}$ elements (sensitivity matrix)

$\{\beta\}$ = matrix of $\frac{\Delta X_i^n}{X_i^n}$ elements (change vector)

$[\underline{r}]$ = matrix of $\frac{\Delta v(z)_i^n}{v(z)_i^n}$ elements (residual vector)

The number of recorded voltage points from the TDR trace determines the number of rows in matrices $[F]$ and $[\underline{r}]$; where the number rows in $\{\beta\}$ and the number of columns in $[F]$ depends on the number of unknowns. Solving for $\{\beta\}$:

$$\{\beta\} = \left[F^T F\right]^{-1}\left[F^T\right][\underline{r}] \tag{24}$$

By minimizing the $\{\beta\}$ matrix, solutions for X_i^n (i.e., conductivity (σ), dielectric constant (ε), and the reflection coefficient (Γ)) are found. The minimization of error contained within the residual matrix $[\underline{r}]$ is analogous to the minimization or reduction of error employed in least squared error analysis as elaborated in appendix B. Another type of systematic error is reduced by the method of allocation inherent in the use of the SID approach. The squared error between the actual measurement and the predicted measurement (residual matrix $[\underline{r}]$) is calculated by using the physically correct model of a mixture dielectric to determine the sensitivity of the weighting coefficients for allocating the squared error. It is possible to adjust the model coefficients until there is no squared error remaining. However, because of the presence of random error (i.e., measurement

error in the TDR device), the values of the residual matrix $[\underline{r}]$ should not be forced to zero.

Furthermore, the size of the random errors should be determined by statistical evaluation of repeated TDR measurements that are not presently available. Inherent in this analysis are the minimum number of points (N) from the TDR trace that should be used to provide a reasonably accurate estimate of the dielectric constant. Accordingly, this analysis suggests that using twice as many data points as the number of coefficients to be computed (which would be 6 in this case) would be sufficient in estimated dielectric constant, conductivity, and reflectivity assuming a measurement error of 3 percent in the TDR voltage trace. In this regard, the six points would be selected between the first and second inflection points, where the first and second inflection points are points 1 and 6, respectively, and the other four points were equally distributed between the inflection points.

This approach was used only for the calibration process (step 2) to characterize the manual TDR traces obtained from the installation reports. In the computational program, which was developed for the new approach, all data points between the inflection points were used to determine the dielectric constant because the data are readily available in the automated TDR trace format, allowing the program to interpret a large number of points relatively quickly.

DETERMINATION AND CALIBRATION OF SOIL COMPONENT DIELECTRIC CONSTANTS (STEP 2)

The VMC is currently estimated in the MOISTER program from the measured dielectric constant using regression-type equations 8 or 9. It is suggested from literature that a more fundamental approach would account for the effect of individual constituent soil dielectrics on the moisture content.[12] In this regard, a theory of dielectric properties of composite materials from a micromechanics/self consistent scheme yields a general expression for the composite dielectric constant (ε-for a 2-phase system):[13]

$$v_1\left[\frac{\varepsilon_1-\varepsilon}{\varepsilon_1+2\varepsilon}\right]+v_2\left[\frac{\varepsilon_2-\varepsilon}{\varepsilon_2+2\varepsilon}\right]=0 \qquad (25)$$

Where:

ε_1 = dielectric constant for phase 1
ε_2 = dielectric constant for phase 2
v_1 = volume fraction of phase 1
v_2 = volume fraction of phase 2

The justification for a self-consistent scheme lies in the volume fractional bounds or limits in which the computed VMC fall. In other words, the computed moisture contents (based on equation 28 below) are consistent with bounded values of dielectric constants of the individual phases and their volume fractions. The upper (+) and lower (-) dielectric expressions, illustrated in figure 8, are as follows:

$$\varepsilon_{-} = \varepsilon_1 + \frac{v_2}{\frac{1}{\varepsilon_2 - \varepsilon_1} - \frac{v_1}{2\varepsilon_1}} \tag{26}$$

$$\varepsilon_{+} = \varepsilon_2 + \frac{v_1}{\frac{1}{\varepsilon_2 - \varepsilon_1} - \frac{v_2}{2\varepsilon_2}} \tag{27}$$

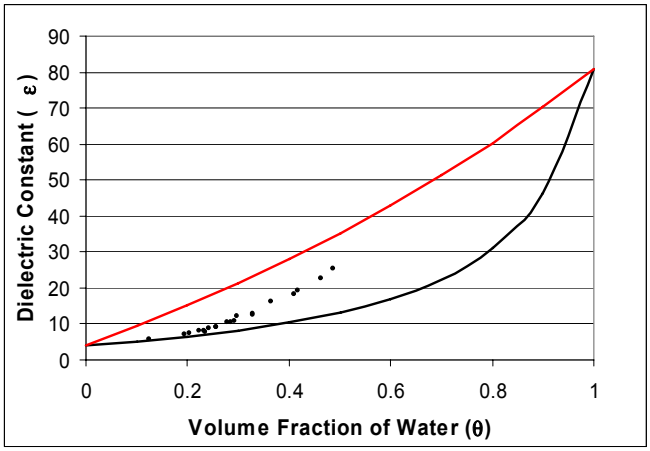

Figure 8. Graph. Bounding of dielectric constant as a function of the computed volumetric moisture content (θ) using equation 28.

Using this concept, an expression can be written based on equation 25 for a three-phase system (air, water, and solids—such as in a soil material):

$$\frac{\gamma_d}{G_s \gamma_w}\frac{\varepsilon_1 - \varepsilon}{\varepsilon_1 + 2\varepsilon} + \theta\frac{\varepsilon_2 - \varepsilon}{\varepsilon_2 + 2\varepsilon} + \left(1 - \frac{\gamma_d}{G_s \gamma_w} - \theta\right)\frac{\varepsilon_3 - \varepsilon}{\varepsilon_3 + 2\varepsilon} = 0 \tag{28}$$

Where:

γ_d = dry density of soil, g/cm^3
Gs = specific gravity of soil
γ_w = density of water, g/cm^3
ε_1 = dielectric constant of solids
ε_2 = dielectric constant of water
ε_3 = dielectric constant of air (= 1)
ε = dielectric constant of the soil determined from step 1
θ = ratio of soil fraction

With a value for ε determined from the SID analysis of a TDR trace, values of ε_1, ε_2, and G_s of the model are adjusted based on the ground truth data of measured values of γ_d and θ. The dielectric constants of the water (ε_2) and the soil solids (ε_1) can be found by applying the SID approach to equation 28. Typical values of ε_1 range between 3 and 5 while typical values of G_s range between 2.6 and 2.9. Using this approach, analysis results of selected TDR traces are shown in tables 6 and 7. Computations of the dielectric constant based on the apparent length method are headed by the notation of "L_a" while the proposed determinations made by the new approach are noted by the heading "new." The calibration shown in table 7 also includes the G_s parameter.

Table 6. Comparison of volumetric moisture contents during TDR installation.*

Section/ TDR #	Soil Type	Dry Density (g/cm3)	Soil Dielectric		Volumetric Moisture Contents (%)			
			L_a	New	Field Measured	MOISTER Program		Micro-mechanics Method
364018/9	Gravel	2.24	9.83	10.04	26.12	17.33	Coarse-K_a	25.71
091803/4	Sand	2.26	14.02	14.33	33.28	22.71	Coarse-K_a	32.92
131031/8	Silt	1.80	12.16	18.40	40.75	20.53	Coarse-K_a	39.86
421606/6	Clay	1.94	7.34	5.76	19.01	17.57	Fine-K_a	18.75

* All information used was obtained from Installation Reports.

Table 7. Calibrated and calculated values determined by micromechanics method.

Section	Dielectric Constant			Specific Gravity (Gs)
	Soil (ε_1)	Water (ε_2)	Air (ε_3)	
364018	3.70	79.7	1.0	2.70
091803	3.65	80.4	1.0	2.74
131031	3.47	79.9	1.0	2.77
421606	3.38	80.0	1.0	2.78

FORWARD COMPUTATION OF WATER CONTENT AND DRY DENSITY (STEP 3)

In the forward calculation of volumetric water content and dry density that is performed in step 3, the self-consistent model in equation 28 is used together with the calibration constants ε_1, ε_2, and G_s to determine the new values of γ_d and θ from values of the dielectric constant for the soil mixture derived from subsequent TDR data collection records. These new dielectric values are determined by analysis of the TDR traces obtained at different times throughout the monitoring period. Thus, once particular soil characteristics ε_1, ε_2, and G_s are "identified" by step 2, all future calculations of γ_d and θ can be determined from the SID in step 3 using a new soil mixture dielectric constant measured in step 1. Along with the calculation of γ_d and θ, the volume relationship of degree of saturation (S), porosity (n), and void ratio (e) can be redefined from step 3:

$$S = \frac{\theta}{1 - \frac{\gamma_d}{G_s \gamma_w}} = \frac{\theta}{n} \tag{29}$$

$$n = 1 - \frac{\gamma_d}{G_s \gamma_w} \tag{30}$$

$$e = \frac{n}{1 - n} \tag{31}$$

It is important to note that two additional sources of systematic error are countered in this approach. First, the three-phase model accounts for the dielectric effect of the air in the soil. Additionally, dry unit weights are obtained from each TDR trace and not assumed to be constant over time.

VALIDATION

The new procedures' effectiveness was analyzed by comparing the moisture content computed both from the MOISTER program and the micromechanics method to laboratory moisture content tests from representative SMP sites. Ground truth data that are linked to specific TDR traces for SMP soils were identified from three sources.

1. Calibration validation – Data captured during the equipment installation at the SMP sites. As part of this process, in situ soil samples were matched to the TDR installation location and tested for moisture content. These data were used in the calibration process previously described.

2. Laboratory validation – Data obtained from Klemunes' [5] study of collecting TDR data in a laboratory setting where soil moisture content and density are known.

3. Field validation – Available information from sites in which forensic evaluations were performed. TDR traces were taken in the field just prior to removal of the equipment and soil sampling.

All three of these sources provide important reference moisture contents to evaluate the capabilities of the micromechanics model. These sources provided the only data available to conduct validation specific to the LTPP equipment and protocols.

The first validation consisted of comparing the moisture content from the laboratory tests in various installation reports to that indicated by the MOISTER program and the micromechanics method. This was presented as part of the calibration process and in table 6. Figure 9 further demonstrates how the calibration of the micromechanics method provides accurate estimates of the ground truth data. While promising, it was necessary to verify the accuracy of the methodology against both laboratory and field data to establish confidence in the micromechanics method.

A second verification effort consisted of computing the moisture content and dry density for the test data noted in Klemunes' thesis work.[5] Data from four of the 28 SMP sections used in the study were selected to provide a range of soil types (i.e., gravel, sand, silt, and clay). For each SMP section, one TDR trace obtained during installation (and corresponding moisture content/dry density) was used to calibrate the micromechanics model. Calibration information relative to the soil and water dielectric constants can be found in table 8. Using this information and the TDR traces obtained at different moisture contents, estimates of moisture content and dry densities were computed and can be found in table 9 along with estimates from the MOISTER program and the laboratory test results. Figure 10 provides the associated difference of each method for all trials. As can be seen, the micromechanics method provides relatively accurate estimates of actual moisture conditions with the majority of estimates falling within 5 percent of the laboratory derived data. Given the circumstances surrounding the collection of the different types of moisture data involved in this analysis, the degree of comparability is remarkable. The evaluation of estimated dry densities was performed through a comparison to measured values obtained from laboratory testing. Figure 11 shows the relatively high capability and accuracy of the micromechanics model in estimating dry density with a maximum resulting difference of less than 6 percent. This verification was considered to be laboratory verification as the soil mixtures and TDR traces were obtained in a laboratory setting where the sampling and data collection were more controlled.

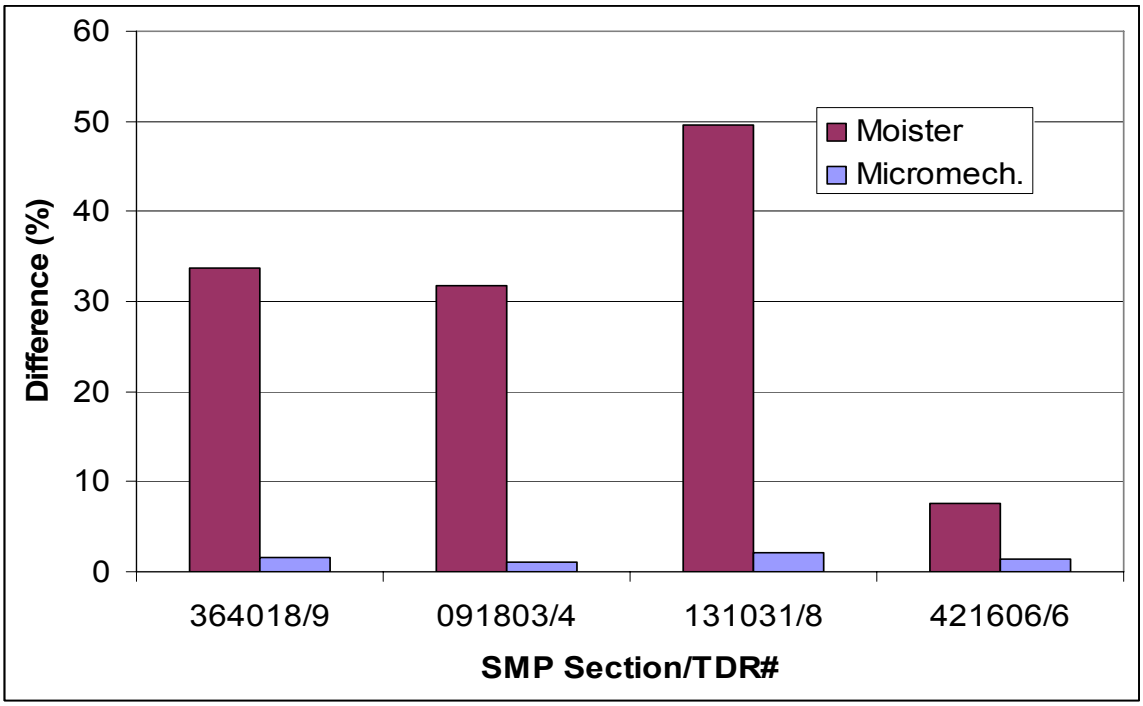

Figure 9. Bar Chart. Errors in volumetric moisture content estimates (calibration validation).

Table 8. Calibration of dielectric constants by transmission line equation.

Section	Soil Type	Spec. Gravity	Dry Density (g/cm^3)	Dielectric Constant		Volumetric Moisture Content (%)
				Soil (ε_1)	Water (ε_2)	
271028	Gravel	2.724	2.017	3.79	80.6	7.06
231026	Sand	2.782	1.960	3.79	80.0	19.35
091803	Silt	2.864	2.264	3.89	81.0	20.38
081053	Clay	2.890	1.634	3.79	80.0	21.57

Table 9. Comparison of moisture contents (continued on next page).

Section		Soil Type	Dry Density (g/cm^3)		Volumetric Moisture Contents (%)			
			Lab.	M.M.[1]	Ground Truth (Lab Result)	Moister Program (3rd Polynomial Equation)		M.M.[1]
271028	C	Gravel	1.730	1.810	7.09	9.36	Coarse-K_a	7.79
	F		1.712	1.700	12.50	13.92	Coarse-K_a	12.17

Section		Soil Type	Dry Density (g/cm^3)		Volumetric Moisture Contents (%)			
			Lab.	M.M.[1]	Ground Truth (Lab Result)	Moister Program (3rd Polynomial Equation)		M.M.[1]
	K		1.766	1.869	18.98	20.06	Coarse-K_a	19.78
231026	B	Sand	1.574	1.558	14.88	15.40	Coarse-K_a	14.25
	F		1.635	1.610	22.98	21.78	Coarse-K_a	21.95
	M		1.605	1.569	7.54	8.34	Coarse-K_a	7.18
091803	C	Silt	0.976	0.989	38.45	29.63	Fine-K_a	38.05
	I		0.965	0.924	27.12	21.01	Fine-K_a	28.07
	P		0.965	0.927	29.65	20.48	Fine-K_a	28.94
	W		0.973	0.923	39.30	32.35	Fine-K_a	38.16
081053	G	Clay	1.406	1.350	44.07	51.80	Fine-Gradation	44.81
	K		1.40	1.321	48.83	51.80	Fine-Gradation	48.03
	U		1.377	1.440	30.72	29.67	Fine-Gradation	31.29

[1]Micromechanics method.

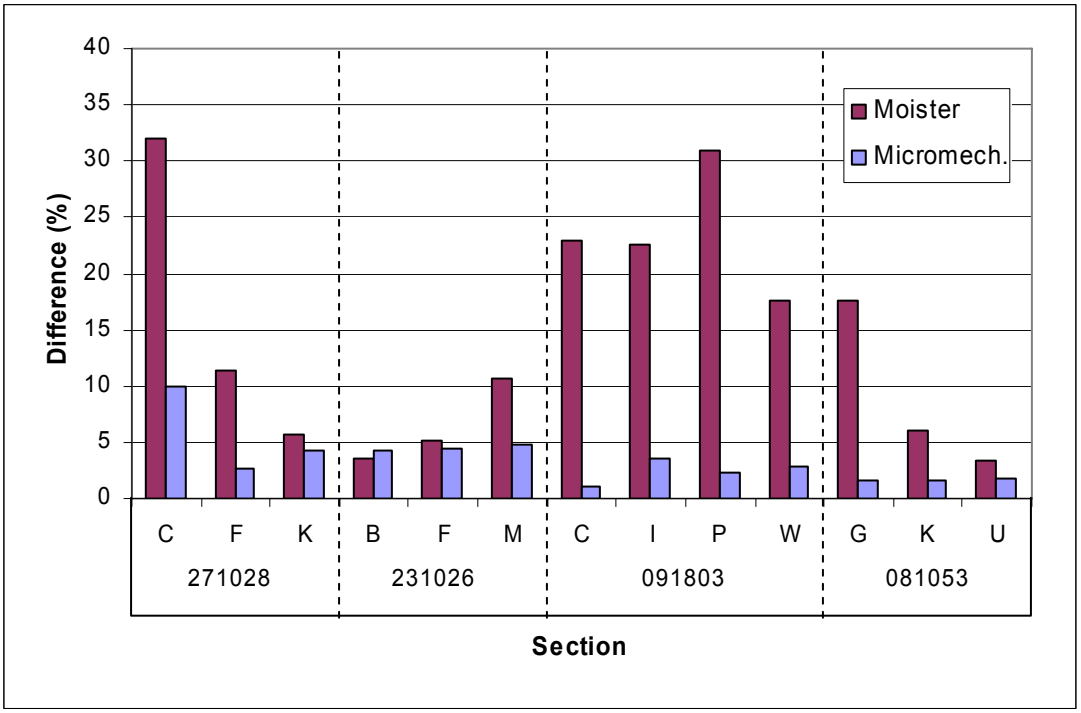

Figure 10. Bar Chart. Errors of volumetric moisture contents on ground truth data (laboratory validation).

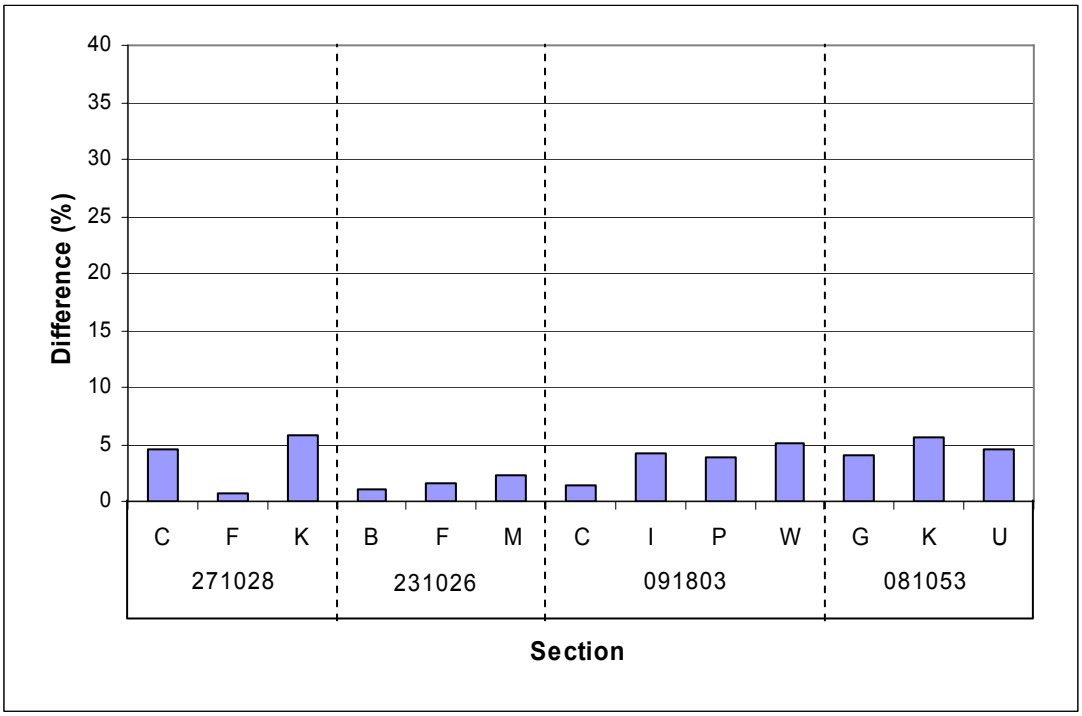

Figure 11. Bar Chart. Errors of laboratory estimated dry density on ground truth data (laboratory validation).

A third evaluation was performed using the data being developed for the forensic report on LTPP-SMP site 091803. In this case, the micromechanics method was calibrated using the laboratory moisture content obtained during the equipment installation as shown in table 10. The calibrated model was used to estimate moisture content based on the TDR traces obtained during the forensic investigation. These resulting moisture estimates were compared to the laboratory test results for samples taken just after the TDR traces were obtained during the forensic activities. Those test comparisons can be seen in table 11 with the resulting difference quantities in figure 12. In general, error of the micromechanics method is very low and is under 5 percent for all but one scenario. The values of dry density estimated by the new approach were evaluated by comparing them to measured values. As shown in figure 13, the resulting differences on measured values were slightly greater than for the laboratory verification but still highly accurate at less than 7 percent.

Table 10. Calibration of dielectric constants for Section 091803.

Layer Type	Specific Gravity	Dry Density (g/cm^3)	Dielectric Constant		Volumetric Moisture Content (%)
			Soil (ε_1)	Water (ε_2)	
Base	2.44	2.255	3.69	79.8	25.71
Subbase	2.74	2.260	3.65	80.4	32.92

Table 11. Comparison of moisture contents for Section 091803.

Layer Type		TDR No.	Depth (mm)	Dry Density (g/cm^3)		Volumetric Moisture Content (%)			
				Field	M.M.[2]	Ground Truth	Moister Program		M.M.[2]
Base	Medium brown gravel	1	330	2.229	2.297	17.39	20.69	Coarse-K_a	16.25
		2	437	2.255	N/A[1]	15.81	N/A[1]	-	N/A[1]
Subbase	Grayish brown silty gravel with large rock	3	584	2.163	2.243	27.94	26.96	Coarse-K_a	26.75
		4	737	2.163	2.293	26.00	22.54	Coarse-K_a	26.34
		5	889	2.166	2.021	19.82	22.54	Coarse-K_a	19.19
		6	1041	2.192	2.343	16.80	20.69	Coarse-K_a	17.11
		7	1194	2.192	2.196	20.75	21.25	Coarse-K_a	21.67
		8	1346	2.091	1.988	25.76	25.94	Coarse-K_a	25.57

[1]Impossible to interpret TDR trace.
[2]Micromechanics method.

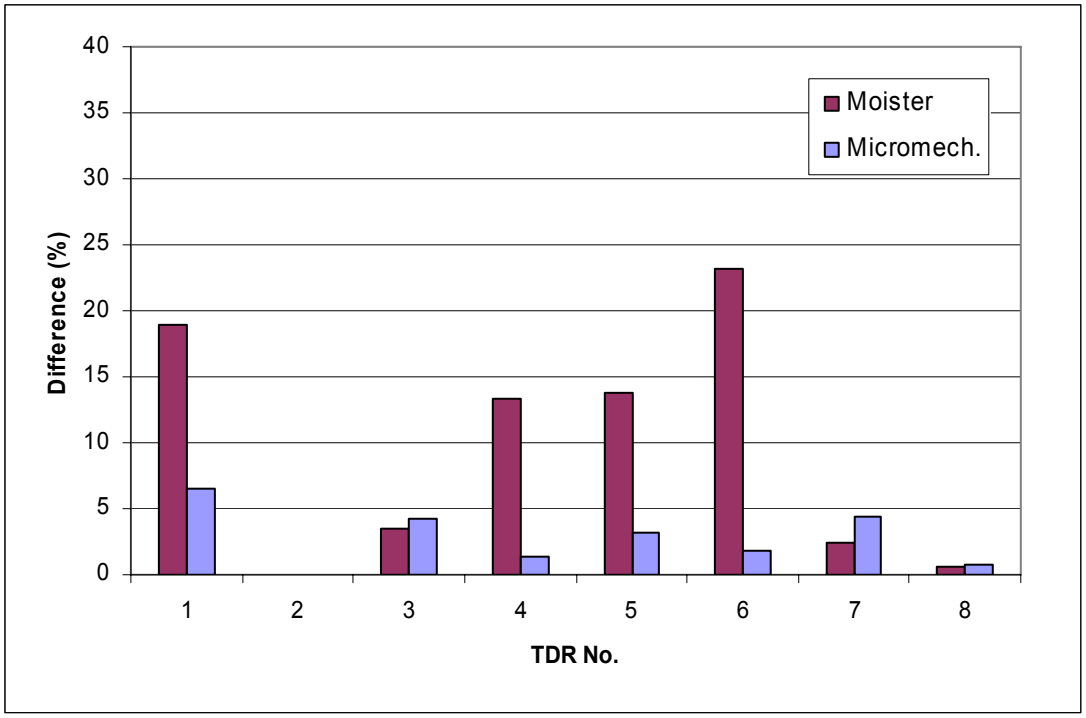

Figure 12. Bar Chart. Errors of volumetric moisture contents on ground truth data (field validation).

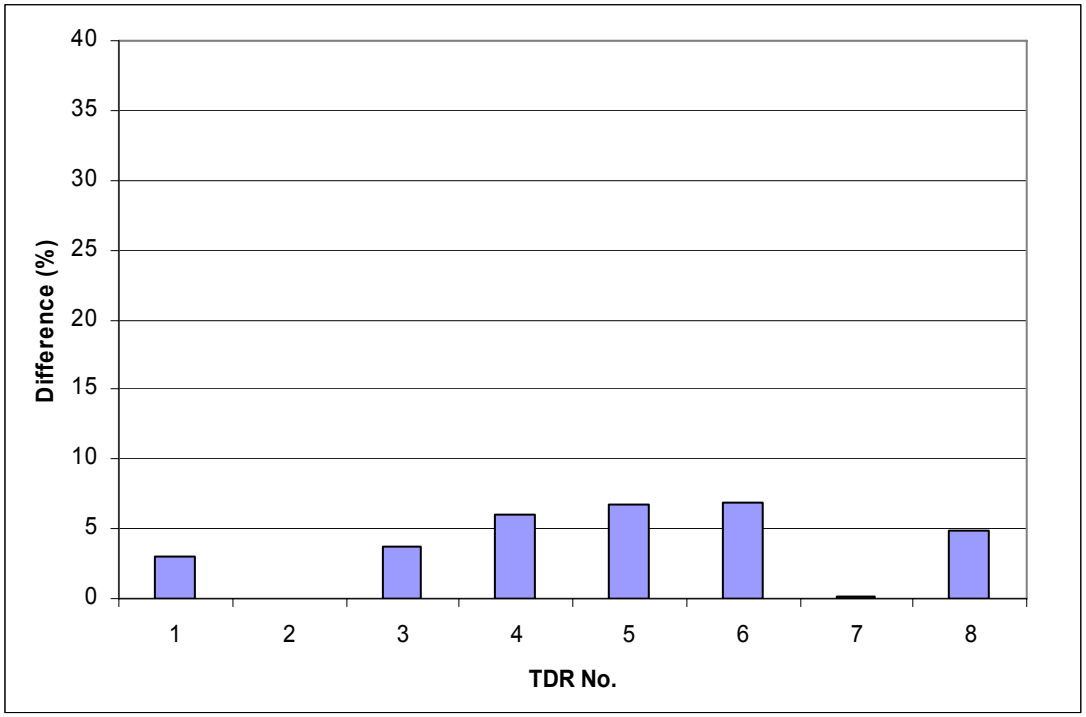

Figure 13. Bar Chart. Errors of estimated dry density on ground truth data (field validation).

Through these three validation exercises, it was found that the micromechanics method is capable of predicting accurate moisture and density results. The largest variation between estimates from the micromechanics method and the measured values was under 10 percent with the vast majority falling under 5 percent.

Based on the results of this evaluation, it was proposed that the micromechanics method be used to compute moisture estimates for all interpretable TDR data in the LTPP database. This approach was approved by FHWA. Developing a computer program and methodologies necessary for computing and reviewing parameters for the LTPP database is described in the next chapter.

CHAPTER 4. COMPUTER PROGRAM DEVELOPMENT

As a part of the study, a computational program was developed to interpret TDR traces and estimate dry density and moisture content using the TLE and micromechanics models. Due to the large differences between the former and current approaches, a new computational program named LTPP MicroMoist was developed to facilitate proper interpretation of the collected traces. However, some of the programming from the MOISTER program was utilized in developing the new program. Much of the appearance and graphical viewing features in the LTPP MicroMoist program were copied from the source code of the MOISTER program.

OVERVIEW OF THE LTPP MICROMOIST PROGRAM

The program was designed to automate the interpretation process with consideration given to certain user input data to ensure the highest quality end product. The program generates output database tables that store data to be uploaded into the LTPP database. The tables can also be used to review data as part of QC processes. Figure 14 shows the main display screen of the new program. A summary of the procedures in the new program can be found in table 12. The user's manual for the program can be found in appendix C.

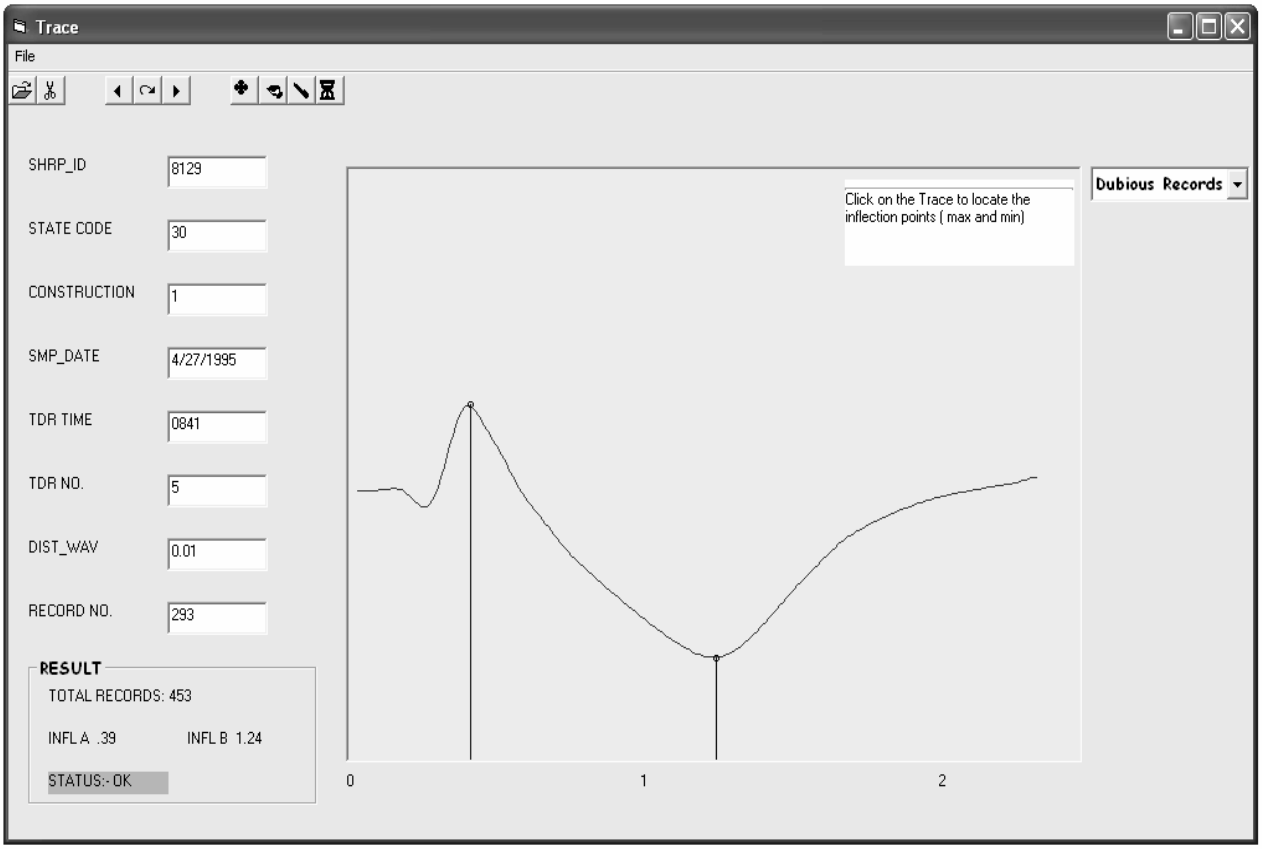

Figure 14. Photo. Interface of new program.

Table 12. Overview of LTPP MicroMoist program.

Procedures	MicroMoist program
Determination of inflection points	Local maxima/minima located and used as beginning/ending points for the range of data to be analyzed.
Calculation of dielectric constant	Transmission line equation (function of dielectric constant, conductivity, and reflectivity of the soil composite)
Calculation of moisture content	Micromechanics/self consistent model (calibrated to site-specific conditions using installation data)
Calculation of dry density	Micromechanics/self consistent model (calibrated to site-specific conditions using installation data)
Input table	SMP_TDR_AUTO SMP_TDR_DEPTHS_LENGTH SMP_TDR_CALIBRATE (developed from TDR traces and moisture contents acquired during installation)
Output table	SMP_TDR_AUTO_DIELECTRIC SMP_TDR_MOISTURES

PROGRAM ALGORITHM

The program logic flow consists of three parts: (1) determination of the TDR trace inflection points, (2) calculation of the soil dielectric constant, and (3) computation of the soil moisture content and dry density. These steps are automatically performed with logical checks and user input incorporated, where applicable.

Inflection Point Determination

A local peak in the TDR trace is created as the electromagnetic wave enters the TDR probe. From this point, the trace falls to a local minimum point and then rebounds upward at a lower rate as the wave hits the end of the probe. Figure 15 depicts the inflection points on TDR traces. The descending portion of the trace represents the waveform at the TDR sensor. This is the portion of the trace that is of interest for soil parameter computation because it represents the characteristics of the in situ soil. Therefore, the inflection points were used to identify the limits for the range of points in the TLE.

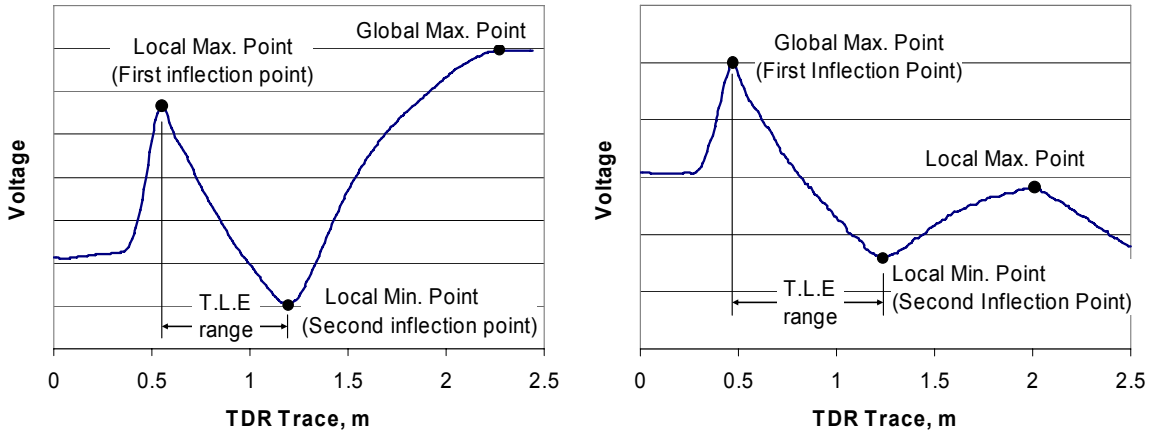

Figure 15. Graph. Inflection points in TDR trace.

The inflection points are determined by the program using a step-wise routine. Depending on the distance between wave points, which usually is 0.01 m but can be 0.02 m, the local maxima search routine is limited to the left portion of the trace. A complete TDR trace consists of 245 data points. For traces with a wave point distance of 0.01 m, the maxima search routine is limited to the first 200 data points. For traces with a wave point spacing of 0.02 m, the maxima search routine only involves the first 100 data points. By doing this, the program reduces the number of iterations and accelerates the process without reducing the utility of the program.

This step-wise iteration consists of the following steps:

1. Identify the global maximum point (P_i) within the probable range (i.e., first 200 or 100 data points as defined above).
2. Find the local maximum point by starting from P_i and comparing it with the three points before and after P_i.
    a. If the point is smaller than one of six points, change to the point to the left (p_{i-1}) and compare again. Continue until the condition in b. below is satisfied.
    b. If the point is larger than all six points, identify the point as the first inflection point.
    c. As in the TDR trace in figure 15 (b), when a local maximum point is not found even though the changes and comparisons are carried on up to first data point (p_1), the global maximum point is identified as the first inflection point.
3. Find the local minimum point (second inflection point) by a routine similar to step 2.
    a. Run the routine from the point to the right of the established first inflection point, as the second inflection point is on the right side of the first in the TDR trace.

4. Flag the TDR trace if the program cannot find the local maximum or minimum point (i.e., uninterpretable trace).

Along with the determination of the inflection points, the above routine helps to locate records without a negative slope. Where both points fall at the same location or the magnitude of the second point is higher than that of first point, the trace is deemed to have a positive slope between inflection points. These cases may indicate that the traces were taken in frozen soil and are flagged as suspect records. Additionally, the program allows the user to review each trace and manually adjust the inflection point locations, if necessary. Figure 16 illustrates the flow chart of the inflection point determination.

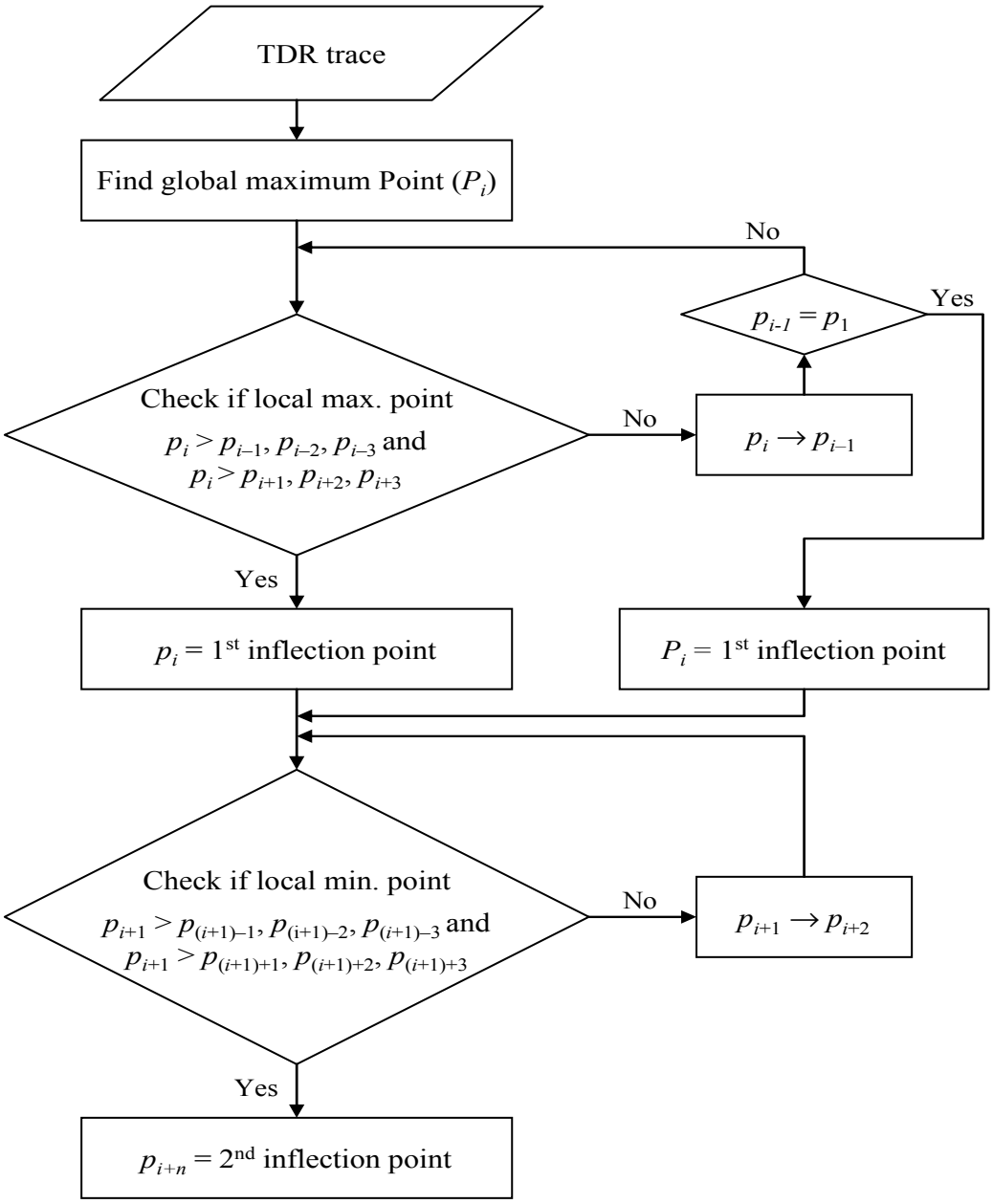

Figure 16. Flowchart. Determination of inflection points.

Calculation of Dielectric Constant, Reflectivity, and Conductivity

Once the inflection points are determined, the program calculates the dielectric constant, conductivity, and reflectivity using the TLE and the SID solution method previously defined. The calculation is conducted based on fitting the measured voltage trace between the inflection points using the iteration process described in chapter 3. While six points from the installation TDR traces were used in the calibration process, all data points between the inflection points were used in the MicroMoist program to determine the dielectric constant. The program calculates the dielectric constant, conductivity, and reflectivity using the automated TDR traces acquired from the LTPP Information Management System (IMS) database. By using all of the data points, the accuracy of the TDR interpretation is improved. The calculation process involves the following steps:

1. Provide initial estimates of dielectric constant, reflectivity, and conductivity as well as the range of acceptable variation.
    a. Equation 5 is used to determine the initial value of the dielectric constant. It serves as an initial estimate and reduces the number of iterations to convergence. The soil dielectric constant ranges between 1 and 85 and is increased or decreased by a constant factor after each iteration. This factor is determined by the change vector (β-matrix) generated from the SID method.
    b. Reflectivity is assigned at 0.1 as an initial value but can vary between -1 and 1. Within the SID iteration, the reflectivity varies by a factor similar to the dielectric constant and is dependent on the change vector.
    c. Conductivity is assigned a value of 0.5 initially, but the range is not fixed. The adjustment factor applied to the conductivity is a function of the change vector.

2. Calculate the parameters based on the SID method.
    a. The change vector, consisting of a 3 by 1 matrix, is determined based on the algorithm implemented in the program. The SID method calculates the relative voltage based on the assumed parameters and then compares it with the measured relative voltage obtained from the trace. The change vector is the measure of variation between each parameter.
    b. This calculation process is contained within a loop that terminates when all elements of the change vector are less than 1.0 percent.

These steps are implemented for each trace, and the values of dielectric constant, reflectivity, and conductivity are stored in the SMP_TDR_AUTO_DIELECTRIC table. The dielectric constant value is then used to calculate moisture content and dry density.

The constants used to compute the dielectric constant are the voltage and relative distance, the magnetic permeability of free space, and the electric permittivity of free space. While the voltage and relative distance are obtained from the TDR trace, the magnetic permeability and electric permittivity values are fixed values, which are $4\pi \times 10^{-7}$ H/m and $1/36\pi \times 10^{-9}$ F/m, respectively. Therefore, users do not need to change any constants

for the computation of the dielectric constant in the program. Figure 17 illustrates this calculation procedure.

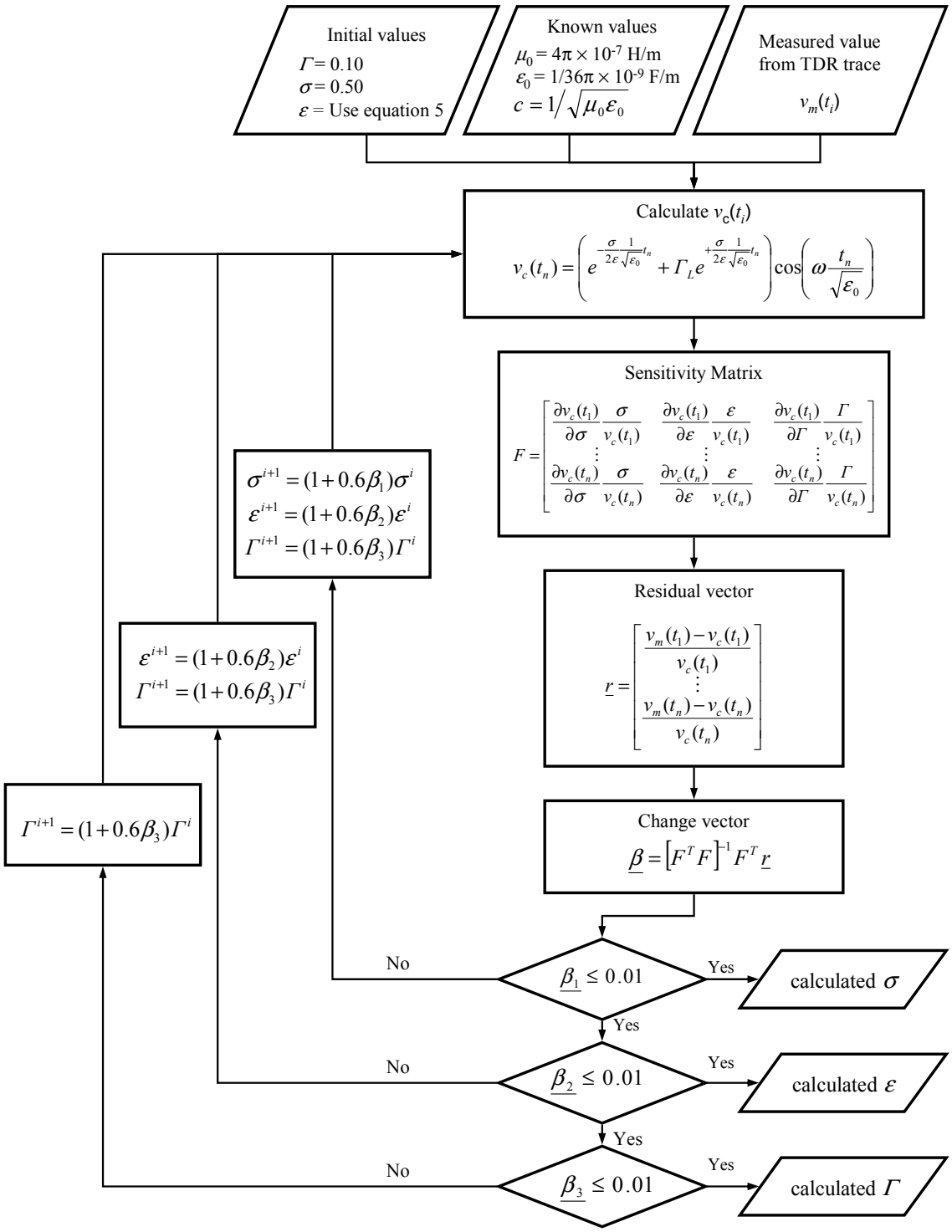

Figure 17. Flowchart. Calculation of dielectric constant, conductivity, and reflectivity.

Calculation of Moisture Content and Dry Density

Moisture content and dry density are calculated based on the micromechanics and self consistent models previously described. The ε_1, ε_2, and G_s parameters in these models are calibrated to site-specific conditions based on TDR traces and moisture content testing performed during installation. The dielectric constant of the soil, determined from the SID iteration process, is also an input into the model. The following routine was used for this calculation in the program:

1. Assign initial values to the unknown parameters of dry density and VMC. Each TDR location has dry density and VMC data measured during the installation process, which are stored in the calibration table. These values are used as seed values for the SID method to calculate the dry density and VMC.

2. Calculate the dry density and moisture content based on the SID method.
    a. The algorithm implemented in the program is a loop system which calculates ε_c using the inputted parameters and then compares it with ε_m. The following equation is used to calculate ε_c:

$$\frac{\gamma_d}{G_s\gamma_w}\frac{\varepsilon_1-\varepsilon_c}{\varepsilon_1+2\varepsilon_c}+\theta\frac{\varepsilon_2-\varepsilon_c}{\varepsilon_2+2\varepsilon_c}+\left(1-\frac{\gamma_d}{G_s\gamma_w}-\theta\right)\frac{\varepsilon_3-\varepsilon_c}{\varepsilon_3+2\varepsilon_c}=0 \qquad (32)$$

    b. The change vector (2×1 matrix) is the measure of variation in dry density and moisture content calculated from ε_c and the inputted parameters.
    c. Once the variation is less than 1 percent, the loop terminates and the values of dry density and moisture content are reported.

The VMC and dry density calculated from the above procedure are presented in the output table, MICROMOIST_SMP_TDR_MOISTURES, and are also used to compute the gravimetric moisture contents.

In this step, the calibrated dielectric constants of solid and water as well as the specific gravity are used as constants. The density of water and the dielectric constant of air are also needed, but they are fixed as 1.0 g/cm^3 and 1.0, respectively. In the micromechanics method, the physical properties of the TDR probe, such as length of TDR, are not considered in the computation process. Therefore, the program can be used to interpret other types of TDR probes as long as calibration data are available. Figure 18 illustrates the procedure for calculating the dry density and moisture content values.

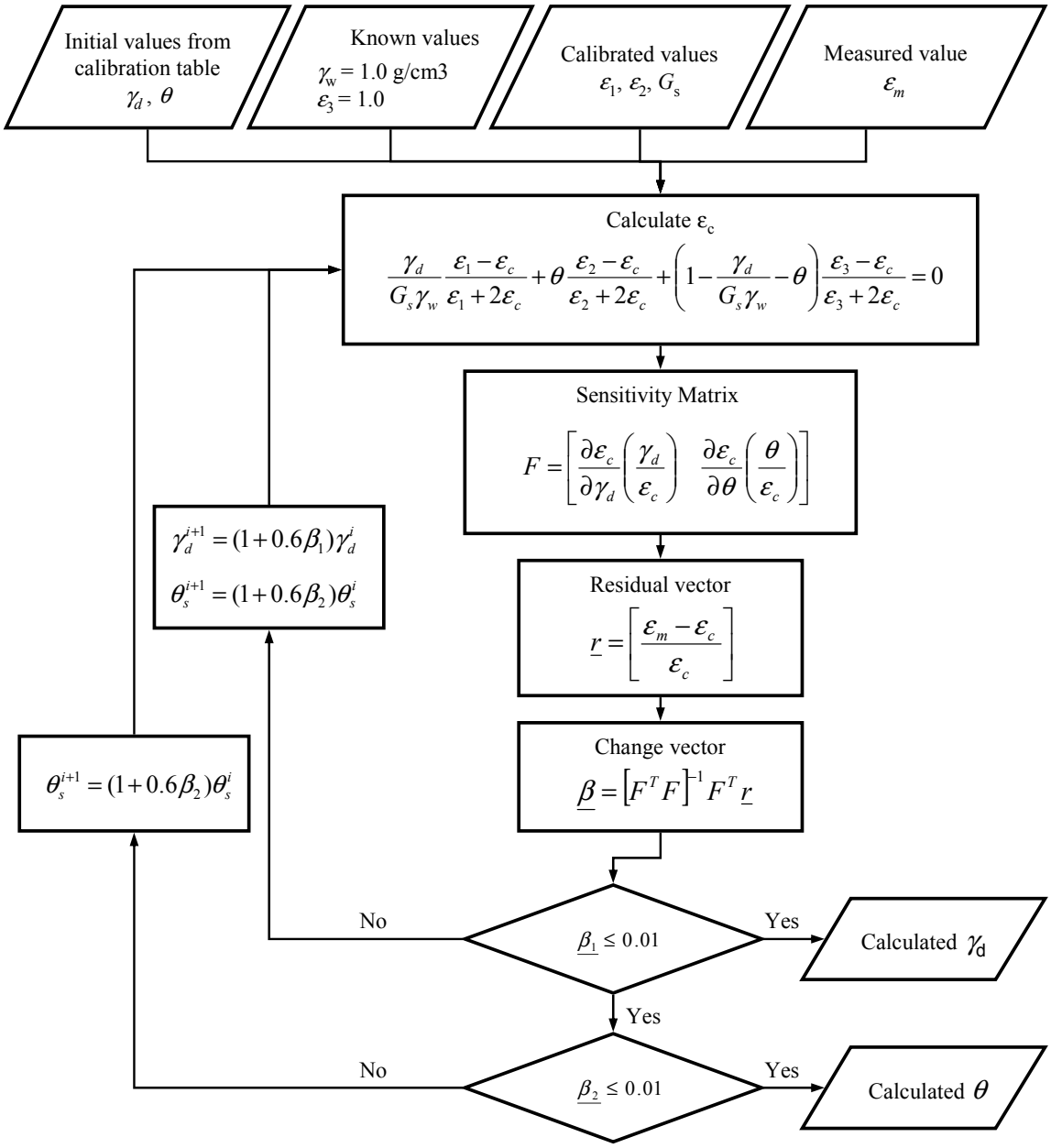

Figure 18. Flowchart. Calculation of moisture content and dry density.

DEVELOPMENT OF THE CALIBRATION TABLE

In order to calculate the moisture content and dry density using the new approach, the program requires the following calibration values for each SMP site and each layer:

- Dielectric constant of solids (ε_1)
- Dielectric constant of water (ε_2)
- Dielectric constant of air (ε_3)
- Specific gravity (Gs)

These values are calibrated using the ground truth data obtained from the LTPP SMP Site Installation and Initial Data Collection reports for each SMP test section. [2] The ground truth data consisted of measured moisture content and manual TDR traces recorded during the installation process as well as dry density values available in the LTPP database. This calibration data are stored in the MICROMOIST_SMP_TDR_ CALIBRATE table.

Calculation of Dielectric Data from Manual TDR Traces

The manual trace taken during installation is used to determine dielectric constant of the soil using the TLE and routine. This dielectric constant is used in the micromechanics equation to determine moisture content and dry density. The micro-mechanics equation is calibrated to each site and layer by adjusting the dielectric constant of solids, dielectric constant of water, and the specific gravity. Adjustments are made to these parameters so that the predicted moisture content and dry density (from manual TDR traces) are equivalent to the measured ground truth moisture content (taken at installation) and the measured ground truth dry density (reported in the LTPP database).

The adjusted values for dielectric of solids, dielectric of water, and specific gravity are then used for subsequent moisture and density estimates for the site/layer combination. In essence, the micromechanics model is calibrated to every site/layer combination before it is used to generate moisture estimates for subsequent TDR traces.

Because the TDR traces obtained during installation were measured manually, they required digitization to obtain actual data points for use in the routine. Data Thief III was used to digitize the manual TDR traces into engineering data points. [14] The digitized TDR trace provided easily identifiable data points including the inflection data points in which to calculate the dielectrics. Figure 19 shows an example of a manually measured TDR trace and its corresponding digitized TDR trace.

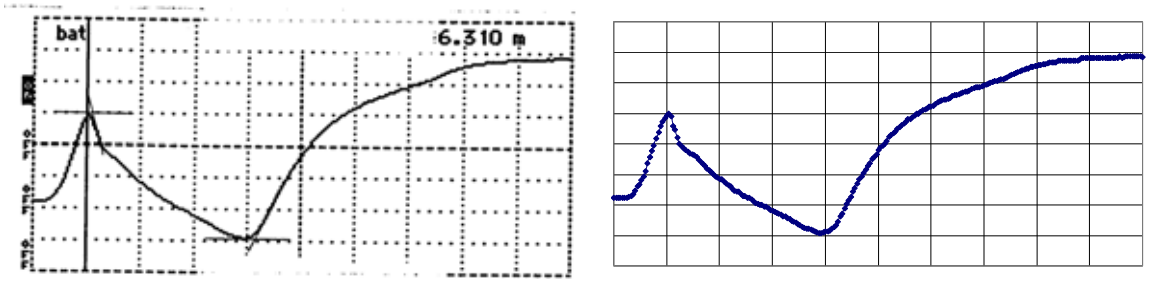

(a) Manually measured trace (b) Digitized trace

Figure 19. Graph. TDR traces of Section 308129, TDR No. 8.

Based on the digitized data points, the dielectric constant, conductivity, and reflectivity were calculated using the TLE and the SID method.

Sources of Ground Truth Dry Density and Moisture Content

To calibrate the dielectric contents of soil components and specific gravity, the measured dry density and VMC were required at each TDR location for all the SMP sites.

Moisture content measured during installation was reported in the SMP Installation Reports and was given in terms of gravimetric moisture content. Equation 18 was used to convert the gravimetric values to VMC for use in the calibration process.

Because in situ dry density data was not always available from the SMP Installation Reports, information was taken from multiple locations within the LTPP database. The following sources were queried to acquire the information:

- SMP Installation Report (priority 1)
- SMP Installation Report – I07 form (priority 2)
- SMP Installation Report – S04 form (priority 3)
- SMP Installation Report – I05 form (priority 4)
- LTPP database table TST_ISD_MOIST (priority 4)
- LTPP database table TST _SS08 (priority 5)
- LTPP database table INV_SUBGRADE (priority 6)
- Appendix C of "Analysis of Time Domain Reflectometry Data From LTPP Seasonal Monitoring Program Test Sections – Final Report" [1] (priority 7)

The dry density of the highest priority source was used if more than one source provided dry density information. [7] Additionally, these dry densities were adjusted based on depth, as described in the following section.

Adjustment of Dry Density

Although the in situ gravimetric moisture contents were measured for each TDR depth, only a single dry density was reported for each layer type. It is known that dry density is influenced by the depth below the surface. Therefore, adjustments to the reported dry density values were required to reflect conditions at each TDR depth. Additionally, it was observed that dry densities and measured moisture contents resulted in unreasonable phase diagram volumetrics. In these cases, adjustments were made to correct for negative air voids in the soil. The following procedure was followed to adjust the reported dry densities:

Step 1. Soil Component Volume and Porosity Calculation

Using the measured gravimetric moisture content and reported dry density, the volume of each component and porosity of soil was calculated using equations 32, 34, and 35.

$$\theta_w = w\frac{\gamma_d}{\gamma_w} \tag{33}$$

$$\theta_s = \frac{\gamma_d}{G_s \gamma_w} \tag{34}$$

$$\theta_a = 1 - \theta_w - \theta_s \tag{35}$$

Where:

θ_w = volumetric moisture content (%)
θ_s = volumetric solid content (%)
θ_a = volumetric air content (%)

Porosity, defined in figure 20, can be calculated as:

$$n = 1 - \theta_s = 1 - \frac{\gamma_d}{G_s \gamma_w} \tag{36}$$

Where:

n = porosity of soil

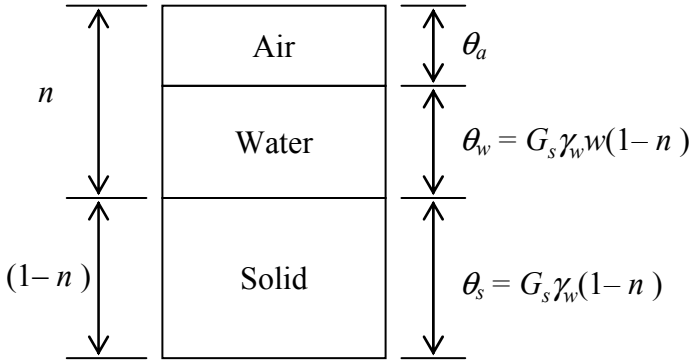

Figure 20. Diagram. Three separate phases of a soil element.

Step 2. Adjust Porosities, Densities, Volumes of Soil Components Based on Depth

Each layer has a single porosity, but due to the assumption that dry density varies as a function of depth, the values of porosity will also vary accordingly within each layer. Therefore, all porosities were adjusted based on vertical location using the following equation.

$$n_i' = n_i\left(1 - 0.1\frac{z_i}{Z_0}\right) \tag{37}$$

Where:

i = number of TDR placed at each layer
n'_i = recomputed porosity of i^{th} TDR depth at each layer (%)

z_i = depth of i^{th} for each layer TDR from surface
Z_0 = depth of last TDR for each layer from surface ($Z_0 > z_i$)

Equation 37 is a general rule useful for checking the consistency of 10 densities and moisture contents based on the assumption porosities should decrease with depth. Figure 21 is provided to illustrate Z_0 and z_i in this adjustment process.

Using the recomputed porosity values, the dry density and volumetric contents of solids, water, and air were recalculated for each TDR using the following equations.

$$\gamma'_{d_i} = G_s \gamma_w (1 - n'_i) \tag{38}$$

$$\theta'_{w_i} = w_i \frac{\gamma'_{d_i}}{\gamma_w} \tag{39}$$

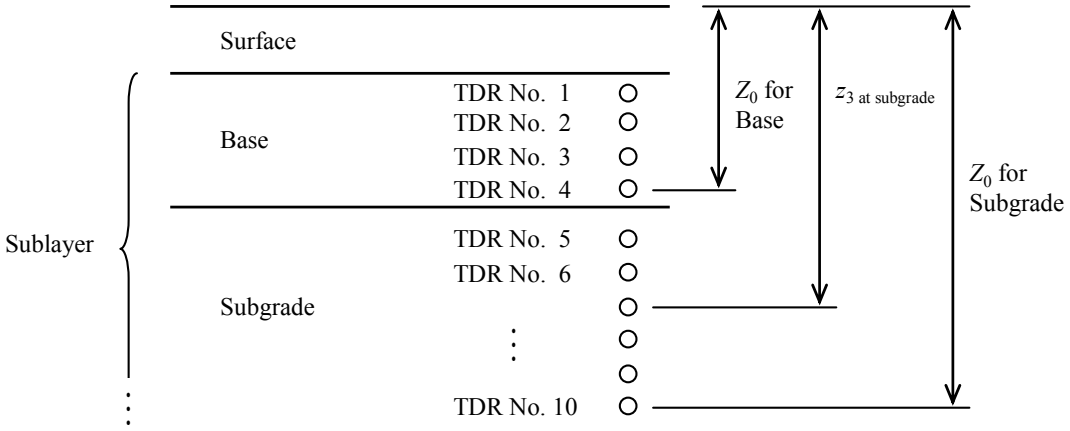

Figure 21. Diagram. Profile of TDR and depth at each layer.

$$\theta'_{s_i} = \frac{\gamma'_{d_i}}{G_{s_i} \gamma_w} \tag{40}$$

$$\theta'_{a_i} = 1 - \theta'_{w_i} - \theta'_{s_i} \tag{41}$$

Where:

γ'_{d_i} = recalculated dry density using n'_i
$\theta'_{w_i}, \theta'_{s_i}, \theta'_{a_i}$ = recalculated volume of water, solids, and air (%)

Step 3. Air volume check and dry density adjustment

The air volume in a soil mixture cannot be less than zero but could be equal to zero if the soil is fully saturated. This condition is defined in terms of the porosity, gravimetric moisture content, and specific gravity:

$$\theta'_a = 1 - \theta'_w - \theta'_s = 1 - (1 - n')(1 + wG_s) \geq 0 \tag{42}$$

Which can be defined as:

$$1 - \frac{1}{1 + wG_s} \leq n' \tag{43}$$

If the air volume recalculated in step 2 was less than zero, it was assumed that the soil was fully saturated and that the air volume was zero:

$$\theta'_a = 1 - (1 - n')(1 + wG_s) = 0 \tag{44}$$

Thus, the porosity was adjusted with equation 43 to achieve an air volume of zero:

$$n'' = 1 - \frac{1}{1 + wG_s} \tag{45}$$

Where:

n'' = adjusted porosity for soil having negative air volume

Using the adjusted porosity, the dry density was also adjusted using equation 46.

$$\gamma''_d = G_s \gamma_w (1 - n'') \tag{46}$$

Where:

γ''_d = adjusted dry density for soil having negative air volume

The volumes of water and solid were also recomputed using the adjusted dry density value (γ''_d):

$$\theta''_w = w \frac{\gamma''_d}{\gamma_w} \tag{47}$$

$$\theta''_s = \frac{\gamma''_d}{G_s \gamma_w} \tag{48}$$

$$\theta''_w + \theta''_s + \theta''_a = \theta''_w + \theta''_s = 1 \tag{49}$$

Where:

$\theta''_w, \theta''_s, \theta''_a =$ adjusted volume of water, solids, and air

This adjustment was only performed if the air volume was found to be less than zero. If the air volumes at TDR probes were larger than zero, the porosity and dry density determined from step 2 were utilized in the calibration process.

As an example, table 13 shows the adjustment process of sections 331001 and 533813. TDR sensor numbers 4 and 5 for section 331001 and numbers 3, 4, and 5 of section 533813 had negative values of air volume based on step 2 calculations. After applying equation 44 and 45, the dry densities were adjusted and the volumes of air were converted to zero. The dry densities of all other TDR sensors remained at the values calculated in step 2 because their air volumes were larger than zero. The final dry densities and VMC were placed in the fields of DRY_DENSITY and VOLUMETRIC_MOISTURE_CONTENT, respectively, in the MICROMOIST_SMP_TDR_CALIBRATE table.

Table 13. Dry density adjustment of Sections 331001 and 533813.

Section	TDR No	Layer Type	w	γ_d	G_s	Step 1				Step 2					Step 3				
						θ_w	θ_s	θ_a	n	n''	γ'_d	θ'_w	θ'_s	θ'_a	n''	γ''_d	θ''_w	θ''_s	θ''_a
331001	1	Base	2.55	2.153	2.695	0.05	0.80	0.15	0.20	0.19	2.18	0.06	0.81	0.13	0.19	2.18	0.06	0.81	0.13
	2	Base	2.16			0.05	0.80	0.15	0.20	0.19	2.19	0.05	0.81	0.14	0.19	2.19	0.05	0.81	0.14
	3	Base	3.75			0.08	0.80	0.12	0.20	0.18	2.21	0.08	0.82	0.10	0.18	2.21	0.08	0.82	0.10
	4	Subbase	10.75	2.105	2.647	0.23	0.80	-0.02	0.20	0.20	2.13	0.23	0.80	-0.03	0.22	2.06	0.22	0.78	0.00
	5	Subbase	11.00			0.23	0.80	-0.03	0.20	0.20	2.13	0.23	0.80	-0.04	0.23	2.05	0.23	0.77	0.00
	6	Subgrade	9.73	1.858	2.647	0.18	0.70	0.12	0.30	0.28	1.90	0.19	0.72	0.10	0.28	1.90	0.19	0.72	0.10
	7	Subgrade	6.16			0.11	0.70	0.18	0.30	0.28	1.91	0.12	0.72	0.16	0.28	1.91	0.12	0.72	0.16
	8	Subgrade	5.85			0.11	0.70	0.19	0.30	0.28	1.91	0.11	0.72	0.17	0.28	1.91	0.11	0.72	0.17
	9	Subgrade	6.99			0.13	0.70	0.17	0.30	0.27	1.93	0.13	0.73	0.14	0.27	1.93	0.13	0.73	0.14
	10	Subgrade	7.89			0.15	0.70	0.15	0.30	0.27	1.94	0.15	0.73	0.12	0.27	1.94	0.15	0.73	0.12
533813	1	Subbase	12.20	1.885	2.734	0.23	0.69	0.08	0.31	0.30	1.91	0.23	0.70	0.07	0.30	1.91	0.23	0.70	0.07
	2	Subbase	12.90			0.24	0.69	0.07	0.31	0.30	1.92	0.25	0.70	0.05	0.30	1.92	0.25	0.70	0.05
	3	Subbase	16.00			0.30	0.69	0.01	0.31	0.29	1.94	0.31	0.71	-0.02	0.30	1.90	0.30	0.70	0.00
	4	Subbase	18.90			0.36	0.69	-0.05	0.31	0.29	1.95	0.37	0.71	-0.08	0.34	1.80	0.34	0.66	0.00
	5	Subbase	15.70			0.30	0.69	0.01	0.31	0.28	1.96	0.31	0.72	-0.02	0.30	1.91	0.30	0.70	0.00
	6	Subbase	13.20			0.25	0.69	0.06	0.31	0.28	1.97	0.26	0.72	0.02	0.28	1.97	0.26	0.72	0.02
	7	Subgrade	14.90	1.821	2.717	0.27	0.67	0.06	0.33	0.31	1.88	0.28	0.69	0.03	0.31	1.88	0.28	0.69	0.03
	8	Subgrade	14.80			0.27	0.67	0.06	0.33	0.31	1.88	0.28	0.69	0.03	0.31	1.88	0.28	0.69	0.03
	9	Subgrade	13.20			0.24	0.67	0.09	0.33	0.30	1.90	0.25	0.70	0.05	0.30	1.90	0.25	0.70	0.05
	10	Subgrade	14.90			0.27	0.67	0.06	0.33	0.30	1.91	0.28	0.70	0.01	0.30	1.91	0.28	0.70	0.01

Calculation of Calibrated Values

Using the dielectric constant (determined from the manual TDR trace taken at installation) and the ground truth measured moisture content and dry density, ε_1, ε_2, and G_s values were calculated. The value of ε_3 was defined as 1.0. The calibrated dielectric constants of solids and water ranged between 3 and 4.5 and 78 and 82, respectively.

The fundamental assumption associated with the micromechanics and self consistent scheme is that each layer is statistically homogeneous. Therefore, one set of ε_1, ε_2, and G_s values were used for each test section/layer combination. That is, the same ε_1, ε_2, and G_s values were utilized to calculate moisture content and dry density for all TDR probes placed in the same layer. The ε_1, ε_2, and G_s values used were averages from all TDR traces in the layer. Table 14 shows the calibrated values and average values at each layer for LTPP sections 331001 and 533813 as an example.

Table 14. Calibrated values of Sections 331001 and 533813.

Section	TDR No	TDR Depth	Layer Type	Soil Type	Measured Values			Calibrated Values				Average Values			
					w	γ_d	θ	ε_1	ε_2	ε_3	G_s	ε_1	ε_2	ε_3	G_s
331001	1	0.362	Base	Gravel	2.55	2.153	5.49	3.90	80.06	1.0	2.695	3.90	80.06	1.0	2.695
	2	0.518	Base	Gravel	2.16	2.153	4.65	3.89	80.06	1.0	2.694				
	3	0.683	Base	Gravel	3.75	2.153	8.07	3.92	80.07	1.0	2.695				
	4	0.819	Subbase	Sand	10.75	2.105	22.63	4.08	80.02	1.0	2.647	4.08	80.02	1.0	2.647
	5	0.953	Subbase	Sand	11.00	2.105	23.16	4.07	80.02	1.0	2.647				
	6	1.121	Subgrade	Sand	9.73	1.858	18.08	4.05	80.01	1.0	2.647	4.03	79.98	1.0	2.647
	7	1.276	Subgrade	Sand	6.16	1.858	11.45	4.03	80.00	1.0	2.647				
	8	1.438	Subgrade	Sand	5.85	1.858	10.87	4.03	79.97	1.0	2.646				
	9	1.740	Subgrade	Sand	6.99	1.858	12.99	4.03	79.96	1.0	2.646				
	10	2.045	Subgrade	Sand	7.89	1.858	14.66	4.01	79.96	1.0	2.647				
533813	1	0.357	Subbase	Sand	12.20	1.885	23.00	4.03	80.12	1.0	2.735	4.05	80.12	1.0	2.734
	2	0.505	Subbase	Sand	12.90	1.885	24.32	4.04	80.12	1.0	2.734				
	3	0.660	Subbase	Sand	16.00	1.885	30.16	4.07	80.11	1.0	2.735				
	4	0.810	Subbase	Sand	18.90	1.885	35.63	4.06	80.14	1.0	2.735				
	5	0.962	Subbase	Sand	15.70	1.885	29.59	4.05	80.13	1.0	2.732				
	6	1.116	Subbase	Sand	13.20	1.885	24.88	4.05	80.11	1.0	2.734				
	7	1.255	Subgrade	Sand	14.90	1.821	27.13	4.07	80.12	1.0	2.717	4.08	80.13	1.0	2.717
	8	1.415	Subgrade	Sand	14.80	1.821	26.95	4.09	80.13	1.0	2.717				
	9	1.721	Subgrade	Sand	13.20	1.821	24.04	4.10	80.13	1.0	2.715				
	10	2.020	Subgrade	Sand	14.90	1.821	27.13	4.06	80.13	1.0	2.718				

MICROMOIST INPUT AND OUTPUT DATA TABLE

As with all computational programs, a specific format of input data is required to process the TDR traces and compute the soil dry density and moisture content.

Input Tables

The program needs the following three input tables: MICROMOIST_SMP_TDR_AUTO for TDR trace reading, MICROMOIST_SMP_TDR_DEPTHS_LENGTH for TDR depth information, and MICROMOIST_SMP_TDR_CALIBRATE for calibrated soil data. The first two tables are available directly from the LTPP database while the third was developed as part of this study.

The program extracts the TDR trace point data from the MICROMOIST_SMP_TDR_AUTO table containing TDR sensor response waveforms. The measured waveform consists of 245 intervals and stored in the WAVP_1 through WAVP_245 fields. The distance interval between data points is recorded in the DIST_WAV_POINTS field and is either 0.01 or 0.02 m. This raw TDR trace data can be acquired from the LTPP database. Table 15 shows the field information included in the table. The table structure is required to match the SMP_TDR_AUTO table in the LTPP IMS database.

Table 15. Field names and description of MICROMOIST_SMP_TDR_AUTO table.

Field Name	Description
SHRP_ID	Test section identification number
STATE_CODE	Numerical code for state or province
CONSTRUCTION_NO	Event number used to relate changes in pavement structure with other time dependent data elements
SMP_DATE	Measurement date
TDR_TIME	TDR measurement time (HHMM)
TDR_NO	ID number of TDR probe
DIST_WAV_POINTS	Distance between waveform points (meters)
WAVP_1 ~ 245	245 data points defining TDR waveform

As shown in table 16, the MICROMOIST_SMP_TDR_DEPTHS_LENGTH table contains the physical characteristics of the TDR probes, including the installed depth below the pavement surface and probe length for each TDR probe at each site. The table links to the SMP_TDR_AUTO table using SHRP_ID, STATE_CODE, TDR_NO and CONSTRUCTION_NO to identify the depth of each TDR. This table is populated in the LTPP database. The table structure is required to match the SMP_TDR_DEPTHS_LENGTH table in the LTPP IMS database.

Table 16. Field names and description of MICROMOIST_SMP_TDR_DEPTHS_LENGTH table.

Field Name	Description
SHRP_ID	Test section identification number assigned by LTPP
STATE_CODE	Numerical code for state or province
CONSTRUCTION_NO	Event number used to relate changes in pavement structure with other time dependent data elements
INSTALL_DATE	Instrumentation installation date
TDR_NO	ID number of TDR probe
TDR_DEPTH	Depth from pavement surface to TDR probe
TDR_PROBE_LENGTH	Actual length of TDR probe

The data contained in the MICROMOIST_SMP_TDR_CALIBRATE table are the calibrated dielectric constants of the soil components and specific gravity. The calibration was accomplished using the micromechanics and self-consistent scheme and the SID approach previously described. The calibrated values are used to calculate moisture content by linking SMP_TDR_CALIBRATE by STATE_CODE, SHRP_ID and TDR_NO fields. The installation date, TDR depth, and layer and soil types are obtained from the SMP installation report. Information included in this table is shown in table 17.

Table 17. Field names and description of MICROMOIST_SMP_TDR_CALIBRATE table.

Field Name	Description
SHRP_ID	Test section identification number assigned by LTPP
STATE_CODE	Numerical code for state or province
INSTALL_DATE	Instrumentation installation date
TDR_NO	ID number of TDR probe
TDR_DEPTH	Depth from pavement surface to TDR probe at installation
LAYER_TYPE	Type of sublayer at TDR probe installation
SOIL_TYPE	Soil type of layer at TDR probe installation
DRY_DENSITY	Measured dry density of soil at installation (g/cm^3)
VOLUMETRIC_ MOISTURE_CONTENT	Measured volumetric moisture content of soil at installation
CONSTRUCTION_NO	Event number used to relate changes in pavement structure with other time dependent data elements
DIELECTRIC_SOILDS	Calibrated dielectric constant value of solid
DIELECTRIC_WATER	Dielectric constant value of water (= 1.0)
DIELECTRIC_AIR	Calibrated dielectric constant value of air
SPECIFIC_GRAVITY	Calibrated specific gravity of soil

Output Tables

Two tables are generated upon running the program: MICROMOIST_SMP_TDR_AUTO_DIELECTRIC and MICROMOIST_SMP_TDR_ MOISTURE.

The dielectric constant, conductivity, and reflectivity parameters determined from the analysis of automated TDR traces are stored in the MICROMOIST_SMP_TDR_AUTO_DIELECTRIC table. The table structure is summarized in table 18. The dielectric constant values reported in this table are used to compute moisture content and dry density values.

Table 18. Field names and description of MICROMOIST_SMP_TDR_AUTO_DIELECTRIC table.

Field Name	Description
SHRP_ID	Test section identification number
STATE_CODE	Numerical code for state or province
CONSTRUCTION_NO	Event number used to relate changes in pavement structure with other time dependent data elements
SMP_DATE	Measurement date
TDR_TIME	TDR measurement time (HHMM)
TDR_NO	ID number of TDR probe
INFLEC_A	First inflection point in TDR trace (meters)
INFLEC_B	Second inflection point in TDR trace (meters)
SOIL_DIELECTRIC_CONSTANT	Computed dielectric constant of soil
SOIL_CONDUCTIVITY	Computed conductivity of soil
SOIL_REFLECTIVITY	Computed reflectivity of soil

The MICROMOIST_SMP_TDR_MOISTURE table contains dry density, VMC, and gravimetric moisture content data computed from TDR traces. The dry density is used to convert moisture content from volumetric to gravimetric using equation 18. Table 19 shows the field name and descriptions in SMP_TDR_MOISTURE.

Table 19. Field names and description of MICROMOIST_SMP_TDR_AUTO_MOISTURE table.

Field Name	Description
SHRP_ID	Test section identification number
STATE_CODE	Numerical code for state or province
CONSTRUCTION_NO	Event number used to relate changes in pavement structure with other time dependent data elements
SMP_DATE	Measurement date
TDR_TIME	TDR measurement time (HHMM)
TDR_NO	ID number of TDR probe
TDR_DEPTH	Depth from pavement surface to TDR probe at installation
LAYER_TYPE	Type of sublayer at TDR probe installation
SOIL_TYPE	Soil type of layer at TDR probe installation
SOIL_DIELECTRIC _CONSTANT	Computed dielectric constant of soil
DRY_DENSITY	Computed dry density of soil
VOLUMETRIC_ MOISTURE_CONTENT	Computed volumetric moisture content
GRAVIMETRIC_ MOISTURE_CONTENT	Computed gravimetric moisture content
ERROR_COMMENT	Assigned error code

The program was developed to produce quality data for the LTPP database. To this end, features were incorporated into the program to ensure quality. Additional measures were implemented for manual review, including a thorough program testing process during development. This will be described in the following chapter.

CHAPTER 5. PARAMETER COMPUTATION AND QUALITY REVIEW

To ensure the highest quality data were provided to FHWA for inclusion into the LTPP database, various QC measures were incorporated into the MicroMoist program. Manual review procedures were also developed and implemented as part of the data processing activities. This chapter provides details on all of the QC and quality assurance tools used in this process.

INTERNAL PROGRAM QUALITY CONTROL FEATURES

Due to the large quantity of data analyzed, MicroMoist was developed to process all TDR traces and compute parameters automatically, but additional consideration was given to unique data requiring user input to ensure the highest quality end product. For example, TDR traces not exhibiting a negative slope could not be analyzed using the proposed method. Also, some computed parameters, especially dry density, could be unreasonable. Therefore, a flagging function was developed to assign comment codes to the TDR traces exhibiting suspect characteristics and/or resulting in questionable computed parameters. The error codes are assigned in the ERROR_COMMENT field of the SMP_TDR_MOISTURE output table.

An example of an uninterpretable TDR trace that did not exhibit a negative slope between the inflection points is shown in figure 22. These traces may be caused by abnormal TDR device operation or the environmental effects near TDR probes, such as temperature or very high salinity of the soil.

Figure 23 provides an example of a TDR trace in which the first inflection point was not captured. The TLE can still be used to estimate dielectric constant from these traces. While the method can interpret dielectric constant using only a small portion of the TDR trace, the prediction error is greatly reduced as the portion of the TDR trace utilized in the computation increases.

A check for these types of traces was included in the program. If the program could not capture a negative slope between the inflection points, the traces were flagged as uninterpretable TDR traces in the program. The number of the questionable TDR trace is displayed as “Dubious Trace” in the program display. Also, a comment code of “TDR_ERR” is assigned to the ERROR_COMMENT field in the SMP_TDR_MOISTURE table.

The program was also designed with a visual feature to allow user review of all TDR traces. Every trace in the input tables can be visually reviewed by a user. This feature allows users to identify unique traces not detected by the automated checks, while also providing a visual verification of those traces that were flagged. As part of the viewing function, the user has the capability of modifying the ranges used in the TLE for cases where they were improperly identified by the program.

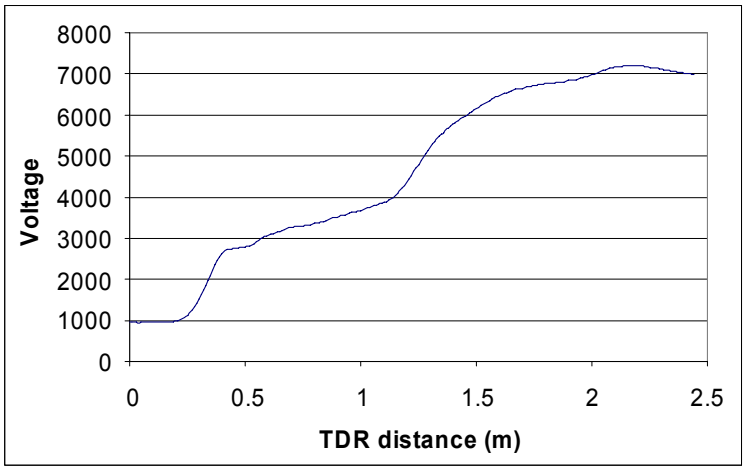

Non-negative slope

Figure 22. Graph. Uninterpretable TDR trace.

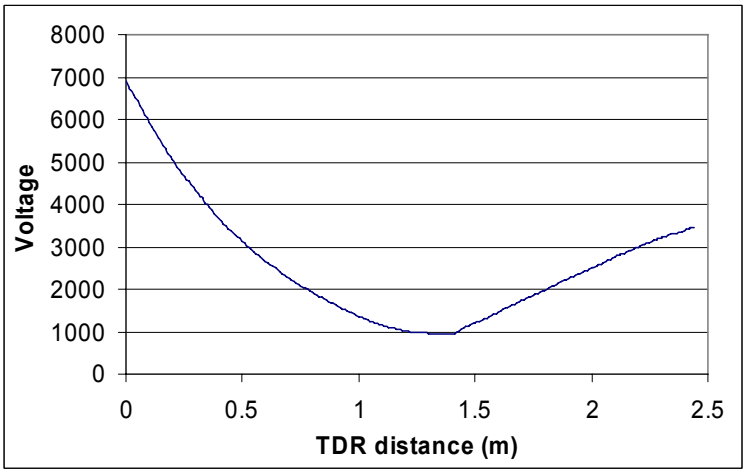

Figure 23. Graph. Incomplete TDR trace.

The measured ground truth values of dry density reported in the LTPP database were in the range of 1.3 to 2.5 g/cm^3. Most of the dry densities calculated from the program were also within this range as well. However, the dry density values of some TDR traces were calculated to be less than 1.3 g/cm^3, most likely due to unreasonably high moisture content or frozen soil material. In these instances, the program assigns a comment of "DD_ERR" in the SMP_TDR_MOISTURE table.

One of the key advantages of this computation process over previous methods is the calibration of the micromechanics model to site specific conditions and equipment. In order to calibrate the micromechanics model, ground truth measured moisture content and dry density were required. Without this information, the model could not be calibrated and accurate computations could not be generated. It was discovered that ground truth data were unavailable at five SMP sites installed on the Specific Pavement

Study (SPS)-5 and SPS-9 in New Jersey. For these cases, a comment code of "CALI_ERR" is assigned to ERR_COMMENT field. The error codes used to identify TDR trace inconsistencies are listed in table 20.

Table 20. Error codes used in the program.

Error Code	Description
TDR_ERR	TDR trace does not have a negative slope.
DD_ERR	Calculated dry density is less than 1.3 g/cm^3.
CALI_ERR	Calibration data from installation activities are unavailable.

SHIFT ZONE IN TREND LINE BETWEEN DIELECTRIC CONSTANT AND MOISTURE CONTENT

Moisture content is expected to decrease as the dielectric constant is reduced. However, in a few TDR sensors, a shift in the VMC occurs even though the dielectric constant decreases, as illustrated in figure 24. The data trends in this figure are from LTPP section 091803. TDR sensor number 7 exhibits a shift in the relationship for dielectric constant values between 3 and 5. Also, the dry density values of the left side of the shift were a little higher than those of the right side. The shift is associated with the circumstances related to the calibration for the soil moisture content. This shift occurred on other sections as well.

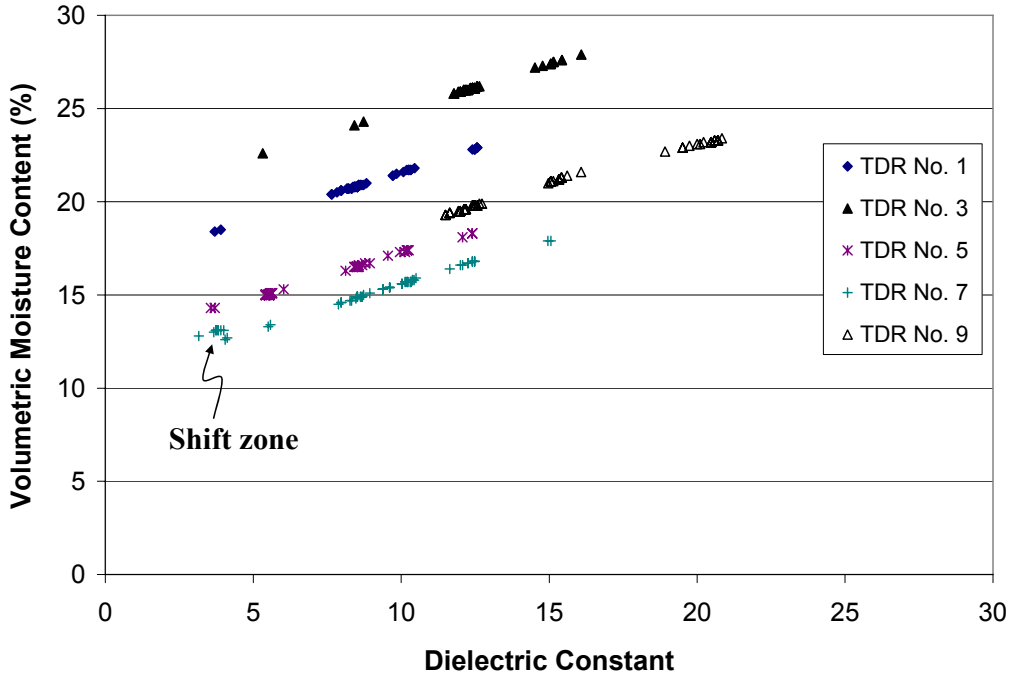

Figure 24. Graph. Shift zone in LTPP section 091803, TDR sensor No. 7.

Soil-Water Characteristic Curve

As the water content of the soil is reduced, the matric suction is increased as a result of the change of pore-water pressure in the soil-moisture system. The relationship between the matric suction and the water content of a soil is called the soil-water characteristic curve (SWCC) as shown in figure 25.

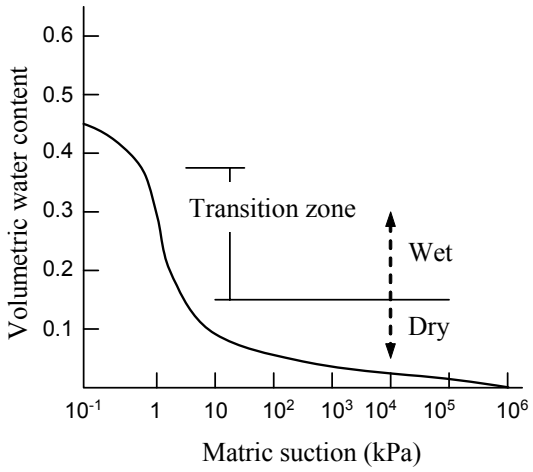

Figure 25. Graph. Soil-water characteristic curve for sandy soil.

As seen in figure 25, the SWCC has a transition zone at which the volumetric water content rapidly drops compared to the matric suction variation. This is particularly prevalent in sandy soils.

The TDR sensors located in soils associated with a shift zone most likely have been calibrated with moisture data on the wet side of the SWCC. Figure 26 illustrates two density-moisture conditions in the same soil. The wet condition shown in figure 26 (b) has higher VMC and lower dry density values than the dry condition, but the weight of solids is the same.

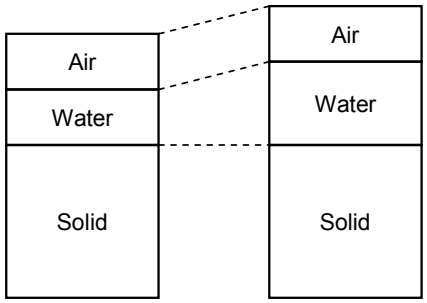

(a) Dry condition (b) Wet condition

Weight of solid, W_s	=
Volumetric Moisture Content, θ	<
Dry density, γ_d	>
Dielectric Constant, ε	<

Figure 26. Diagram. Diagrams of soil having different volume.

Figure 27 also shows the relationship between the SWCC and the VMC trend.

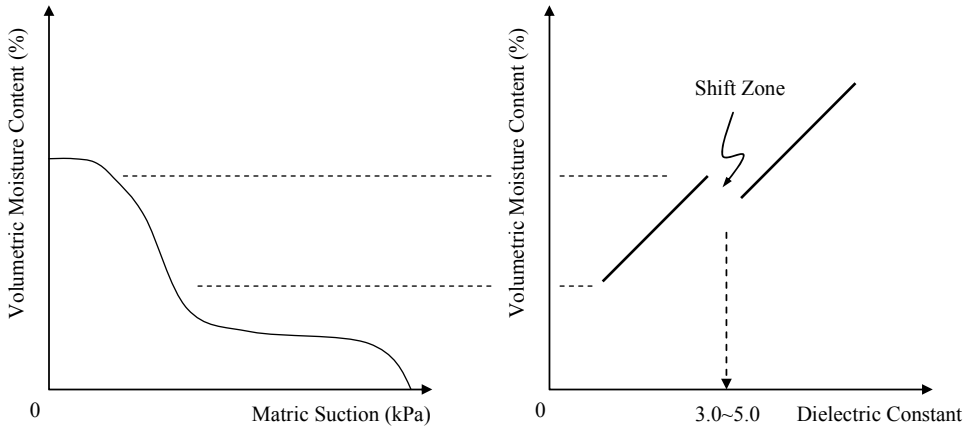

(a) Soil-water characteristic curve (SWCC) (b) VMC-DC trend

Figure 27. Graph. Comparison of SWCC and VMC-DC trend.

Recalibration for Shift Zone

As seen in figure 27, when the calibration of a TDR sensor was carried out on the wet side, the higher dry density soil exhibits a lower dielectric constant but similar VMC because the volume of water was smaller (on a percentage basis) in the higher density material.

As a consequence, any TDR trace containing a shift in the moisture content-dielectric constant trend indicates that an additional calibration needs to be carried out in order to

determine the correct interpretation of the TDR trace over the full range of moisture contents. Because the LTPP database did not have additional ground truth data to perform further calibrations, the values in the transition zone were adjusted (and flagged) accordingly.

POST-PROCESSING QUALITY CONTROL REVIEW

Moisture content and dry density estimates generated from the program were plotted to review seasonal trends and variation with depth using pivot tables in Microsoft Excel. An example of moisture content seasonal trends can be found in figure 28.

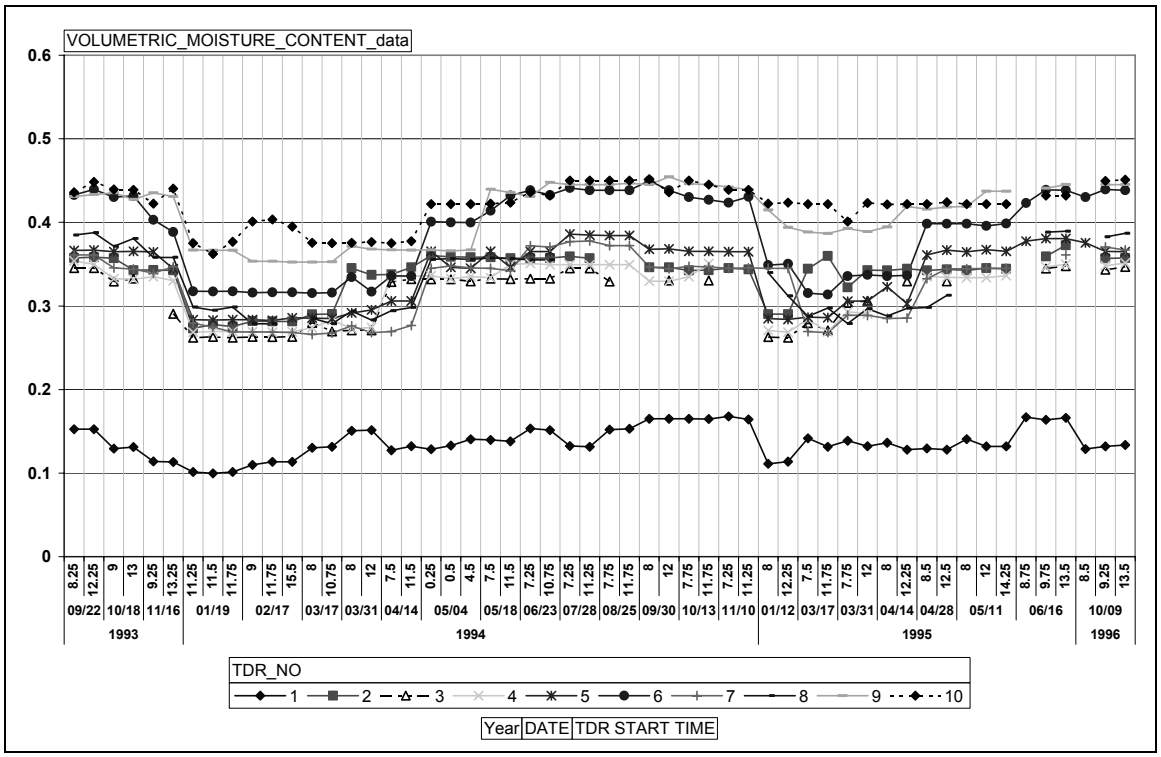

Figure 28. Graph. Sample plot of moisture content seasonal trend.

The pivot table configuration allowed large quantities of data to be reviewed relatively quickly, while the graphical nature made questionable or anomalous data readily identifiable. Problematic or frequently occurring trends in the data could also be easily recognized through the process.

During the program development phase of the project, the pivot tables served as a critical part of the beta testing. The review provided valuable insight, identified issues with the software, and was an integral part of the debugging process. Multiple programming and testing iterations were conducted in completing the MicroMoist program.

The pivot tables were also used after MicroMoist was finalized to perform a 100 percent review on all computed moisture content and dry density estimates. Outliers and anomalous data identified were manually flagged in the final data submittal to FHWA.

The QC measures incorporated into the program and the post-processing reviews were designed as a supplement to the LTPP database QC checks. Coupling the LTPP checks with the reviews conducted by the analysis team, the data provided to FHWA for inclusion into the LTPP database underwent a very rigorous QC process.

ESTIMATE OF ERROR

Unlike an empirical approach, which provides an error of estimate based on the fit of the regression equation, the micromechanics approach provides no such comparison. The micromechanics model is solved through an iterative process, which closes on a solution with an error of less than one percent. This, however, does not give a realistic error estimate on the resultant moisture content and dry density because there are multiple steps involved in the computation process (i.e., TLE and micromechanics model).

The best estimate of error for this type of approach is achieved by comparing the computed moisture content solutions to those obtained from both the laboratory and field moisture tests. This was described in chapter 3 as part of the validation discussion. Data from Klemunes' work with TDR data in soils from SMP sites were considered from laboratory tests. The field moisture tests used in this validation were obtained during a forensic analysis of LTPP-SMP test section 091803. The differences between the micromechanics solution and the laboratory tests are shown in figure 10, while those from the field tests are shown in figure 12.

For most of the test results, the differences were less than five percent, with one set of test results indicating a difference of 10 percent. Based on this information, a conservative estimate of the possible error in the computations of the micromechanics approach is approximately 10 percent.

CHAPTER 6. LTPP DATABASE DELIVERY

This chapter provides details on the data delivered for upload into the LTPP IMS database. Two tables were developed specifically to store data from this study: SMP_TDR_CALIBRATE and SMP_TDR_MOISTURE.

Table 21. Description of SMP_TDR_CALIBRATE table for the LTPP IMS Database.

Field	Comment
STATE_CODE	Numerical code for State or Province.
SHRP_ID	Test section identification number assigned by LTPP.
TDR_NO	TDR sensor number.
CAL_DRY_DENSITY	Retrieved from other LTPP tables or assumed.
SOURCE_DRY_DENSITY_TDR	Code indicating source of CAL_DRY_DENSITY. 1-SMP installation report 2-SMP installation report - I07 form 3-SMP installation report - S04 form 4-SMP installation report - I05 form 5-IMS table TST_ISD_MOIST 6-IMS table TST_SS08 7-IMS table INV_SUBGRADE 8-From Appendix C of "Analysis of Time Domain Reflectometry Data From LTPP Seasonal Monitoring Program Test Sections-Final Report" FHWA-RD-99-115
CAL_DRY_DENSITY_ADJUSTMENT_METHOD	Code indicating type of adjustment made to CAL_DRY_DENSITY. 1-Adjustment based on vertical variation 2-Adjustment based on vertical variation and air volume
CAL_VOLUMETRIC_MOISTURE_CONTENT	Measured VMC from samples taken during installation.
CAL_SOIL_DIELECTRIC	Dielectric constant estimated from manual TDR trace taken at installation (from SMP Installation Report).
CAL_DIELECTRIC_SOLIDS	Computed using measured VMC and TDR trace taken during installation. This is used to calibrate the micromechanics equation to the specific TDR sensor for subsequent VMC computations.
CAL_DIELECTRIC_WATER	Computed using measured VMC and TDR trace taken during installation. This is used to calibrate the micromechanics equation to the specific TDR sensor for subsequent VMC computations.
CAL_DIELECTRIC_AIR	Computed using measured VMC and TDR trace taken during installation. This is used to calibrate the micromechanics equation to the specific TDR sensor for subsequent VMC computations.
CAL_SPECIFIC_GRAVITY	Computed using dry density and TDR trace taken during installation. This is used to calibrate the micromechanics equation to the specific TDR sensor for subsequent density computations.

The SMP_TDR_MOISTURE table contains dielectric constant, moisture, conductivity, and reflectivity data estimated from automated TDR traces. A description of each field can be found in table 22.

Table 22. Description of SMP_TDR_MOISTURE table for the LTPP IMS Database.

Field	Comment
STATE_CODE	Numerical code for State or Province.
SHRP_ID	Test section identification number assigned by LTPP.
SMP_DATE	Date TDR trace was obtained.
TDR_TIME	Time TDR trace was obtained.
TDR_NO	TDR sensor number.
TLE_BEGIN	Starting point of interval on TDR trace captured for use in the Transmission Line Equation.
TLE_END	Ending point of interval on TDR trace captured for use in the Transmission Line Equation.
SOIL_DIELECTRIC	Dielectric constant estimated from TDR trace (from SMP_TDR_AUTO).
SOIL_CONDUCTIVITY	Conductivity estimated from TDR trace (from SMP_TDR_AUTO).
SOIL_REFLECTIVITY	Reflectivity estimated from TDR trace (from SMP_TDR_AUTO).
DRY_DENSITY	Dry density estimated from SOIL_DIELECTRIC and calibrated micromechanics equation.
VOLUMETRIC_ MOISTURE_CONTENT	VMC estimated from SOIL_DIELECTRIC and calibrated micromechanics equation.
GRAVIMETRIC_ MOISTURE_CONTENT	GMC estimated from VMC and DRY_DENSITY.
TDR_COMPUTATION_ COMMENT_CODE	Codes to describe traces that could not be interpreted. 1-TDR trace uninterpretable due to lack of negative slope 2-Questionable data due to low dry density value 3-Calibration data from installation activities are unavailable 4-Outlier data based on time series analysis 5-Volumetric moisture content was in transition zone and was adjusted

CHAPTER 7. DATA OBSERVATIONS

As discussed in previous parts of this report, TDR trace data as well as computed parameters developed under this project were thoroughly reviewed. Observations discovered during the project are described in this chapter.

COMPARISON BETWEEN NEW AND EXISTING DATA

Limited comparisons were made between data computed using the TLE micromechanics method and the moisture estimates computed previously using the apparent length method. A series of comparisons (discussed in chapter 3 of this report) were performed to validate the new procedure.

Additional comparisons were made during the development phase to ensure that the MicroMoist program was working properly. In many cases, the same trends show up for both computational processes and the resultant estimates are very similar. However, in some cases, significant differences are present, typically in higher moisture content settings. In these situations, the TLE/micromechanics method results in a moisture content that is closer to the in situ moisture content (acquired during equipment installation) as compared with the apparent length method. This is expected because the micromechanics model was calibrated to the in situ moisture content at each site/layer.

As an example, results for LTPP section 063042 from the apparent length approach and the TLE/micromechanics method can be found in figures 29 and 30, respectively. Also included in the figures are the in situ VMC obtained during equipment installation. As can be seen in figure 29, VMC from the apparent length approach ranged from 35 to 55 percent (with the majority of values falling between 35 and 39 percent). For some of the TDR sensors, the predictions are drastically higher than the measured in situ moisture content. The results from the TLE/micromechanics method shown in figure 30 correlate more closely with the measured in situ moisture content trends.

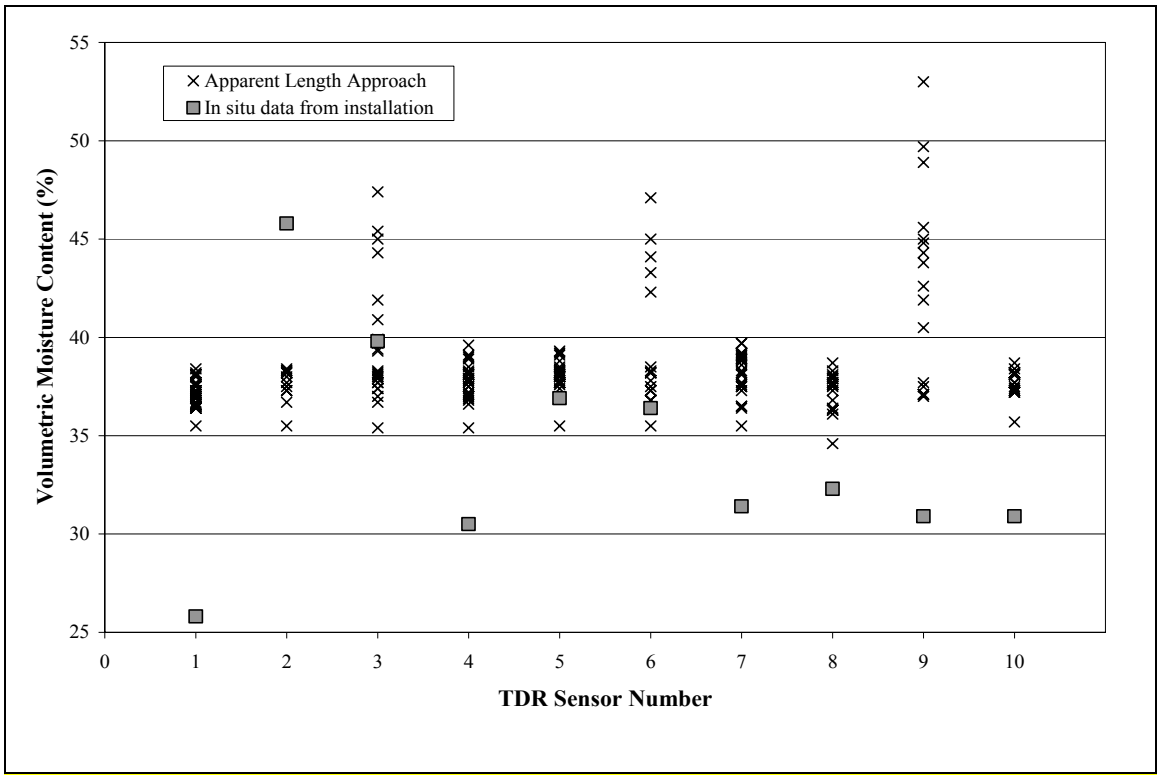

Figure 29. Graph. Results from the apparent length approach for LTPP section 063042.

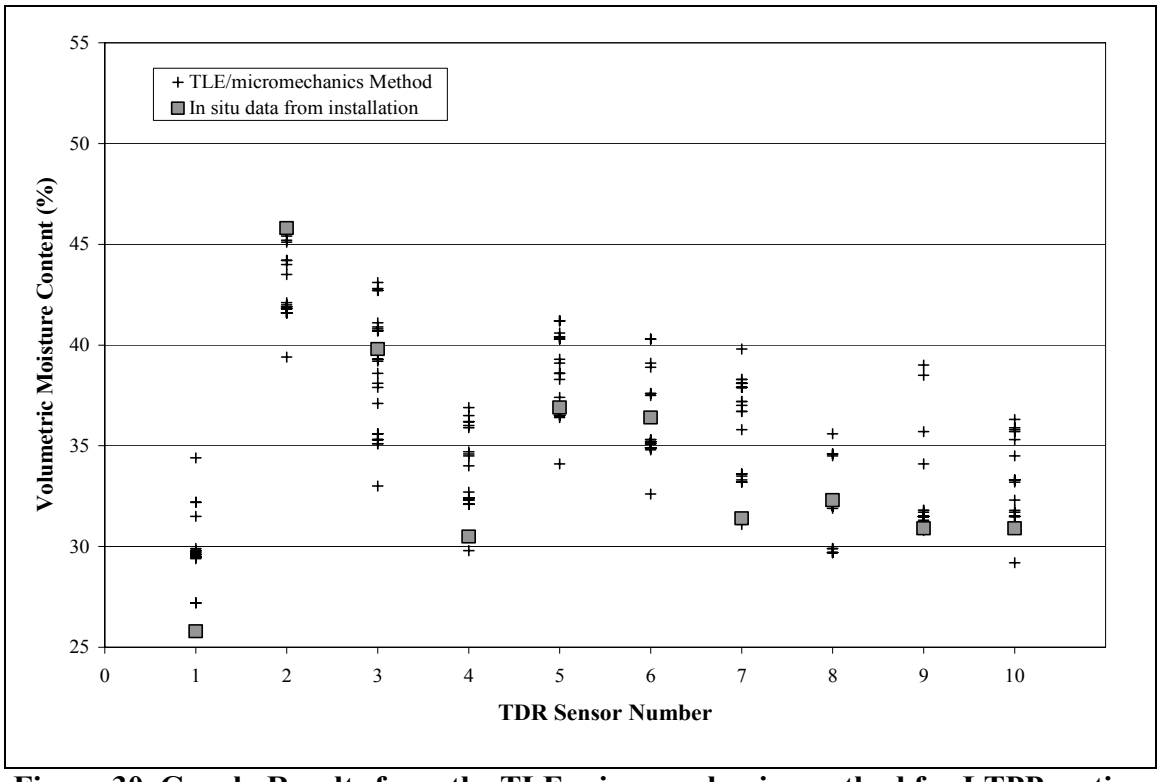

Figure 30. Graph. Results from the TLE micromechanics method for LTPP section 063042.

Figures 31 and 32 provide similar information for LTPP site 313018. The data for both computational processes range from 5 to 22 percent with similar distributions.

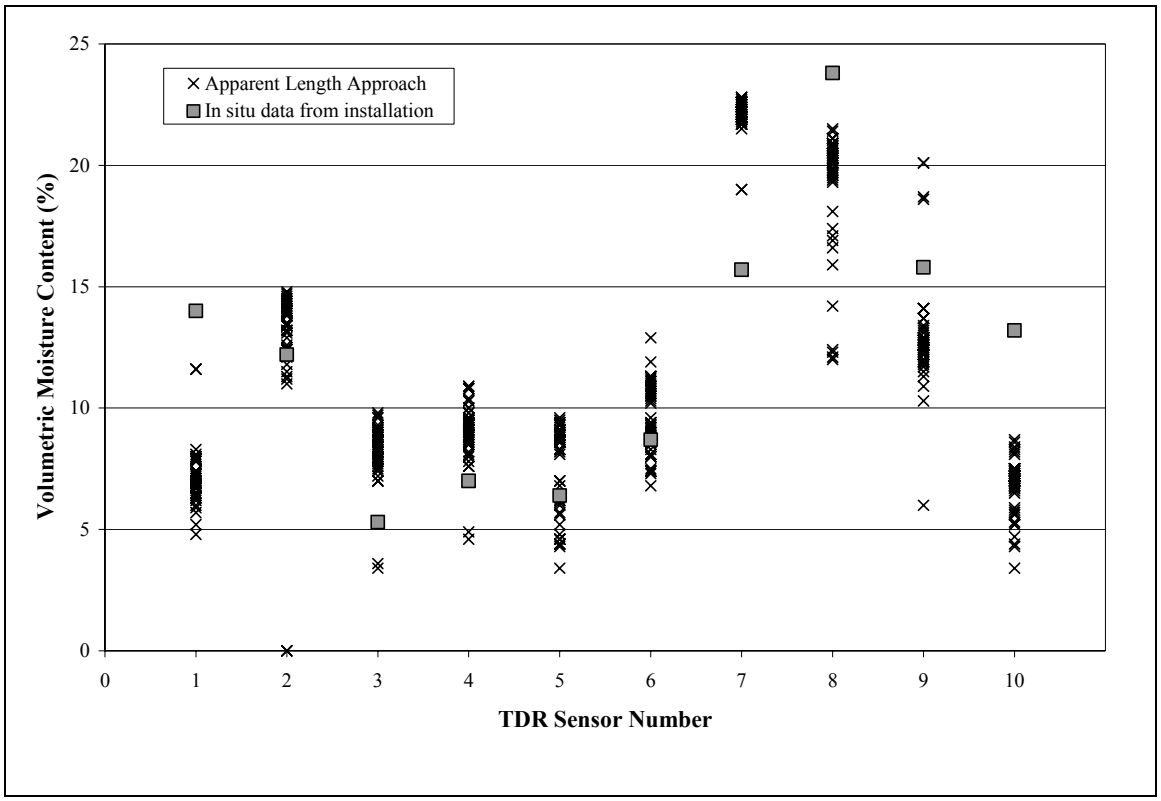

Figure 31. Graph. Results from the apparent length approach for LTPP section 313018.

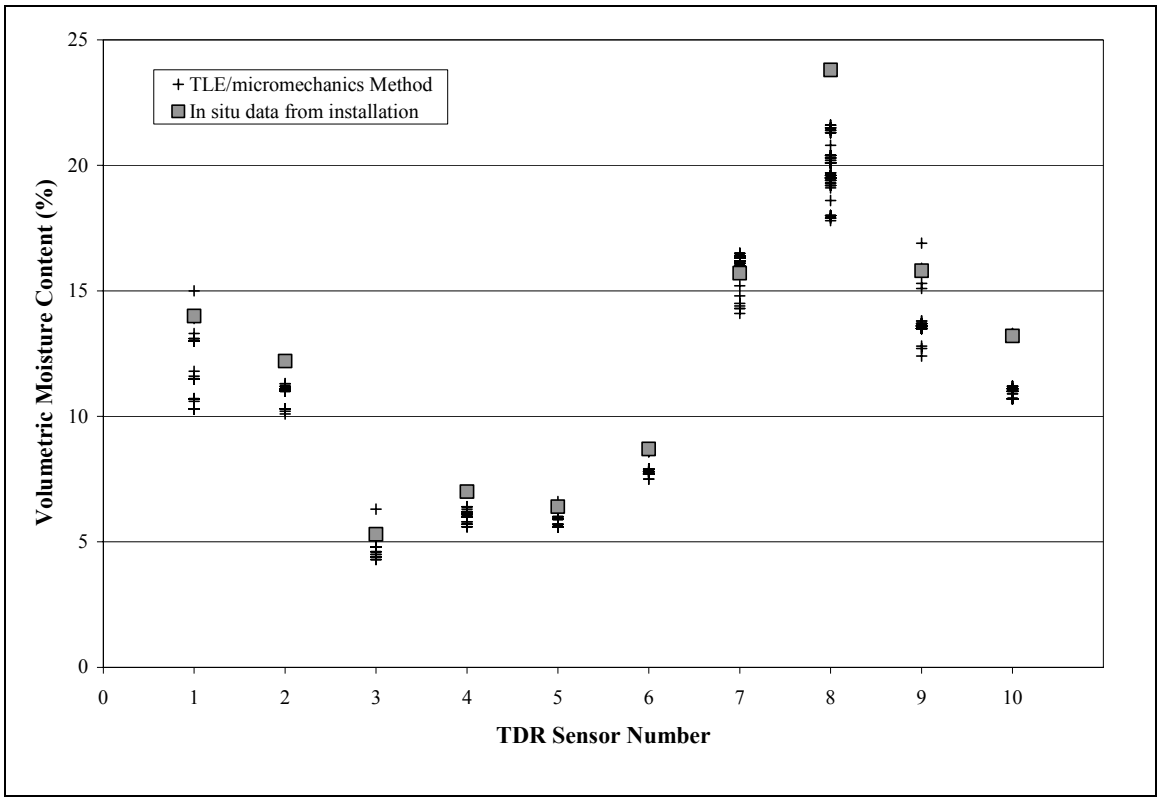

Figure 32. Graph. Results from the TLE micromechanics method for LTPP section 313018.

Differences between the two approaches are generally site specific and largely dependent on the measured in situ data. The TLE/micromechanics method is calibrated to the measured data and, therefore, yields estimates that are closer to the measured data as compared with the apparent length approach. The apparent length approach is a general empirical regression model that can vary significantly from ground truth data under certain circumstances.

FROST EFFECTS

Limited frost effects show up in the new data. In general, there is an expectation that the VMC values will decrease as the moisture in the ground freezes in both the wet and dry freeze regions. This can be seen in the values computed for site 274040. Where there is a distinct reduction in the volumetric moisture values during the winter months of 1993-1994, 1994-1995 and 1996-1997. There were no measurements recorded during the winter of 1996 at that location. It has been documented that frozen ground results in a TDR trace that does not have a negative slope between inflection points (i.e., an "open trace"). [(15)] These traces cannot be interpreted using the TLE/micromechanics method. Therefore, TDR traces flagged as uninterpretable during the winter months are indicative of frost effects.

SOURCES OF ERROR IN CALIBRATION DATA

The ability to calibrate to measured in situ data is one of the key advantages of the TLE/micromechanics method. Computed parameter estimates are directly affected by measurement errors in the ground truth data.

The in situ information came from limited soil tests performed during equipment installation. At that time, the apparent length approach was the accepted method for interpreting TDR traces to determine moisture estimates and was independent of the ground truth data. The soil was tested for in situ moisture content for general background information regarding the installation, not for calibration of moisture estimate algorithms. The procedure established for collection of the in situ moisture consisted of heating samples in an open pan over a propane stove in the field. The in situ dry density values were determined for each soil type based on a one point proctor test. Both of these tests have errors associated with them that directly affect soil parameters developed in this study.

A very likely source of error associated with moisture content testing in the field is soil loss due to either exploding aggregate (caused by rapid heating) or loss of fines (blown away during heating and stirring). Loss of soil during the drying process will produce moisture content results that can be up to five percent higher than the actual moisture content.

The dry density values used to calibrate the MicroMoist program often came from the one point proctor test performed on the soil samples taken during installation (when available). While the results from the one point proctor test provide reasonably accurate estimates of in situ densities, the findings are derived from disturbed samples, which can be another source of error. For some sites, dry density values reported were extremely high and not physically possible as they would result in a negative percentage of air voids. These cases were discussed in chapter 4 along with details on an adjustment procedure used to mitigate the problem. However, no correction was made for densities that were relatively low. These results were likely from deeper depths, where standard proctor densities would likely have provided more reasonable density values.

Future endeavors utilizing TDR equipment to monitor in situ conditions should focus on obtaining more accurate ground truth moisture and density data for use in the calibration of the TLE/micromechanics method. As such, soil from each layer should be sampled from a second hole and taken to the laboratory for testing. The moisture content could then be determined using a standard moisture test. The density could be estimated for each layer from a standard proctor test based on the moisture content established for each layer. For the deeper layers the density used may be 90 to 95 percent of the standard proctor density, assuming the in situ densities were below the influence area of the normal construction process. The ideal approach would be to dig test pits and perform nuclear density tests on each layer as it is excavated. However, the costs of this approach

may be prohibitive and could require placement of the TDR probes in the shoulder next to the traveled lane.

CHAPTER 8. RECOMMENDATIONS FOR FUTURE RESEARCH

This section provides recommendations on future research needed to improve and/or further the TLE/micromechanics approach to estimating soil parameters. These recommendations would provide complete validation of the process and improve the overall accuracy while reducing variability in the estimates.

INVESTIGATE THE EFFECTS OF SOIL SUCTION ON THE COMPOSITE DIELECTRIC CONSTANT

As discussed in chapter 5 of this report, a shift was observed in the relationship between composite dielectric constant and VMC. This shift typically occurred at dielectric constant values below five. Upon investigation, the research team believed that this phenomenon was caused by soil suction influences. However, the data needed to fully examine this issue is not currently available.

It is recommended that additional research be conducted to more fully investigate the effects of soil suction on the composite dielectric constant as it is used to compute moisture content using the micromechanics models used in this project. This would require laboratory evaluation of TDR traces in soils at different stages of the soil water characteristic curve.

INVESTIGATE THE USE OF CONDUCTIVITY AND REFLECTIVITY

As a result of this project, conductivity, reflectivity, and dielectric constant were computed and reported. Only the dielectric constant was used for estimating the VMC and dry density on this project. In some cases this seemed to lead to unrealistic values for the dielectric constant relative to the moisture content. While the resulting moisture content values were reasonable as compared to the ground truth calibration moisture content, the composite dielectric constant was very low relative to the moisture content estimate. It is likely that the soil reflectivity and conductivity information obtained from TDR traces would account for these anomalous data. It is recommended that further research in this area be conducted to fully document the relationship of all components of the TDR trace on soil parameters.

INVESTIGATE REPEATABILITY OF TDR TRACES

This project did not address the relative accuracy, variability, or repeatability of the computation process. Because the project dealt with existing data, there was no option available to obtain better information on the relative accuracy of the procedure other than to provide basic estimates from observations.

It is recommended that future research be conducted to investigate the accuracy and repeatability of the micromechanics-based procedure used on this project. The relative

accuracy of the procedure was tested against the existing data from the site installations, as well as the data from Klemune's thesis data. [5]

It is also recommended that more in situ information be collected and utilized to quantify the repeatability of the models. One such source of information would be from additional soil samples collected at the end of the TDR data collection sequence. This information could be used to compare estimates from the last TDR trace to ground truth data at a point in time other than during installation. In addition, it is recommended that repeated TDR traces be taken to determine the resultant variation in soil parameter estimates.

SENSITIVITY OF MICROMOIST PROGRAM OUTPUT TO VARIATION IN INPUT VALUES

The data needed to fully evaluate and document the sensitivity of the MicroMoist program were not available for this study. This would require a series of laboratory tests where moisture content and/or dry density is changed using a constant soil sample. The TDR traces from multiple conditions over a range of soil types and conditions could be used to fully document sensitivity. This information could also be compared to ground truth values derived from moisture content and dry density laboratory testing.

CHAPTER 9. SUMMARY AND CONCLUSIONS

TDR traces have been used to estimate the subsurface moisture content for unbound layers in pavement structures. In particular, the moisture content of the various roadway sublayers at SMP test sections were monitored with TDR instrumentation because it is relatively fast and accurate and provides a nondestructive in situ measurement. The TDR waveforms, however, do not provide moisture content estimates directly. In situ conditions of interest must be derived from the TDR waveforms and are largely dependent on the methodology used. However, it is clear that interpretation of electrically induced reflectometry depends not only on the material dielectric constant but also the reflectance and conductance attributes.

Moisture parameters had been estimated from TDR traces in the LTPP database previously, but significant quantities of TDR data have been collected since the completion of the original study. Therefore, one objective of this current study was to develop soil parameter estimates from TDR waveforms not previously analyzed. An additional objective was to investigate new methodologies or improvements to existing processes for interpreting TDR waveforms.

Based on the investigation conducted in phase 1 of the study, a new approach utilizing TLEs to compute dielectric constants from the TDR waveform and micromechanic models to estimate moisture and density parameters was proposed. This approach was approved by FHWA and was used to interpret 274,000 automated TDR traces in the LTPP database.

This new approach for calculation of the VMC consists of four steps:

Step 1*:* Calculate the dielectric constant, conductivity, and reflectivity from the TDR trace using the TLE.

- The TLE uses the shape of the trace to provide a more complete estimate of the dielectric constant.
- The solution method is the SID, which can minimize the error between the actual measurement and the calculated measurement.

Step 2: Given the moisture content and density data from the installation reports, along with the parameters calculated at step 1, backcalculate the permittivity of the solids and calibrate the micromechanics volumetric water model.

- This backcalculation is based on a theory of dielectric properties of composite materials from the micromechanics and self consistent scheme as follows:

$$\frac{\gamma_d}{G_s\gamma_w}\frac{\varepsilon_1-\varepsilon}{\varepsilon_1+2\varepsilon}+\theta\frac{\varepsilon_2-\varepsilon}{\varepsilon_2+2\varepsilon}+\left(1-\frac{\gamma_d}{G_s\gamma_w}-\theta\right)\frac{\varepsilon_3-\varepsilon}{\varepsilon_3+2\varepsilon}=0 \qquad (50)$$

- The dielectric constant of soil and water (ε_1, ε_2) and specific gravity of soil (G_s) are calibrated, based on the in situ information obtained during equipment installation, using the SID approach.

***Step 3*:** Given the calibrated micromechanics volumetric water model, forward calculate the volumetric water content and the dry density of the soil for other times and seasons based on the TDR traces and the associated dielectric constant.

- The self-consistent model was used together with the calibration constants ε_1, ε_2, and G_s to calculate soil dry density (γ_d) and VMC (θ).
- Systematic error was removed through consideration of the effect of individual constituent soil dielectrics.

***Step 4**:* Compute the gravimetric moisture content using the VMC and dry density from step 3.

The TLE method used to determine dielectric constant is able to consider the soil conductivity and reflectivity influence on the dielectric value. Additionally, the micromechanics models are calibrated to site-specific conditions and equipment using ground truth measured data. These two processes work together to minimize systematic errors in the resulting moisture and density estimates.

An evaluation of the new approach was conducted by comparing moisture estimates to measured values using data from SMP Installation Reports, Klemunes' thesis, and LTPP forensic studies. The estimates were relatively accurate and were all within 10 percent of the measured values. The previous LTPP interpretation procedures did not have a mechanism for estimating dry density for the soils represented by the TDR trace, but the new method provides the capability of estimating dry density values from TDR measurements.

A key advantage to the new micromechanics-based procedure is that it incorporates the engineering properties associated with the TDR measurements, as well as the mechanical properties of the soils being measured. Beyond this, it makes use of the physical and electrical properties of the materials being measured.

In order to quickly and efficiently compute soil parameters for the large quantity of records in the LTPP database, a new program, LTPP MicroMoist, was developed. The program utilized many of the same graphical and visual features as the MOISTER program. The new program was designed to calculate all components of the soil parameters automatically. Logic and reasonableness checks were incorporated into the program to ensure anomalous data were manually reviewed and verified. Data not passing established checks were flagged as part of the process. The program was designed so that quality took precedence over the computation efficiency and ensured that the highest quality data were obtained in a practical manner.

External to the program, post-processing graphs were developed and used in beta testing and debugging of the program. These graphs were also used to perform a 100 percent review of the final set of computed parameters. Anomalous or outlier data were manually flagged in the dataset delivered to FHWA for inclusion into the database.

As a result of this study, approximately 274,000 automated TDR traces were analyzed. Some were not interpreted due to questionable TDR trace characteristics or questionable results. The vast majority of those not interpreted were from the five sites in New Jersey where ground truth moisture content data were unavailable.

The analysis team worked with FHWA contractors to deliver the data in the most efficient manner and provided table and field descriptions for their use. It is anticipated that the data will be available in the 2008 LTPP Standard Data Release.

APPENDIX A. TRANSMISSION LINE EQUATION

The new approach for calculating dielectric constant in this project utilizes the transmission line equation (TLE). The following describes the basic theories and concepts of electromagnetics and the TLE.

MAXWELL'S EQUATIONS

In the study of electromagnetics, the four vector quantities called electromagnetic fields, which are functions of space and time, are involved: [12]

E = electric field strength (volts per meter, V/m)
D = electric flux density (coulombs per square meter, C/m^2)
H = magnetic field strengths (amperes per meter, Am/m)
B = magnetic flux density (webers per square meter, wb/m^2)

The fundamental theory of electromagnetic fields is based on Maxwell's equations governing the fields E, D, H, and B:

$$\nabla \times E = -\frac{\partial B}{\partial t} \tag{51}$$

$$\nabla \times H = J + \frac{\partial D}{\partial t} \tag{52}$$

$$\nabla \cdot B = 0 \tag{53}$$

$$\nabla \cdot D = \rho_V \tag{54}$$

Where:

J = electric current density (Am/m^2)
ρ_v = electric charge density (C/m^3)

J and ρ_v are the sources generating the electromagnetic field. The equations express the physical laws governing the E, D, H, and B fields and the sources J and ρ_v at every point in space and at all times.

In order to understand concepts of Maxwell's equations, some definitions and vector identities are described. The symbol ∇ in Maxwell's equations represents a vector partial-differentiation operator as following,

$$\nabla = \hat{x}\frac{\partial}{\partial x} + \hat{y}\frac{\partial}{\partial y} + \hat{z}\frac{\partial}{\partial z} \tag{55}$$

Where $\hat{x}$, $\hat{y}$, *and* $\hat{z}$ = unit vectors along the x, y, and z axes

If A and B are vectors, the operation $\nabla \times A$ is called the curl of A, and the operation $\nabla \cdot B$ is called the divergence of B. The former is a vector and the latter is a scalar. In addition, if

$\phi(x, y, z)$ is a scalar function of the coordinates, the operation $\nabla\phi$ is called the gradient of ϕ. The operator as a vector is only permissible in rectangular coordinates.
Some useful vector identities are as follows: [12]

$$\nabla\times(\nabla\times A)\equiv\nabla(\nabla\cdot A)-\nabla^2 A, \quad (56)$$
$$\nabla\cdot(\nabla\times A)\equiv 0, \quad (57)$$
$$\nabla\times\nabla\phi\equiv 0, \text{ and} \quad (58)$$
$$\nabla\cdot(A\times B)\equiv B\cdot(\nabla\times A)-A\cdot(\nabla\times B) \quad (59)$$

Where: $\nabla^2=\frac{\partial^2}{\partial x^2}+\hat{y}\frac{\partial^2}{\partial y^2}+\hat{z}\frac{\partial}{\partial z^2}$ (60)

CONSERVATION LAW OF ELECTRIC CHARGE

The Maxwell equation (55) can be presented using the vector identity (57) and multiplying both sides by ∇ as follows:

$$\nabla\cdot J+\frac{\partial}{\partial t}\nabla\cdot D=\nabla\cdot(\nabla\times H)=0 \quad (61)$$

Being replaced with equation 54, the conservation law for current and charge densities is defined as the following:

$$\nabla\cdot J+\frac{\partial\rho_V}{\partial t}=0 \quad (62)$$

The conservation law means that the rate of transfer of electric charge out of any differential volume is equal to the rate of decrease of total electric charge in that volume. This law is also known as the continuity law of electric charge. In fact, to solve electromagnetic field problems, it is essential to assume that the sources J and ρ_v are given and satisfy the continuity equation. [12]

CONSTITUTIVE RELATIONS

Constitutive relations can provide physical information for the environment in which electromagnetic fields occur, such as free space, water, or composite media. Also, they can characterize a simple medium mathematically with a permittivity, ε, and a permeability, μ, as follows:

$$D=\varepsilon E \quad (63)$$
$$B=\mu H \quad (64)$$

For free space such as air, $\mu=\mu_0=4\pi\times10^{-7}$ H/m and $\varepsilon=\varepsilon_0=8.85\times10^{-12}$ F/m

MAXWELL'S EQUATIONS FOR TIME-HARMONIC FIELDS

Time-harmonic data is the large class of physical quantities that vary periodically with time. While physical quantities are usually described mathematically by real variables of space and time and by vector quantities, the time-harmonic real quantities are represented by complex variables.[12] A time-harmonic real physical quantity $V(t)$ that varies sinusoidally with time can be expressed as follows:

$$V(t) = V_0 \cos(\omega t + \phi) \tag{65}$$

Where:

V_0 = amplitude,
ω = angular frequency (= $2\pi f$)
f = frequency of $V(t)$
t = time
ϕ = phase of $V(t)$

Figure 33 illustrates $V(t)$ as a function of time t.

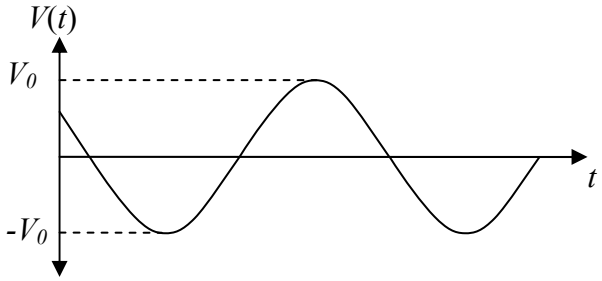

Figure 33. Graph. Time-harmonic function $V(t)$.[12]

The V(t) can be expressed by using the symbol of Re{ }, which means taking the real part of the quantity in the brace as follows:

$$V(t) = \mathrm{Re}\{Ve^{j\omega t}\} = \mathrm{Re}\{V_0 e^{j\phi} e^{j\omega t}\} \tag{66}$$

Hence, the derivation with respect to time can be expressed as

$$\frac{\partial}{\partial t} V(t) = -\omega V_0 \sin(\omega t + \phi) = \mathrm{Re}\{j\omega V_0 e^{j\phi} e^{j\omega t}\} \tag{67}$$

So,

$$\frac{\partial}{\partial t} V(t) \leftrightarrow j\omega V \tag{68}$$

As shown in equation 67, the time derivative ∂/∂t can be replaced by $j\omega$ in the complex representation of time-harmonic quantities.

Maxwell's equations can be expressed with respect to the complex representations for the time-harmonic quantities as follows:

$$\nabla \times E = -\frac{\partial B}{\partial t} = -j\omega B \tag{69}$$

$$\nabla \times H = J + \frac{\partial D}{\partial t} = J + j\omega D \tag{70}$$

$$\nabla \cdot B = 0 \tag{71}$$

$$\nabla \cdot D = \rho_V \tag{72}$$

UNIFORM PLANE WAVES IN FREE SPACE

Given that electromagnetic fields are generated in free space by source J and ρ_v in a localized region, then, for electromagnetic fields outside the region, J and ρ_v are equal to zero and Maxwell's equation can be expressed with free space constitutive relations of equations 63 and 64 as the following: [11]

$$\nabla \times E = -j\omega B = -j\omega\mu_0 H \tag{73}$$

$$\nabla \times H = j\omega D = j\omega\varepsilon_0 E \tag{74}$$

$$\nabla \cdot B = \nabla \cdot H = 0 \tag{75}$$

$$\nabla \cdot D = \nabla \cdot E = 0 \tag{76}$$

By taking the curl of (73) and substituting (74), the following can be obtained:

$$\nabla \times (\nabla \times E) = \omega^2 \mu_0 \varepsilon_0 E \tag{77}$$

The wave equation for E can be obtained with regard to vector identity (56) and equation 74 as follows:

$$\nabla^2 E + \omega^2 \mu_0 \varepsilon_0 E = 0 \tag{78}$$

The wave equation (78) is a vector second-order differential equation. The simple solution is expressed as follows;

$$E = \hat{x} E_0 e^{-jkz} \tag{79}$$

From equations 78 and 79, the following is obtained;

$$k^2 = \omega^2 \mu_0 \varepsilon_0 \tag{80}$$

The magnetic field H of the wave can be determined from equation 73 or 74:

$$H = \hat{y}\sqrt{\frac{\varepsilon_0}{\mu_0}}E_0 e^{-jkz} \tag{81}$$

In equation 81, the factor $\sqrt{\varepsilon_0/\mu_0}$ is known as the intrinsic impedance of free space,

$$\eta = \sqrt{\frac{\mu_0}{\varepsilon_0}} \tag{82}$$

The wave has the electric field E in the $\hat{x}$-direction and the magnetic field H in the $\hat{y}$-direction and propagates in the $\hat{z}$-direction. Figure 34 shows the velocity of propagation with time in a sinusoidal wave.

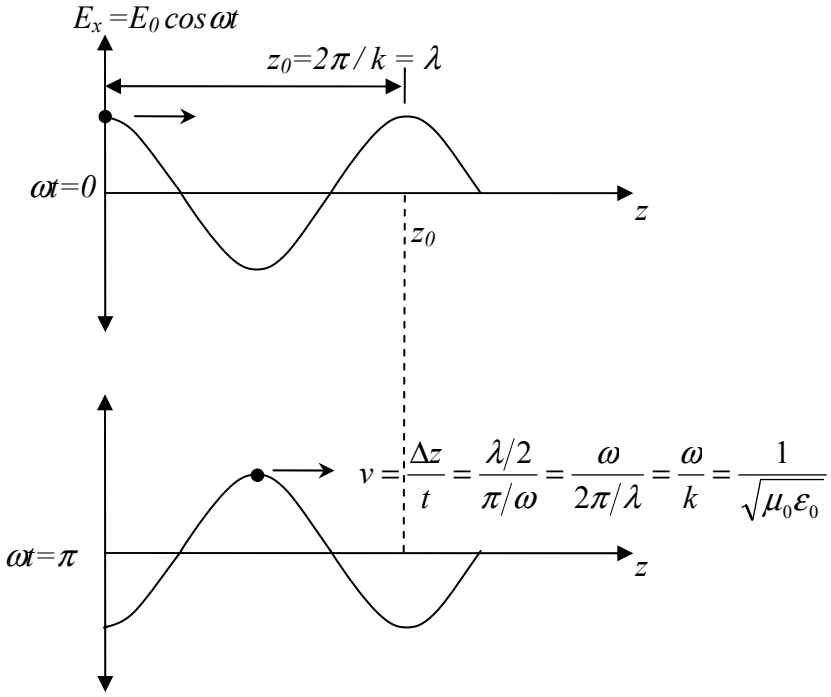

Figure 34. Graph. Electric field as a function of z direction at different times. [12]

Therefore, the velocity of light in free space becomes:

$$v = \frac{\omega}{k} = \frac{1}{\sqrt{\mu_0 \varepsilon_0}} \tag{83}$$

Where:

ω = angular frequency

k = propagation constant

TRANSMISSION LINE EQUATION OF COAXIAL TRANSMISSION LINE

In the case that electromagnetic waves propagate in free space, the path of the wave is straight, and the intensity is uniform on the transverse plane. However, if the wave is guided along a curved and limited path, the wave is not uniform on the transverse plane and the intensity is limited to a finite cross-section. The finite structure transmitting electromagnetic waves is called a transmission line or waveguide. The wave can be transmitted along different types of waveguides: parallel-plate waveguides, rectangular waveguides, and coaxial lines. This study considers the coaxial lines, which are involved in TDR.

COAXIAL LINES

The most commonly used transmission line to guide the electromagnetic wave is the coaxial line. The coaxial line consists of inner and outer conductors and an inner dielectric insulator. As shown in figure 35, a coaxial line has an inner conductor of radius, *a,* and an outer conductor of inner radius, *b*, insulated by a dielectric layer of permittivity, ε. Figure 36 presents the cylindrical coordinate system for the solution inside coaxial lines.

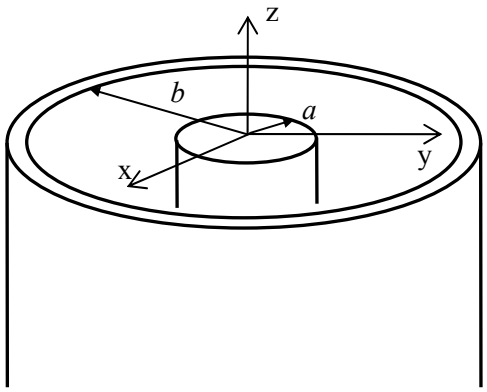

Figure 35. Diagram. Coaxial line. [(11)]

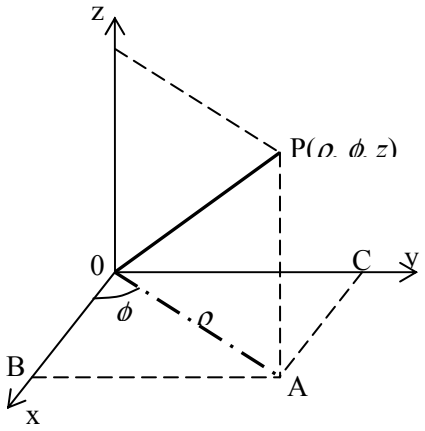

Figure 36. Cylindrical coordinate system. [12]

In the cylindrical coordinate system, coordinate ρ is the distance from the z-axis or length 0A, ϕ is the angle between 0A and the x-axis, and z represents the distance from the *x-y* plane. The three coordinates, ρ, ϕ, and *z* represent the point *P* and are expressed in terms of unit vectors, $\hat{\rho}$, $\hat{\phi}$ and $\hat{z}$.

TRANSVERSE ELECTRIC AND MAGNETIC (TEM) MODE IN A COAXIAL LINE

In order to explain the fundamental mode on the coaxial line, it is necessary to consider the case where the inner radius, *a*, is close to the outer radius, *b*. When the coaxial line is cut along the *x-y* plane and unfolded into a parallel strip, the line can be illustrated as figure 33:

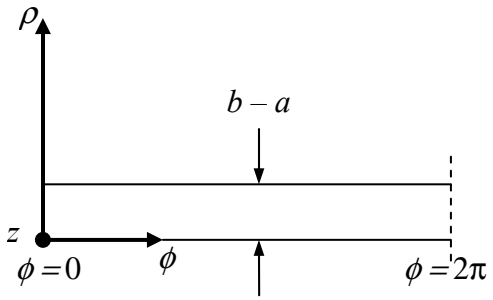

Figure 37. Diagram. Coaxial line developed into a parallel-plate waveguide. [12]

From Figure 37, it is realized that the wave has the electric field *E* in the $\hat{\rho}$-direction and the magnetic field *H* in the $\hat{\phi}$-direction and propagates in the $\hat{z}$-direction. Therefore, *E* and *H* can be expressed as follows:

$$E = \hat{\rho}\frac{V_0}{\rho}e^{-jkz} \tag{84}$$

$$H = \hat{\phi}\frac{V_0}{\eta\rho}e^{-jkz} \tag{85}$$

Where:

k = propagation constant, $\omega\sqrt{\mu\varepsilon}$

η = intrinsic impedance, $\sqrt{\frac{\mu}{\varepsilon}}$

Since the *E* and *H* are transverse to the direction of wave propagation, the set of equations 84 and 85 is called the transverse electromagnetic mode (TEM) of the coaxial line.

TRANSFORMATION RULES FOR TRANSMISSION LINES

The following rules are for transforming the field quantities into network parameters. [12]

Rule 1. Voltage $V(z) = \alpha_1 \int_{C_t} E \cdot ds$ (86)

Where:

α_1 = proportional constant
C_t = integration path transverse to z

Rule 2. Current $I(z) = \alpha_2 \oint_{C_0} H \cdot ds$ (87)

Where:

α_2 = proportional constant
C_0 = closed contour of integration

The power relationship must hold:

Rule 3. $1/2\,\mathrm{Re}[V(z)I(z)] = \int_A dA\,\hat{z} \cdot 1/2\,\mathrm{Re}[E \times H]$ (88)

Where A = cross-sectional area of the line or waveguide

TRANSMISSION LINE EQUATION

The electric and magnetic fields *E* and *H* for a coaxial line in the TEM mode are:

$$E_\rho = \frac{V_0}{\rho} e^{-jkz} \tag{89}$$

$$H_\phi = \frac{V_0}{\eta\rho} e^{-jkz} \tag{90}$$

By applying the field equations to the transformation rule, the following equations can be defined as:

$$V(z) = \alpha_1 \int_a^b d\rho E_\rho = \alpha_1 V_0 \ln\frac{b}{a} e^{-jkz} \tag{91}$$

$$I(z) = \alpha_2 \oint_{C_0} \rho\, d\phi\, H_\phi = \alpha_2 \frac{2\pi V_0}{\eta} e^{-jkz} \tag{92}$$

Where:

α_1, α_2 = calibration constants
V_0 = applied voltage
a, b = inside and outside coaxial transmission line diameters (figure 13)

If the calibration constants are one ($\alpha_1 = \alpha_2 = 1$), equations 91 and 92 become:

$$E_\rho = \frac{V(z)}{\ln(b/a)} \frac{1}{\rho} \tag{93}$$

$$H_\rho = \frac{I(z)}{2\pi} \frac{1}{\rho} \tag{94}$$

Maxwell's equations for electric and magnetic fields can be cast in the standard form of TLEs in terms of voltage and current, *V* and *I,* by using cylindrical coordinates. Maxwell's two curl equations are defined as the following TLEs:

$$\frac{dV}{dz} = -j\omega\mu \frac{I}{2\pi} \ln(b/a) \tag{95}$$

$$\frac{dI}{dz} = -j\omega\varepsilon \frac{V}{\ln(b/a)} 2\pi \tag{96}$$

By eliminating *I* from equation 95, a wave equation for the voltage *V* can be obtained as follows:

$$\frac{d^2V}{dz^2} = -\omega^2 \mu\varepsilon V \tag{97}$$

V has two solutions of $e^{-j\omega\sqrt{\mu\varepsilon}}$ and $e^{+j\omega\sqrt{\mu\varepsilon}}$. Each solution has an integration constant as a multiplier. *V* can be expressed by introducing two constants, V_+ and V_-, as:

$$V = V_+ e^{-jkz} + V_- e^{+jkz} \tag{98}$$

Where $k = \omega\sqrt{\mu\varepsilon}$

The amplitude of V_+ represents a wave traveling in the positive z-direction and the amplitude of V_- represents a wave traveling in the negative z-direction.

APPENDIX B. CHARACTERIZATION OF ERROR IN THE SID

Relative to the least squares error associated with linear regression, assuming that $y_i = ax_i + b$, then the error (r_i) and the variance (r_i^2) at a point can be expressed as:

$$r_i = \left(y_i - ax_i - b\right) \tag{99}$$

$$r_i^2 = \left(y_i^2 + a^2x_i^2 + b^2 - 2ax_iy_i - 2by_i + 2abx_i\right) \tag{100}$$

The total variance over all points *n* is:

$$\sum_{i=1}^{n} r_i^2 = \sum_{i=1}^{n}\left(y_i^2 + a^2x_i^2 + b^2 - 2ax_iy_i - 2by_i + 2abx_i\right) \tag{101}$$

Setting the derivatives of the variance with respect to the coefficients a and b to zero gives:

$$\frac{\partial\sum_{i=1}^{n} r_i^2}{\partial a} = \sum_{i=1}^{n}\left(2ax_i^2 - 2x_iy_i + 2bx_i\right) = 0 \tag{102}$$

$$\frac{\partial\sum_{i=1}^{n} r_i^2}{\partial b} = \sum_{i=1}^{n}\left(2b - 2y_i + 2ax_i\right) = 0 \tag{103}$$

and yields two equations in the two unknown coefficients a and b:

$$\begin{bmatrix} 2\sum_{i=1}^{n} x_i^2 & 2\sum_{i=1}^{n} x_i \\ 2\sum_{i=1}^{n} x_i & 2\sum_{i=1}^{n} 1 \end{bmatrix}\begin{Bmatrix} a \\ b \end{Bmatrix} = \begin{bmatrix} 2\sum_{i=1}^{n} x_iy_i \\ 2\sum_{i=1}^{n} y_i \end{bmatrix} \tag{104}$$

Which expresses the definition of linear regression. In matrix form, where there are a number (*i*) independent variables x_i associated with observations y_j (dependent variable) that form a matrix of independent variables, $x_{i,j}$ can be expressed as:

$$\underline{y} = X\,\underline{a} - \underline{r} \tag{105}$$

Where:

$\underline{y}$ = vector of *j* observations

X = matrix of $x_{i,j}$

$\underline{a}$ = vector of unknown coefficients

$\underline{r}$ = vector of regression errors

Solving for $\underline{a}$:

$$X^T \underline{y} = X^T X \underline{a} - X^T \underline{r} \tag{106}$$

$$X^T X \underline{a} = X^T \underline{y} + X^T \underline{r} \tag{107}$$

$$\underline{a} = \left[X^T X \right]^{-1} X^T \underline{y} + \left[X^T X \right]^{-1} X^T \underline{r} \tag{108}$$

Where the second part of the above expression represents the residual regression error. Formulating this on the basis of partial derivatives:

$$\underline{r} = \underline{y} - X \underline{a} \tag{109}$$

$$\sum_{i=1}^{n} r_i^2 = \underline{r}^T \underline{r} = \left[\underline{y} - X \underline{a} \right]^T \left[\underline{y} - X \underline{a} \right] \tag{110}$$

Differentiating with respect to the vector of unknown coefficients $\underline{a}$ and setting to zero:

$$\frac{\partial \sum_{i=1}^{n} r_i^2}{\partial \underline{a}} = \frac{\partial \left[\underline{r}^T \underline{r} \right]}{\partial \underline{a}} = \frac{\partial \left\{ \left[\underline{y} - X \underline{a} \right]^T \left[\underline{y} - X \underline{a} \right] \right\}}{\partial \underline{a}} = \underline{0} \tag{111}$$

$$\frac{\partial \left\{ \left[\underline{y} \right]^T \left[\underline{y} - X \underline{a} \right] - \underline{a}^T X^T \underline{y} + \underline{a}^T X^T X \underline{a} \right\}}{\partial \underline{a}} = \underline{0} \tag{112}$$

$$= \frac{\partial \left\{ \left[\underline{y} \right]^T \underline{r} \right\}}{\partial \underline{a}} - X^T \underline{y} + X^T X \underline{a} = \underline{0} \tag{113}$$

Rearranging and solving for $\underline{a}$:

$$X^T X \underline{a} = X^T \underline{y} - \frac{\partial \left[\underline{y}^T \underline{r} \right]}{\partial \underline{a}} \tag{114}$$

$$\underline{a} = \left[X^T X \right]^{-1} X^T \underline{y} - \left[X^T X \right]^{-1} \frac{\partial \left[\underline{y}^T \underline{r} \right]}{\partial \underline{a}} \tag{115}$$

Where again the second part of the above expression represents the residual regression error. Drawing the analogy to the system identification method (SID):

$$\underline{y} = \underline{y}_m \left(\underline{a} \right) - \frac{\partial \underline{y}_m \left(\underline{a} \right)}{\partial \underline{a}} \partial \underline{a} \tag{116}$$

Where $\underline{y}_m \left(\underline{a} \right)$ is the matrix of model predictions. Rearranging:

$$\frac{\partial \underline{y}_m \left(\underline{a} \right)}{\partial \underline{a}} \partial \underline{a} = \underline{y} - \underline{y}_m \left(\underline{a} \right) = \underline{r}$$
$$\left[F \right] \{ \beta \} = \left[\underline{r} \right] \tag{117}$$

Where:

$[F]$ $= \left[\frac{\partial y_m}{\partial \underline{a}}\right]$ which is a rectangular sensitivity matrix (k x n); k = number of coefficients a

$\{\beta\}$ $= \partial \underline{a}$ which is the matrix of change in the model coefficient (n x 1)

$[\underline{r}]$ = the matrix of change in the model prediction or the residual error (k x 1)

Therefore:

$$\left[\frac{\partial \underline{y}_m(\underline{a})}{\partial \underline{a}}\right]^T \left[\frac{\partial \underline{y}_m(\underline{a})}{\partial \underline{a}}\right] \{\partial \underline{a}\} = \left[\frac{\partial \underline{y}_m(\underline{a})}{\partial \underline{a}}\right]^T \{\underline{r}\} \tag{118}$$

$$\{\partial \underline{a}\} = \left\{\left[\frac{\partial \underline{y}_m(\underline{a})}{\partial \underline{a}}\right]^T \left[\frac{\partial \underline{y}_m(\underline{a})}{\partial \underline{a}}\right]\right\}^{-1} \left[\frac{\partial \underline{y}_m(\underline{a})}{\partial \underline{a}}\right]^T \{\underline{r}\} \tag{119}$$

This yields a solution for the changes in the model coefficients based on the residual error in the model prediction.

APPENDIX C. MICROMOIST USER'S MANUAL

The user's manual documents and describes the various features of the MicroMoist program. This will serve as a tool in the installation, navigation, and data processing components of the program. The program was developed to automate, to the extent practical, procedures in interpreting time domain reflectometry (TDR) traces to estimate soil parameters such as moisture content and dry density. MicroMoist was developed specifically for use on data stored in the LTPP database. The program requires input tables to be in a specified format. Other data can be analyzed in with MicroMoist as long as the input data are structured in accordance with this manual.

This manual is divided into three main sections:

- Introduction to the Program
- Getting Started in the Program
- Program Features

INTRODUCTION TO THE PROGRAM

In 1992, the Seasonal Monitoring Program (SMP) was initiated within the LTPP study in order to understand the environmental factors and the relationship with pavement performance. Sixty-four LTPP test sections were selected for the SMP according to pavement type, thickness, environment, and subgrade type. Several instruments were installed at each section to acquire data on in situ moisture content and temperature of sublayers, frost penetration, and depth to ground water. As part of this program, TDR technology was selected to measure in situ moisture content of pavement sublayers. TDR data were collected with 8-inch TDR probes developed by FHWA. Ten TDR probes were installed for each SMP test section at specified depths in the unbound base and subgrade layers below the outer wheel path.

This program was developed based on the approach of using transmission line equations (TLE) and micromechanic models to estimate soil parameters from TDR traces. In this approach, the TLE is used to solve for the dielectric constant of the soil. The dielectric value was then employed in a micromechanics model calibrated specifically to each site and layer combination to determine soil parameters. MicroMoist allows users to view and process TDR traces based on this approach.

MicroMoist extracts data from three input tables that are in Microsoft Access format and shows the smoothed trace on the screen. The trace shown on the screen is processed automatically using the algorithm implemented by the program, which identifies the inflection points and displays the points on the trace. The soil dielectric constant is determined using the data points on the TDR trace between the inflection points.

The program can process TDR traces in the following ways:

- MicroMoist automatically processes all the TDR traces collectively and shows the identified inflection points on the screen for review.

- For QC purposes, users can view all traces and have the option of adjusting the location of the inflection points. Changed inflection points automatically get recorded as new points on the trace and are hence used for the calculation.

The resultant soil parameters and supporting computations are provided in two Access database tables.

The program was designed with features that make it an efficient tool for reviewing TDR traces and computing parameters of interest.

GETTING STARTED IN THE PROGRAM

Getting started with the new program is easy, especially if Windows XP operating system is currently installed on the target workstation.

System Requirements

To run MicroMoist, the following minimum hardware and software requirements must be met:

- IBM-compatible Pentium processor
- 512 MB of RAM (1 GB recommended)
- 1 MB of available hard disk space, depending on the size of the TDR trace table
- Super video graphics adapter with at least 800*600 resolution and 256 colors
- Microsoft mouse or compatible pointing device
- Microsoft Windows XP operating system.

Installing and Running the Program

The MicroMoist program is an executable file which does not need to be installed. The program can be run once the program files are copied to the appropriate drive.

PROGRAM FEATURES

MicroMoist was developed to allow users to view TDR traces as well as to automate the process of estimating soil parameters from the traces. In light of this, the following functions and features were incorporated into the program. MicroMoist is a powerful tool for the analysis of TDR traces; however, users must be familiar with TDR data collection principles, equipment, and techniques.

Raw TDR Trace Data

The program extracts raw TDR trace data points from an Access database into an Access table. This table should be the same format and structure as the SMP_TDR_AUTO table in the LTPP database. The table contains a flat representation of the TDR waveform sampled at 245 intervals and stored in the WAVEP_1 through WAVP_245 field. The table to be queried by MicroMoist can have any name. A sample table is provided with the program. This table must be provided with the following two tables (SMP_TDR_DEPTHS_LENTH and SMP_TDR_CALIBRATE) together in one Access database prior to running the program.

TDR Depth Records

The MicroMoist program also requires the SMP_TDR_DEPTHS_LENGTH table in the Access database to extract information on installation depths of TDR sensors. This table needs to be the same structure and format as the SMP_TDR_DEPTHS_LENGTH table in the LTPP database, which contains the physical information of the TDR probes such as the depths at which the probes are installed, their installation date, and the length of TDR probes. This table is used to link to SMP_TDR_AUTO to determine the depth corresponding to a TDR trace, using the STATE_CODE, SHRP_ID, TDR_NO, and CONSTRUCTION_NO. A sample table is provided with the program. This table must be provided with the raw TDR trace table and the following table (i.e., SMP_TDR_CALIBRATE) in one Access database prior to running the program.

TDR Calibration Records

MicroMoist also utilizes calibration information for each site and TDR sensor. A table named SMP_TDR_CALIBRATE is required in the Access database. The SMP_TDR_CALIBRATE table contains the calibrated dielectric constants of soil components and specific gravity. The calibrated values are required to calculate moisture content and dry density values by linking SMP_TDR_CALIBRATE by STATE_CODE, SHRP_ID, and TDR_NO fields. A sample table is provided with the program. This table must be provided with the raw TDR trace table and the SMP_TDR_DEPTHS_LENGTH table in an Access database prior to running the program.

Starting the Program

When MicroMoist is started, the main TDR data processing window appears. The user must first open an Access database containing the raw TDR trace table as described in "Raw TDR Trace Data."

TDR Program Menus

Menus in MicroMoist are context sensitive; both the available menus and their contexts change according to which part of the program is active. Menu features are briefly discussed in this section.

The toolbar buttons provide shortcuts to all the menu items. The menu items and corresponding toolbar buttons are both described below.

Menu bar:

- ***OPEN:*** Opens dialog box to select the database for processing.
- ***EXIT:*** Ends the program, closing all the connections and the database.

Toolbar: Contains icons in the order listed below:

- ***OPEN:*** Open dialog box to select the database for processing.
- ***CLOSE:*** Ends the program, closing all the connections and the database.
- ***Previous Trace:*** View previous TDR trace in database.
- ***Go To:*** View a specific TDR trace based on location in the database.
- ***Next Trace:*** View next TDR trace in database.
- ***Show Trace:*** Refresh current TDR trace.
- ***Change Inflection Points:*** Manually select inflection points on TDR trace.
- ***Write Dielectric Output:*** Compute dielectric constant of TDR trace and store in database.
- ***Write Moisture Output:*** Compute moisture content and store in database.

The screen contains a combo box, labeled "Dubious Records," which lists TDR traces that do not pass criteria checks. Traces with positive slope or wrong inflection points fall into this category. Additional information is also provided on the screen, including SHRP_ID, STATE CODE, CONSTRUCION NUMBER, SMP DATE, TDR TIME, and TDR NUMBER, DIST_WAV of the TDR trace currently displayed.

Output Table after Running Program

Utilizing data from the input database tables described above, the program generates two output tables: SMP_TDR_AUTO_DIELECTRIC and SMP_TDR_ MOISTURE. These tables are automatically generated in the Access database containing the input data tables.

The SMP_TDR_AUTO_DIELECTRIC table contains dielectric constant, conductivity, and reflectivity values computed from interpretable TDR records in SMP_TDR_AUTO. This table is generated by running the ***Write Dielectric Output*** option on the toolbar.

The SMP_TDR_ MOISTURE table contains the dry density, volumetric moisture content, and gravimetric moisture content values computed from interpretable TDR traces in the SMP_TDR_AUTO table and is generated by running the ***Write Moisture Output*** option on the toolbar.

REFERENCES

[1] Jiang, Y.J., and Tayabji, S.D. *Analysis of Time Domain Reflectometry Data from LTPP Seasonal Monitoring Program Test Sections – Final Report*, FHWA-RD-99-115, Federal Highway Administration, 1999.

[2] *LTPP SMP* (CD-ROM), Version 1.2, Federal Highway Administration, 2004.

[3] Rada, G.R., Elkins, G.E., Henderson, B., Sambeek, R.J., and Lopez, A., *LTPP Seasonal Monitoring Program: Instrumentation Installation and Data Collection Guidelines*, Report No. FWHA-RD-94-110, Federal Highway Administration, 1995.

[4] FHWA-LTPP Technical Support Services Contractor. *LTPP Manual for Falling Weight Deflectometer Measurements Operational Field Guidelines*, Federal Highway Administration, 2000.

[5] Klemunes, J.A. *Determining Volumetric Moisture Using the Time Domain Reflectometry Response*, M.S. Thesis, University of Maryland, 1995.

[6] Klemunes, J.A., *Determining Soil Volumetric Moisture Content Using Time Domain Reflectometry*, FHWA-RD-97-139, Federal Highway Administration, 1998.

[7] Roth, K., Schulin, R., Flühler, H., and Attinger, W. Calibration of Time Domain Reflectometry for Water Content Measurement Using a Composite Dielectric Approach, *Water Resource Research*, Vol. 26, No. 10, 1990.

[8] Topp, G.C., Davis, J.L., and Anna, A.P. Electromagnetic Determination of Soil Water Content: Measurement in Coaxial Transmission Lines, *Water Resource Research*, Vol. 16, No. 3, 1980.

[9] LTPP Information Management System, Database Scheme and QC specification for SMP_TDR_MANUAL_MOISTURE Tables-Draft Final, Federal Highway Administration, 2002.

[10] Das, B.M. *Principles of Geotechnical Engineering*, PWS Engineering: Boston, 1985.

[11]Lytton, R.L. *Backcalculation of Pavement Layer Properties*, *Nondestructive Testing of Pavements and Backcalculation of Moduli. ASTM 1026.* (A.J. Bush III and G.Y. Baladi, eds.), American Society of Testing Materials: Philadelphia, 1989, pp. 7–38.

[12] Shen, L.C., and Kong, J.A. *Applied Electromagnetism*, Brooks/Cole Engineering Division: Monterey, CA, 1983.

[13] Hashin, Z. Theory of Composite Materials, in *Mechanics of Composite Materials*, Pergamon Press: Oxford, UK, 1969, pp. 201–242.

[14] Tummers, B. *DataThief III manual v.1 β*, http://www.datathief.org/, 2005.

[15] *Interpretation of Manual TDR Traces*. Long Term Pavement Performance Program Directive SM-28, FHWA, August 7, 1998.

HRTI-13/03-08(1.5M)E